DSE Final Report

Floating Airborne Wind Energy System Farm

AE3200: Design Synthesis Exercise

Group 19: *Deep WattAir*

Delft University of Technology

TU Delft

Cover Image: Artist Impression of the AWES

This page was intentionally left blank

DSE Final Report

Floating Airborne Wind Energy System Farm

by

Student Name	Student Number
Bogaert, Joshua	5298601
Bononi Bello, Felipe	5069238
van den Heuvel, Gerwin	5004888
Johary, Antra	5238218
Kohlhéb, Áron	5094704
Teunissen, Robin	4562895
Trịnh, Thế Minh	5216958
Verhas, Toon	5006546
Vermeulen, Fleur	5071372
van Zuylen, Coen	4835565

Instructor:	Prof. dr. S.J. Watson
Coaches:	S.R. Turteltaub, PhD and V.O. Bonnin, PhD
Teaching Assistant:	K. Regnery
Institution:	Delft University of Technology
Place:	Faculty of Aerospace Engineering, Delft
Date:	Tuesday 27th June, 2023

Cover Image: Artist Impression of the AWES

TU Delft

Executive Summary

The aim of this Design Synthesis Exercise was to design a floating large-scale wind farm of 1 GW in deep water using an Airborne Wind Energy System (AWES) that is cost-competitive, largely recyclable and uses less material than conventional wind turbines. By exploring the project foundation, carrying out an iterative single-system design process, and delving into the farm layout and management, this project assesses the feasibility of this novel concept. This report proposes an initial design with the resources currently available to the team while highlighting the next steps that need to be taken in order to pursue further design iterations, prototyping, and testing of this concept. This initial design, the tool developed to carry out the sizing, and a detailed reflection on the limitations of this design process and concept could be stated as the main contribution of this project to the field of airborne wind energy.

The main user requirements this project bases itself upon are as follows [1]:

- The AWES-based floating offshore wind farm should have a rated output of 1GW
- The system should have 95% availability (in terms of availability to generate)
- The AWESs in the wind farm must operate safely (no risk to shipping or air traffic)
- The components should be 90% recyclable
- 95% of the components should be capable of being removed at end of life
- The mass of all components in the wind farm should be less than 50% of an equivalent fixed bottom-mounted or floating horizontal axis wind turbine (HAWT) based wind farm
- The projected levelised cost of energy (LCoE) assuming eventual technology maturity for the AWES-based wind farm should be less than an equivalent HAWTbased system (assuming 50 €/MWh)
- The lifetime of the AWES-based wind farm should be 20 years (though components may be replaced at intervals)

Part 1: Project Plan

Trade-off Summary

Over the course of the project, the team converged on a few airborne concepts that were deemed feasible, namely a rigid wing fly-gen, a rigid wing ground-gen, and a soft wing ground-gen. As their names suggest, the first two concepts use rigid wings, however, differ in the way they produce energy; the fly-gen concept generates electricity through rotating rotors placed on the wing (or wings) along the element's flight path, while the ground-gen concept generates electricity by pulling the tether, which connects the airborne to the seaborne element, as it follows the airborne element's flight path. The soft wing ground-gen concept uses a soft wing, a collapsable and flexible material while using the ground-gen system for energy production. A trade-off was performed between these concepts based on what was considered the most important criteria, which were, in order of importance, the cost, reliability, mass, operability, sustainability, and development effort. From this trade-off, the rigid wing fly-gen turned out to be the best option.

For the seaborne element, existing floater concepts were explored. The concepts considered were a spar buoy, a semi-submersible platform, and a tension-leg platform. The criteria decided upon for this trade-off were Mass, Production Cost, Lifetime, Stability, Transportation, and Installation. This trade-off showed the semi-submersible to be the best option for the floater. This option was then scaled to suit the complete design needs.

For both these trade-offs, a sensitivity analysis was performed to ensure that the trade-off was robust. The impact of changing weights and scoring of criteria showed that the chosen concepts from the trade-off won more than 70% of the time.

Market Analysis

The energy markets are transitioning from fossil fuels to sustainable energy due to increased agreements and pledges to combat climate change. The Paris Agreement, for instance, has been signed by 175 countries to set the goal of net-zero emissions by 2050. In reaching this goal, renewable energy sources worldwide are expected to grow from 29% in 2020 to 90% in 2050, most of which will be solar and wind energy.
In the Netherlands, the current rated wind power capacity of the Netherlands is equal to about 9 GW, of which 5 GW is onshore and 4 GW is offshore. The onshore wind capacity is expected to grow by a factor of two to four by 2050. The expected offshore wind capacity in 2050 sits between 30 GW and 52 GW. For reference, the electricity consumption of the Netherlands has fluctuated around 120 TWh yearly, which equals 33 GW continuous power.
The potential for Airborne Wind Energy Systems (AWES) lies in the opportunity of generating the same amount of power with fewer materials and thus more sustainably. There is limited available surface area for bottomfixed wind turbines. Therefore the opportunity for AWES lies in floating offshore wind since there is a lot of available surface area and there is currently little competition from conventional floating turbines. The Levelised Cost of Energy (LCOE) of the European baseload price is expected to range between 60 and 80 €$/MWh$ in 2050. The LCoE of offshore wind is expected to drop from 200 €$/MWh$ to below 40 €$/MWh$ in 2050. Therefore the aim for floating AWES is to become comparable to the LCoE of offshore wind.

Risk Assessment
A large-scale AWES concept has much that yet needs to be validated, resulting in many uncertainties, especially during the operating life of the system. Therefore, possible risks with their likelihood and severity have been identified. This led to 79 identified risks, including 1 probable catastrophic risk and 54 other unacceptable risks due to high severity and likelihood. Consequently, risk mitigation strategies were implemented to reduce the likelihood or severity of a risk.

Materials
The overall design consists of three main elements: the airborne element, the tether and the seaborne element. Many different materials are analysed in order to appropriately design them. For the airborne element, amongst materials that were explored, aluminium alloys and carbon fibre composite were selected as most promising. Due to its high strength-to-weight ratio, Dyneema was selected as the material for the tether. For the seaborne element, different types of maritime steel were analysed. While most are similar in terms of price and strength, only Q1N-steel is about twice as strong but six times as expensive.
The system will be positioned far offshore where the maritime environment can cause different types of corrosion. An analysis performed on the susceptibility of different materials to corrosion found that there is no significant influence on composites however does affect aluminium and steel. To decrease the susceptibility of these materials to corrosion the airborne element can make use of a coating and the seaborne element can make use of sacrificial metals, where sacrificial metals corrode earlier due to a lower electric potential.

Part 2: Single System Design

Power Generation
The amount of power generated by the farm will depend on the number of systems, the rated power of each system, and the capacity factor. Firstly, based on the rigid wing fly-gen concept, the amount of power that can be extracted from the wind is dependent on the wind speed and bound by the Betz limit of $\frac{16}{27}$. The power relations from Loyd's paper on *Crosswind Kite Power* have been adapted in Trevisi's master's thesis *Configuration Optimisation of Kite-Based Wind Turbines* to include losses due to elevation, side angles and gravity effects. Additionally, the lift and drag coefficients of the airborne element and the drag coefficient of the rotors have an

effect. These formulas have been derived for straight flight and thus do not account for the chosen flight path. The formula was further expanded by introducing a flight path model in the chosen figure eight shape and analysing the power generation over the flight path. Although it provides a lower yield, this path is preferred over a circular flight path as it is safer and less complicated due to the tether not twisting. To calculate the capacity factor, a wind frequency histogram must be used at different wind speeds. For the analysis of the wind in the North Sea, the data of Meteomast Ijmuiden was used.

Sizing of the Airborne element
In order to ensure the airborne element generates the desired power output, the power generation equations can be used to size it. This can be done by changing the wing surface area, the lift and drag coefficient of the airborne element, the drag coefficient of the rotors and the rated wind speed. Firstly the diameter of the rotors will be sized, where a trade-off can be made between the number of rotors and the diameter of each rotor. Then, the wing can be designed by performing a trade-off on the airfoil, the number of wings, the span and the aspect ratio of the wing. The goal is to have a wing structure optimised for power generation while still being able to withstand the loads. Thus an airfoil specialised for rigid AWES was selected. The number of wings was also looked into, where an extra wing causes a decrease in lift coefficient, an increase in total lift, and an increase in parasitic drag. Furthermore, the tether was sized to be able to withstand the maximum amount of load plus a safety factor while transporting electricity to and from the airborne element. Lastly, the tail and tail boom are sized making use of empirical and structural relations.

Airborne Design Code
A code has been scripted to utilise the relations found in an iterative manner. As power is the main criterion, which mainly consists of the drag and lift coefficients, they are found first by choosing an airfoil. The drag of the other components is found by approximating the mass and nominal velocity of the craft. Once these attributes are given, the surface area and nominal velocity are computed based on the power formula. Then the mass and drag coefficients are computed by sizing each subsystem, which gives the option to reiterate with more accurate results. The process is repeated until convergence which takes three to four iterations.

Airborne and Tether Design
The airborne design code led to the final design of the airborne element with the following specifications:

(a) Airborne Element Specifications

Parameter	Value	Unit
Surface area	118	m^2
Wingspan	30	m
Rotor diameter	3.2	m
Mass	2312	kg

(b) Tether Specifications

Parameter	Value	Unit
Length	400	m
Diameter	3.7	cm
Mass	375	kg

Different block diagrams are set up to showcase the hardware and electronics of the design. Where the power source is connected to the control pod, control surfaces, generators and communication subsystem. The generators are connected in pairs of two, and each pair is then connected in series. Causing the voltage through the cable to be equal to four times the voltage of one generator, which decreases the power loss. The power loss of the overall AWES is dependent on the efficiency of the generator, the generator controller, the tether and the step-up converter at the base. This leads to an estimated total efficiency of one system to be 90%. After a definitive site for the AWES farm is decided the transmission losses can be

estimated.

Seaborne Design
The seaborne element, a semi-submersible, is designed to function during all scenarios of operation. It should stay buoyant and stable while the airborne element is positioned in the air or on the floater. A maximum tilt angle is established to be 15 degrees which is a 50% increase compared to conventional floating wind due to having less influence on power generation. This lead to the height of the columns submerged and above the water line, the radius of the columns and the spacing between them. The semi-submersible is moored to the seabed to be kept in place, where the tension of the mooring lines keeps the system in place. One mooring line is sized to be able to carry the load of the waves, the drag of the seaborne element and the tether. To summarise the overall parameters of the seaborne element are:

Table 2: Seaborne parameters

Parameter	Value	Unit
Above water height	30	m
Below water height	3.7	m
Column spacing	44.4	m

Part 3: Farm Design

Farm Design
To make the design more tangible a site, the Hornsea IV, has been selected for the development of the 1 GW farm. The spacing between each system will depend on the different elevation angles, the side angles and the length of the tether during flight. Leading to a spacing of 566 m in the southwest direction and 352 m in the southeast direction.

This spacing will influence the layout of the electrical network which is necessary to supply the electricity to the national grid. Groups of ten to eleven systems will be connected in series and these groups will be connected in parallel to a substation. Each system will have a bypass positioned at the base in case of failure, to minimise downtime of the group. Inside the substation, the 40 $kVDC$ of the group of systems will be transformed to 220 $kVDC$ to transport to shore. This configuration can in the future be optimised to minimise power losses and costs.

One of the main benefits of AWESs over conventional wind turbines is the decrease in the amount of mass necessary. The mass of a 1 GW scale farm of AWES is estimated to be around 40 % of a conventional floating wind turbine farm.

Operations & Logistics
The operational expenses or OpEx of conventional wind turbines contribute to about 30% of the lifetime cost of the project. A trade-off can be made between OpEx and the availability of the AWES, which should be optimised for the lowest LCoE. The transportation and installation of the AWES farm consist of different trade-offs regarding time and money spent. The AWESs can be assembled in the port and transported to the farm location removing the need for costly floating cranes. Different tug and supply vessels can be used to transport the AWESs to the farm location. The faster vessels are more expensive but have less of a chance of delays due to unforeseen weather conditions. The installation phase is started off by cable-laying vessels placing the electrical cables on the seabed and connecting the end to floaters at the position of an AWES and the substations. Then using Anchor Handling Tug and Supply vessels (AHTSs) each AWES will be anchored into place by three chains. Lastly, the floating ends will be connected to the AWES.

While operating the AWES farm maintenance and repair will need to be performed on a predetermined schedule and when a condition is met. Conditions can vary from a failure or anomaly to a weather condition. Once more data is known on the rate and cause of failures of different parts the maintenance schedule can be optimised to be preventive. The maintenance will mostly occur at low wind speeds and low wave heights for safety and cost reasons.
There exist three options for the end-of-life of the AWES: decommissioning, life-extension or re-empowerment. For decommissioning of the AWES farm, all components must be removed by ship, disassembled in the port and recycled. If the OpEx stays below the proceeds of the generated power, the life of the farm could be extended by a few years. It might make sense to re-empower the farm by replacing old elements with newer and more efficient elements. A decision can be made to overdesign the seaborne element and the electricity network to account for this possibility.

The availability of the system is highly dependent on the failure rate and the time to repair an AWES. It is required that the AWES farm is 95% available. The wind speed is expected to be below the cutout speed for 2.5% of the time. As the airborne elements are all stationed at the base this time will be fully used for maintenance. The share of unexpected failures is currently expected to be in the order of 1 %. This leads to the fact that 6.5% of the farm may be unavailable at one time. For safety reasons, the surrounding groups will be stopped to keep the maintenance crew safe.

For a floating offshore AWES farm to be feasible the system must be fully autonomous. The farm should measure data, perform system checks, forecast weather conditions and communicate this to each AWES. An individual system should be able to autonomously launch, generate power, land and deal with catastrophic risks.

Project Finances
One of the most important parts of an energy-generating system is its LCoE. The LCoE is set up breaking down the cost into the Capital Expense (CapEx), the Operating Expense (OpEx) and the Decommissioning Cost (Decex). The LCoE is set up by adapting the cost breakdown of floating wind turbine per MW to the AWES design. Regarding the CapEx of the project, the conventional turbine is replaced by an airborne element, the seaborne element is scaled and the electrical system is larger. The cost of the airborne element is modelled by a top-down and a bottom-up approach, which both make use of a scaling law for more systems. The seaborne element will have a smaller mass due to lower forces acting on the system, thus decreasing the cost. The AWES farm will have more systems, but less space between each system, causing an increase in the number of cables. The OpEx will depend largely on the maintenance and operating cost. It is expected that the frequency of maintenance trips to the AWES farm will increase with respect to floating wind farms, however, this will be counteracted due to the decrease in cost of smaller ships being needed.

Table 3: Simplified Cost Breakdown per MW

Expense	HAWT	HAWT ES	RW FG pessimistic	RW FG optimistic
CapEx	€ 4,380,000	€ 3,750,000	€ 3,590,000	€ 2,390,000
OpEx per year	*€ 80,480*	*€ 70,600*	*€ 71,100*	*€ 67,660*
DecEx	€ 162,450	€ 138,000	€ 83,780	€ 0

Using the Cost breakdown the LCoE can be computed by dividing the sum of the Net Present Value (NPV) of the expenses each year by the NPV of the power generation each year. The power produced depends on the rated power the capacity factor and the availability. The rated power of 1 MW will not always be reached when in flight due to wind speed, flight path

or availability. The yearly output is expected to be 8,760 GWh with a capacity factor of 63% and availability of 95%, leading to a total output of 5,243 GWh. Depending on the case this leads to an LCoE of 49.5 to 69.0 €$/MWh$ at a discount rate of 5%.

To calculate the Return on Investment, the revenue of the farm will be divided by the total cost of the farm. This is highly dependent on the electricity price per MWh and the costs of the farm. The ROI will range from -13% to +265%.

Sustainable Development Strategy
In the first part, the sustainability aspects of the project are addressed, including environmental, social, and economic sustainability. In each aspect, mitigation plans are also included. The environmental mitigation plans focus on material recyclability, minimising the impact on marine wildlife, and discussing the potential threats/ opportunities to avian wildlife. The social aspects involve supporting the climate-neutral goal of the EU, contributing to local energy security, reducing noise and air pollution, and creating job opportunities. From an economic perspective, the longevity and repairability of the system are emphasised, along with market potential, resource depletion levels, the possibility of renewable energy grants and subsidies, optimising costs through technological advancements, and the importance of designing an onsite maintenance lot. These measures aim to ensure a sustainable and successful implementation of the Deep WattAir project.

The second part of the sustainable development strategy presents a Life Cycle Analysis (LCA) of a project, focusing on the five main phases of a product's life cycle: material extraction, manufacturing, transportation, operations, and end of life. CO_2 emissions and embodied energy are used as metrics, with a preference for Global Warming Potential. The CO_2 emissions per kilogram of various materials are estimated, and conservative values are chosen for materials with unavailable data. The LCA results show that the manufacturing phase contributes the most emissions, followed by raw material extraction. Overall, the project emits nearly 3 million metric tonnes of CO_2 over its 20-year operation. To mitigate these emissions, proposed actions include local sourcing, transparency in the supply chain, sustainable procurement, resource efficiency, promoting the 3R principles (Reduce, Reuse, Recycle), adopting cleaner production technologies, waste management strategies, implementing renewable energy sources for maritime vessels, and repurposing the seaborne element for floating offshore wind turbines.

Verification & Validation
To ensure that the design is able to fulfil the set requirements a compliance matrix is set up. Where compliance regarding the user requirements is checked. The design is compliant or intends to comply with most requirements, except for the LCoE requirement of 50 €$/MWh$. By changing certain parameters the sensitivity of the design to these parameters can be checked. For instance, by changing the discount rate to 1.02 the LCoE will become 48.5 $\pm$ 7.5 €$/MWh$. Therefore compliance with respect to the LCoE is incredibly sensitive to a change in the discount rate.
Validating newer concepts can be rather difficult, therefore a system validation plan is set up. Where the different parts of the system are validated independently after which the total design is validated.
Firstly the aerodynamics of the airborne element must be validated using computational fluid dynamics model and wind tunnel testing, to validate the lift and drag calculations. Secondly, the structural components of the airborne element will be validated using Finite Element Methods and physical tests. Then, stability and autonomous launch and landing capabilities will be validated. Furthermore, the tether tensile strength, strain and lifetime will be validated using stress, resistivity and cyclic testing. The stability and lifetime of the seaborne element will be validated using a scale model. Before going offshore the airborne element and the tether-winch assembly will be tested onshore. Lastly, the full-scale system will be tested offshore.

Part 4: The Next Steps

Project Design & Development

A high-level design and development plan is discussed. This plan is used to gain insight into the required time from the current state of the design up to a fully operational farm. This starts by hiring personnel after which the current design is further detailed. With this more detailed design, an aerodynamic and structural analysis will be performed to get a better estimate of the power generation. When these analyses are completed, a prototype will be made which will then be tested from component level up to complete system level. This will then give the data required for the verification and validation of the design. When the system is validated, the systems will be integrated into a farm layout after which the final design is documented.

Additionally, a high-level production plan was written. To produce a large-scale wind farm, you start by producing the required parts. There are many different parts, each of which requires a different manufacturing technique. The parts will be produced in batches. When the parts are available, sub-assemblies using these parts will be produced. These sub-assemblies are then integrated into the subsystem, being the airborne element or the seaborne element. These subsystems will be integrated into the port, where the complete system will be constructed out of the seaborne element, airborne element and tether. When a full system is completed, it will be towed towards the site location where it will be connected to the grid and start operation.

Discussion and Recommendations

In the discussion, the team presents the limitations of the analyses performed. Furthermore, recommendations are given on future research topics and the feasibility of an offshore airborne wind farm as a concept. Limitations of the analyses include the inaccuracy of the mass estimation, assuming constant aerodynamic properties over the flight path and limited validation data. Additionally, limited research on the control and stability of the airborne element and its ability to steer along a flight path of the figure eight is also included. Recommended further research includes: improving upon the limitations of the analyses within this project, investigating tether wear in saline conditions, optimising power fluctuation reduction, investigating the effect of AWES farms on birds and other wildlife, determining floater stability requirements for launch and landing, performing continuous operation test to determine reliability and safety, performing detailed aerodynamic analyses on multi-element lifting wing concepts and performing a more thorough analysis on the stability of the airborne element. Finally, the team believes that, while there are tangible improvements compared to conventional wind, airborne wind farms are much more complex. For this reason, the technology should first be developed onshore, since the offshore environment introduces even more complexity. Once the airborne wind has been commercially proven, projects for offshore airborne wind farms will have a higher chance of attracting investors. However, it is important to continue the development of the offshore aspects of airborne wind energy, since it shows the potential of being cost-competitive with conventional wind energy while promising a higher capacity factor and less material usage.

Conclusion

The team has achieved the goals outlined in the mission need statement, showing the feasibility of a gigawatt-scale wind farm using airborne wind technology. However, it remains uncertain if airborne wind energy is better than conventional turbines. The airborne wind energy system has an advantage in the decrease in required material. However, a major drawback is the limited scale of a single system, which the team has not fully solved. The complexity of a fly-gen system can lead to complete failure with a single component issue, and uncertainties exist in launching and landing on a dynamic platform. Therefore, the team believes that much more testing and development is needed for a 1 MW scale single system before the focus should shift towards an offshore wind farm.

Contents

List of Figures

List of Tables

Nomenclature

Abbreviation	Definition
AC	Alternating Current
AHTS	Anchor Handling Tug and Supply vessel
AoA	Angle of Attack
AWE	Airborne Wind Energy
AWES	Airborne Wind Energy System
CapEx	Capital Expences
CAN	Control Area Network
CCUS	Carbon Capture, Utilisation and Storage
CFD	Computational Fluid Dynamics
CFRP	Carbon Fiber-Reinforced Plastic
CPU	Central processing unit
DC	Direct Current
DecEx	Decomission Expences
DOT	Design Option Tree
DSRC	Dedicated short-range communication
DSE	Design Synthesis Exercise
EOL	End of Life
ERFF	ensemble random forest filter
FBS	Function Breakdown Structure
FEM	Finite Element Methods
FFD	Functional Flow Diagram
FMS	Failure Management System
GPS	Global Positioning System
HAWT	Horizontal Axis Wind Turbine
HV	High Voltage
IMU	Inertial measurement unit
LCoE	Levelised Cost of Energy
LCA	Life Cycle Analysis
LIN	Local interconnect network
LV	Low Voltage
M/G	Motor/Generator
MBL	Minimum Break Load
MPC	Model Predictive Controller
MV	Medium Voltage
N.A.	Neutral Axis
NZE	Net Zero Energy
O&G	Oil and Gas
OpEx	Operational Expences
PEEK	Poly-Ether-Ether-Ketone
PID	Proportional integral derivative
PLC	Programmable Logic Controller
PPS	Poly-Phenil-Sulfide
PV	Photo Voltaic
RAMS	Reliability, Availability, Maintainability, Safety
R&D	Research and Development
RDT	Requirement Discovery Tree
ROI	Return On Investment
RPM	Revolutions Per Minute
RTK	Real time kinematic
RW	Ridged Wing
SPL	Sound Pressure Level
SW	Soft Wing
SWOT	Strength, Weakness, Opportunity, Threat
TLP	Tension Leg Platform
T&I	Transport and Installation
UAV	Unmanned Arial Vehicle
VTOL	Vertical Take-Off and Landing
V&V	Verification and Validation
V2X	Vehicle to everything
V2I	Vehicle to interface
V2V	Vehicle to vehicle
W2W	Walk to Work
WBS	Work Breakdown Structure
WFD	Work Flow Diagram

1 Introduction

The world is currently facing an immense challenge: climate change caused by green house gasses from fossil fuel emissions. To address this issue, a worldwide push is underway to transition to renewable energy sources. One of the fastest-growing renewable energy sources is wind energy. Offshore wind energy in particular has much potential because of the higher and more constant winds they can access. Moreover, offshore wind turbines have a less disruptive effect on the public making them preferable. Though there is an abundance of space offshore, there are limited shallow areas suitable for bottom-fixed wind turbines. For this reason, floating wind power is emerging to make deep water areas accessible.

With the emergence of the floating wind energy market lies an opportunity. Instead of placing large, top-heavy wind turbines onto floating bases, a different type of wind energy system can be used. Airborne wind energy systems are systems that can generate power by using flying elements. With these systems, there is no need for a heavy tower making them much lighter than conventional turbines. Furthermore, the components that are not airborne can be much closer to sea level. These features combined have the potential to reduce the size of the floater, leading to further weight savings. This means that a lot less materials will be needed compared to conventional wind farms.

This opportunity has led to the following mission need statement:
"Provide a cost-competitive way to harvest wind energy in deep water with a more sustainable alternative to conventional wind turbines." [1]

How this problem will be solved is formulated in the project objective:
"To design a floating large-scale wind farm in deep water using an Airborne Wind Energy System that is cost-competitive, largely recyclable and uses less material than conventional wind turbines, with ten students in ten weeks." [1]

This is the final of four reports, documenting the design process to reach the project objective. It builds upon the work of the previous reports ([1]–[3]) and establishes an initial design tool for a rigid wing fly-gen airborne wind energy system. Furthermore, this report shows the first iteration of the design of the floating airborne wind farm.

This report is separated into four parts. First, part 1 will consist of chapters summarising and building on the content of the previous reports. First, chapter 2 provides a summary of the trade-off performed in the midterm report [3]. Next, chapter 3 shows the functional flow and breakdown diagrams containing an overview of the flow of tasks performed during the project. Then, chapter 4 contains a market analysis, in which the market opportunities for the airborne wind farm are investigated. Next, chapter 5 shows the expected risks and the mitigation steps to reduce these risks. Lastly, the material options and characteristics are presented in chapter 6.

Part 2 then discusses the single airborne wind energy system design process. First, the power estimation relations are discussed in chapter 7. Next, chapter 8 explains the design process and the subsystem relations. After this, chapter 9 explains the sizing tool that has been developed for the design process. Then, chapter 10 shows the single system design generated with this tool which meets the requirements set by the user. Chapter 11 then explains the electronic components and layout for this design. Lastly, chapter 12 discusses the design process and results for the seaborne element, which consists of the floater, base and mooring.

Part 3 describes the wind farm design, where the farm consists of the airborne wind energy systems designed in the previous part. Chapter 13 investigates the farm design for a chosen exemplary farm site. Then, chapter 14 discusses the logistics and operations of the floating airborne wind farm and compares these to conventional wind farms. Next, in chapter 15 an estimation of the levelised cost of energy and return on investment is calculated for the farm. Chapter 16 contains the sustainable development plan of the farm as well as a life cycle analysis. Lastly, chapter 17 discusses the compliance with the user requirements, as well as the verification and validation of the final farm design.

Lastly, part 4 presents the concluding chapters of the report. Chapter 18 will discuss the steps needed after the preliminary design phase to achieve the goal of a functioning airborne wind farm. Next, chapter 19 will present the discussion and recommendations of the team. Finally, chapter 20 contains the conclusion.

Part 1

Project Foundation

In this part the foundation of the project is presented. A trade-off summary highlighting the reasons for the chosen design is covered. It also includes logic diagrams showcasing different steps that will be taken during the design, operational, and post operational phases. A market analysis is conducted to analyse the place that floating Airborne Wind Energy (AWE) will take in the energy market, along with a risk assessment highlighting different technical risks. Lastly, different possible materials are analysed.

2 Trade-off Summary

This chapter will summarise the results of the trade-off performed in the midterm report. In the baseline report, multiple concepts were thought up for both the airborne and seaborne elements, collected in the Design Option Tree (DOT). A shortened version of the DOT is shown in figure 2.1, which shows the concepts for which the trade-off was performed.

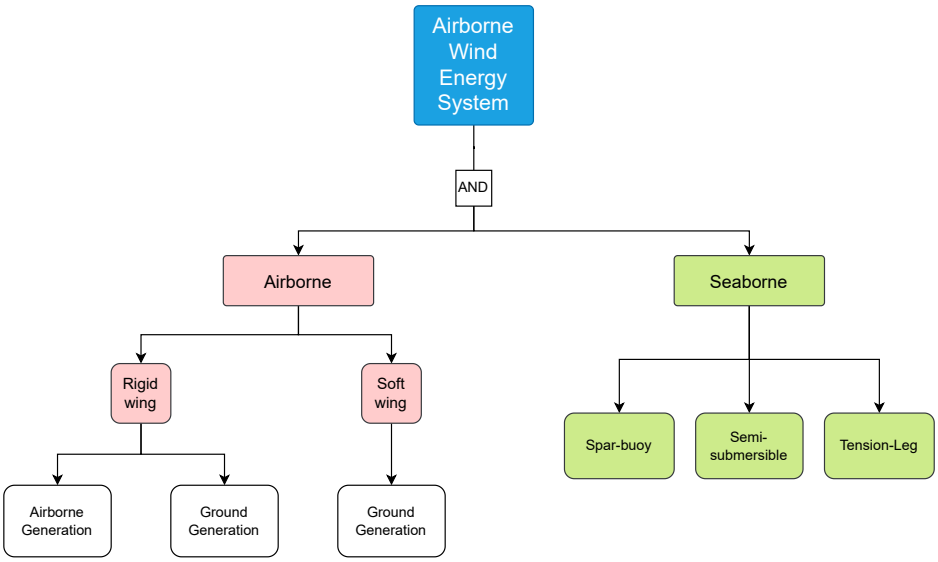

Figure 2.1: Design Option Tree with the trade-off concepts.

As shown in the figure, the concepts considered for the airborne element are rigid wing airborne generation (fly-gen), rigid wing ground generation (ground-gen), and soft wing ground generation. Before starting the trade-off, six criteria were decided upon by the team, and weights were assigned to them based on their importance according to the team. The criteria and their weights are shown in table 2.1.

Table 2.1: Airborne trade-off criteria and their weights [3].

Criterion	Cost	Reliability	Mass	Operability	Sustainability	Development Effort
Weight	5	5	4	4	3	2

Along with the airborne element, there is also a seaborne element. The team had decided that the focus of the project would be on the airborne element and that the seaborne element would be a scaled version of an existing concept. From the literature study, it was shown that three concepts are currently used for floater design, those being a spar buoy, a semi-submersible, and a tension-leg platform. These three concepts were also scored on six criteria decided upon by the team. These criteria and their weights are shown in table 2.2.

Table 2.2: Seaborne trade-off criteria and their weights [3].

Criterion	Mass	Production Cost	Lifetime	Stability	Transportation	Installation
Weight	4	3	3	2	2	2

From these trade-offs, the final concept that emerged for the airborne element was the rigid wing fly-gen. The soft wing concept was discarded due to the immense size needed for it to generate significant amounts of power, which would also cause problems in terms of controlling it, as well as the expected maintenance trips required and the low ability for recycling. The rigid wing fly-gen won out over the ground gen due to the fact that it is easier to land and launch due to the vertical take-off and landing (VTOL) capabilities, as well as the reduced tether wear, which introduces less micro-plastics in the surrounding environment.

The winning concept for the seaborne trade-off was the semi-submersible platform. The tension-leg platform was ruled out because of the possibility of fatigue failure of the mooring lines. The semi-submersible was selected over the spar buoy due to the easier installation and transportation processes. The mooring was chosen to be catenary mooring, due to its simplicity and low cost for installation.

To reduce the possibility that the trade-off results were biased, a sensitivity analysis was also performed. The sensitivity analysis changed some criteria weights and scores to see how that influenced the outcome of the trade-off. A code was written to iterate this process. The results of this analysis are shown in table 2.3.

Table 2.3: An overview of the results of the sensitivity analyses [3]

Airborne		**Seaborne**	
Concept	Win percentage [%]	Concept	Win percentage [%]
Soft wing	0.8	Spar buoy	1.2
Rigid wing ground-gen	17.4	Semi-submersible	71.5
Rigid wing fly-gen	76.8	tension-leg platform	6.2
Tie	4.9	Tie	10.1

These results show that the rigid wing fly-gen combined with the semi-submersible floater is indeed the appropriate choice of concept to explore the 1 GW offshore wind farm.

Considerations

It is important to consider the interactions between the floating and airborne elements selected. Two main interactions have been identified. Firstly, the tether connects both elements. If the seaborne platform moves because of waves, the tension in the tether changes. This affects the dynamics of the airborne element. Next to this, the tether will pull on the seaborne element, causing pitching and displacement of the seaborne element as well as loads on the mooring system. This load on the seaborne element must be taken into account during the design. Additionally, the airborne element flight control must be able to compensate for changes in tether tension.

Next, the fact that the airborne element must be able perform take-off and landing on the floating base must be considered. The platform should be stable enough for the airborne element to land. The launch and landing method chosen is a VTOL method, which is expected to require a high degree of stability. Even though it was found that the semi-submersible is more susceptible to wave-induced motion, it is still preferred because it is less dependent on water depth and sea bottom conditions and because it is easier to transport and install. This does mean that, during the detailed design of the seaborne element, this implication must be designed for. This could be done through the floater design. The floater should be designed to reduce wave-induced motion. This however will increase design complexity and cost. Another option is to design a landing point that is actively stabilised with respect to the floating platform. This however would introduce more complexity and maintenance to the system.

3
Logic Diagrams

The logic diagrams are revised from the baseline report [2]. After having revised the final concept, many additions have been made to the functional flow diagram (FFD) (section 3.1) and the functional breakdown structure (FBS) (section 3.2).

3.1. Functional Flow Diagram

To understand the functionality of each design step in each phase, a functional flow diagram (FFD) was made. The diagram showcases possible iterations and junctions found during the different phases. The five phases focused on are the design, production, deployment operation, and EoL phase.

3.2. Functional Breakdown Structure

Following from the FFD, a functional breakdown structure (FBS) is derived. This delves into the functionalities and creates tasks for each block for all the five aforementioned phases. This diagram helps to establish work packages while using the same labelling convention as the FFD.

FUNCTIONAL FLOW DIAGRAM

Arrows: Indicate flow
No Arrows: Indicate parallel tasks

Phase 1.0 | Phase 2.0 | Phase 3.0 | Phase 4.0 | Phase 5.0

1 - Design AWES

1.1: Follow Project Timeline
- 1.1.1 Follow Project Plan
- 1.1.2 Perform, Implement and Submit all Review Milestones

1.2: Implement Feedback
- 1.2.1 Receive Feedback from TAs and Tutors
- 1.2.2 Implement Feedback

1.3: Establish Design Parameters
- 1.3.1 Produce Technical Drawings and BoM
- 1.3.2 Estimate Weight of Complete System
- 1.3.3 Calculate Engineering Performance Parameters
- 1.3.5 Establish Farm Location
- 1.3.4 Calculate Material and Structural Parameters

1.4: Configure the Farm
- 1.4.1 Design Preliminary Farm Configuration
- 1.4.2 Optimize Configuration for Power Production

2 - Produce AWES

2.1: Prepare for the production
- 2.1.1 Apply for Grants and Find Investors
- 2.1.2 Market the System
- 2.1.3 Hire Required Personnel

2.2: Create Prototype
- 2.2.1 Create Airborne Prototype
- 2.2.2 Create Seaborne Prototype
- 2.2.3 Create Full AWES prototype

2.3: Perform tests
- 2.3.1 Perform Component Tests
- 2.3.2 Perform Integration Tests
- 2.3.3 Perform Subsystem Tests

2.4: Decide Production Process
- 2.4.1 Decide Production Method or Outsourcing Entity
- 2.4.2 Establish Production Facility Location, Layout, and Storage

2.5: Source Materials
- 2.5.1 Ensure Material Source Sustainability
- 2.5.2 Ensure Material Sourcing Budget

2 - Produce AWES

2.6: Provide Adequate Infrastructure
- 2.6.1 Source Correct Machines, Tools, Labour
- 2.6.2 Ensure Purchases are within the Budget

2.7: Produce Parts
- 2.7.1 Initiate Proper Production Sequence
- 2.7.2 Carry out Appropriate Quality and Management Checks
- 2.7.3 Replace Tools and Machinery when Needed
- 2.7.4 Check Stock, Storage Spaces and Update Manufacturing Process

2.8: Assemble Systems
- 2.8.1 Assemble Airborne Elements
- 2.8.2 Configure Part for Assembly
- 2.8.3 Replace Tools and Machinery when needed

2.9: Test System on Land
- 2.9.1 Perform Complete System Tests
- 2.9.2 Iterate Design

2.9.2 → 1.0

3.1: Check Weather for Transport
- 3.1.1 Inspect Weather and Wave Projection
- 3.2.1 Model Success likelihood

3 - Deploy AWES

3.2: Ship Elements to Location
- 3.2.1 Ensure all Needed Parts are Onboard and Secured
- 3.2.2 Confirm Safe Passage of Elements

3.3: Place Seaborne Elements
- 3.3.1 Attach Floating Base to Seabed
- 3.3.2 Ensure Following of Safety Procedures for Personnel

3.4: Attach Airborne Elements
- 3.4.1 Attach Airborne Element to Seaborne Element
- 3.3.2 Guarantee the Following of Safety Procedures

3.5: Test the System
- 3.5.1 Initiate Power Generation Sequence
- 3.5.2 Run Appropriate Tests on all Components
- 3.5.4 Implement Farm Configuration
- 3.5.3 Implement Design or Production Iterations if Needed

3.5.3 → 1.0 OR 2.0

4 - Operate AWES Farm

4.1: Check Measurements
- 4.1.1 Measure Wind Speed
- 4.1.2 Measure Wind Direction
- 4.1.3 Measurement of Wave Intensity
- 4.1.4 Model Environment of the farm
- 4.1.5 Analyse weather

Go / No Go

4.2: Launch Airborne Systems
- 4.2.1 Initialize Subsystem
- 4.2.2 Launch System
- 4.2.3 Reel Out to Desired Altitude

Communicate failure to operations team

4.3: Control Airborne Systems
- 4.3.1 Control Altitude
- 4.3.2 Control Stability
- 4.3.3 Control Trajectory

4.4: Collect Data
- 4.4.1 Retrieve Position Data
- 4.4.2 Retrieve On-Board Measurements
- 4.4.3 Retrieve Energy Output

4.5: Initiating Generation Phase
- 4.5.1 Initiate flight path

4.6: Generating electricity
- 4.6.1 Generate electricity
- 4.6.2 Control the AWES

5 - End of Life AWES Farm

4.7: Collect data
- 4.7.1 Retrieve position data
- 4.7.2 Retrieve on-board measurements
- 4.7.3 Retrieve energy output
- 4.7.4 Retrieve general telemetry

4.8: Monitor performance
- 4.8.1 Analyse performance degradation
- 4.8.2 Comparing output to initial power rating

4.9: Land Airborne Systems
- 4.9.1 Initialize landing sequence
- 4.9.2 Reel in
- 4.9.3 Attach Airborne Element to base

5.1: Asses End of Life Possibilities
- 5.1.1 Perform EoL study

5.2: Life extension of system
- 5.2.1 Airborne element
- 5.2.2 Seaborne element

5.3: Repower System
- 5.3.1 Research for repowering
- 5.3.3 Seaborne element
- 5.3.2 Airborne element

5.4: Decommission System
- 5.4.1 Airborne element
- 5.4.2 Seaborne element

FUNCTIONAL BREAKDOWN STRUCTURE

1.0 Design AWES

1.1 Follow Project Timeline

1.1.1 Follow Project Plan
- **1.1.1.1:** Assemble all deliverables and key concept reporting
- **1.1.1.2:** Keep track of team progress, roles and decisions

1.1.2 Perform, Implement and Submit all Review Milestones
- **1.1.2.1:** Set internal deadlines
- **1.1.2.2:** Meet internal deadlines
- **1.1.2.3:** Meet external deadlines
- **1.1.2.4:** Communicate intermediate results with users/tutors
- **1.1.2.5:** Present all report reviews

1.2 Implement Feedback from Entities

1.2.1 Receive Feedback from TAs and Tutors
- **1.2.1.1**: Process all feedback
- **1.2.1.2**: Understand user needs and focus points

1.2.2 Carry out Iterations if Needed

1.3 Establish Design Parameters

1.3.1 Produce Technical Drawings and BoM
- **1.3.1.1:** Assemble all components
- **1.3.1.2:** Construct BoM
- **1.3.1.3:** Create technical drawings
- **1.3.1.4:** Create renderings

1.3.2 Estimate Weight of Complete System
- **1.3.2.1:** Create preliminary mass and sizing estimate
- **1.3.2.2:** Establish detailed mass estimates per component
- **1.3.2.3:** Establish mass estimates per subsystem of all elements
- **1.3.2.4:** Iterate and update mass estimates

1.3.3 Calculate Engineering Performance Parameters
- **1.3.3.1:** Establish aerodynamic and stability parameters of all elements
- **1.3.3.2:** Calculate capacity factor
- **1.3.3.3:** Quantify cut in/cut out speed
- **1.3.3.4:** Construct farm layout

1.3.4 Calculate Material and Structural Parameters
- **1.3.4.1:** Size all elements
- **1.3.4.2:** Select suitable materials for main structures

1.3.5 Establish Farm Location
- **1.3.5.1:** Identify available area for farm
- **1.3.5.2:** Compute individual system power requirement

1.4 Configure the Farm

1.4.1 Design Preliminary Farm Configuration
- **1.4.1.1:** Analyse the main wind direction
- **1.4.1.2:** Choose the preliminary configuration

1.4.3 Optimize Configuration for Power Production
- **1.4.2.1:** Calculate the preliminary power yield
- **1.4.1.2:** Calculate the theoretical maximum yield
- **1.4.2.3:** Optimise the farm lay-out for maximum yield

2.0 Produce AWES*

2.1 Prepare for the Production

2.1.1 Apply for Grants and Find Investors

2.1.2 Market the System

2.1.3 Hire Required Personnel

2.2 Create Prototype

2.2.1 Create Airborne Prototype

2.2.2 Create Seaborne Prototype

2.2.3 Create Full AWES prototype

2.3 Perform Tests

2.3.1 Perform Component Tests

2.3.2 Perform Integration Tests

2.3.3 Perform Subsystem Tests

2.4 Decide Production Process

2.4.1 Decide Production Method or Outsourcing Entity

2.4.2 Establish Production Facility Location, Layout, and Storage

2.5: Source Material

2.5.2 Ensure Material Sourcing Budget

2.5.1 Ensure Material Source Sustainability

2.6 Provide Adequate Infrastructure

2.6.1 Source Correct Machines, Tools, Labour

2.6.2 Ensure Purchases are within the Budget

2.7 Produce Parts

2.7.1 Initiate Proper Production Sequence

2.7.2 Carry out Appropriate Quality and Management Checks

2.7.3 Replace Tools and Machinery when Needed

2.7.4 Check Stock, Storage Spaces and Update Manufacturing Process

2.8 Assemble Systems

2.8.1 Assemble Airborne Elements

2.8.2 Configure Part for Assembly

2.8.3 Replace Tools and Machinery when needed

2.9 Test System on Land

2.9.1 Perform Complete System Tests

2.9.2 Iterate Design

*** EXPANDED UPON IN PROJECT D&D AND PRODUCTION PLAN**

3.0 Deploy AWES

3.1 Check Weather for Transport

3.1.1 Inspect Weather and Wave Projection
- **3.1.1.1:** Collect weather data and projections
- **3.1.1.2:** Collect wave data and projections

3.1.1 Model Success likelihood

3.2 Ship Elements to Base

3.2.1 Ensure all Parts are Onboard and Secured
- **3.2.1.1:** Ensure parts (semi- and assembled) are onboard
- **3.2.1.2:** Ensure extra components and tools are onboard
- **3.2.1.3:** Ensure all parts onboard are secured appropriately

3.2.2 Post Transportation, Confirm Safe Passage of Elements
- **3.2.2.1:** Perform component and inventory check
- **3.2.2.2:** Mitigate damages and repair of broken components

3.3 Place Seaborne Elements

3.3.1 Procedure to Attach Floating Base to Seabed
- **3.3.1.1:** Deploy floating base
- **3.3.1.2:** Deploy anchoring procedure

3.3.2 Guarantee Safety Procedures for Personnel
- **3.3.2.1:** Ensure personnel training
- **3.3.2.2:** Establish safety protocols and use safety equipment

3.4 Attach Airborne Elements

3.4.1 Attach Airborne to Seaborne Element
- **3.4.1.1:** Initiate assembly procedures
- **3.4.1.2:** Secure all tether attachment points
- **3.4.1.3:** Secure VTOL attachment points

3.5 Test the System

3.5.1 Initiate Power Generation Sequence
- **3.5.1.1:** Initiate Operate Phase (4.0) for one AWES system
- **3.5.1.2:** Measure performance data and yields of system

3.5.2 Run Appropriate Tests on all Components
- **3.5.2.1:** Analyse performance and power yields
- **3.5.2.2:** Carry out individual component tests
- **3.5.2.3:** Mitigate failures if any

3.5.3 Implement Design or Production Iterations if Needed
- **3.5.3.1:** If catastrophic failures occur, initiate Design Phase 1.0

3.5.4 Implement Farm Configuration
- **3.5.4.1:** If 3.5 successful, initiate 3.3 for multiple systems
- **3.5.4.2:** Construct chosen farm configuration
- **3.5.4.3:** Mitigate failures if any

4.0 Operate AWES

4.1 Check Measurements

4.1.1 Measure Wind Speed
- **4.1.1.1:** Anemometer Measurements
- **4.1.1.2:** Lidar Measurements
- **4.1.1.3:** Pitot Tube Measurements

4.1.2 Measure Wind Direction
- **4.1.2.1:** Wind Vane Measurements

4.1.3 Measurement of Wave Intensity
- **4.1.3.1:** Wavemeter measurements

4.1.4 Model Environment
- **4.1.4.1:** Input variables
- **4.1.4.2:** Output Optimal Launch
- **4.1.4.3:** Output Optimal Flightpath
- **4.1.4.4:** Perform radar measurements for foreign objects (Birds, helicopters, ...).
- **4.1.4.5** :Communicate with neighbouring AWES units

4.1.5 Analyse weather
- **4.1.5.1:** Perform measurement (pressure, humidity, wind velocity, temperature)
- **4.1.5.2:** Perform radar measurements

4.2 Launch Airborne System

4.2.1 Initialize Subsystem
- **4.2.1.1:** Check Airborne unit Health
- **4.2.1.2:** Check Tether Health
- **4.2.1.3:** Check Launching Subsystem

4.2.2 Launch System
- **4.2.2.1:** Point Launch System
- **4.2.2.2:** Perform Launch

4.2.3 Reel Out to Defined Altitude
- **4.2.3.1:** Initiate reel out process
- **4.2.3.2:** Ensure reel out rate in accordance to airborne element climb

4.3 Control Airborne System

4.3.1 Control Altitude
- **4.3.1.1:** Control tether length
- **4.3.1.2:** Initiate reel in/out at given rate when needed
- **4.3.1.3:** Maintain contingency sequence for altitude loss
- **4.3.1.4:** Implement contingency sequence
- **4.3.1.5:** Control altitude based on neighbouring units

4.3.2 Control Stability
- **4.3.2.1:** Actuate control surfaces during VTOL and transition
- **4.3.2.2:** Maintain contingency sequence altitude loss
- **4.3.2.3:** Implement contingency sequence

4.3.3 Control Trajectory
- **4.3.3.1:** Predictive path planning to predict actuator activity
- **4.3.1.3:** Maintain contingency sequence for trajectory deviations
- **4.3.1.4:** Implement contingency sequence
- **4.3.3.4:** Control trajectory based on neighbouring units

4.4 No Energy Generation

4.4.1 Park Airborne Element
- **4.4.1.1:** Perform parking procedure when velocity is outside operational window

4.4.2 Reel-in
- **4.4.2.1:** Asses operational condition
- **4.4.2.2:** Perform real-in procedure (if operation is not possible due to damage or dangerous flight environment/ conditions)

4.5 Initiating generation phase

4.5.1 Initiate Flight path
- **4.5.1.1:** Perform manoeuvre to target path
- **4.5.1.2:** Switch motors from propulsion mode to generation mode

4.6 Generating electricity

4.6.1 Generate electricity
- **4.5.6.1:** Start generating electricity along flight path
- **4.5.6.2:** Transport energy trough the tether to seaborne unit
- **4.5.6.3:** Transport, transform, moderate and regulate energy flow to the national grid

4.6.2 Control the AWES
- **4.6.2.1:** Dynamically adapt the tether to fly along the flight path

4.7 Collect Data

4.7.1 Retrieve Position Data
- **4.7.1.1:** GPS Positional Data

4.7.2 Retrieve On-Board Measurements
- **4.7.2.1:** Retrieve Dynamic Pressure
- **4.7.2.2:** Retrieve Directional Data

4.7.3 Retrieve Energy Output
- **4.7.3.1:** Retrieve energy generation data

4.7.4 Retrieve General Telemetry
- **4.7.4.1:** Retrieve performance levels of airborne element components (power usage/ generation, ...)
- **4.7.4.2:** Retrieve flown flight path
- **4.7.4.3:** Retrieve component failures if applicable

4.8 Monitor Performance

4.8.1 Analyse performance degradation
- **4.8.1.1:** Monitor Energy Output

4.8.2 Compare output to initial power rating
- **4.8.2.1:** Energy Output vs. Theoretical Energy Output

4.9 Land Airborne Systems

4.9.1 Initialize landing sequence
- **4.9.1.1:** Acquire desired POSE and velocity for landing

4.9.2 Reel in
- **4.9.2.1:** Activate reel in at given rate

4.9.3 Attach airborne element to base
- **4.9.3.1:** Perform VTOL attachment procedure

5.0 End of Life (EoL)

5.1 Asses EoL Possibilities

5.1.1 Perform EoL study
- **5.1.1.1:** Perform checks of all elements
- **5.1.1.2:** Validate state of main subsystems
- **5.1.1.3:** Assess EOL options of the farm
- 5.1.1.4: Decide on EOL procedure (Life extension, repower, decomission)

5.2 Life Extension of System

5.3.1 Airborne element
- **5.3.1.1:** Continue operation of the airborne element

5.3.2 Seaborne element
- **5.3.2.1:** Continue operation of the seaborne element

5.3 Repower System

5.3.1 Research for repowering
- **5.3.1.1:** Assess current state of the art and market development
- **5.3.1.2:** Establish components needed for upgrades
- **5.3.1.3:** Market research on best component prices and/or manufacturing processes
- **5.3.1.4:** If needed, resell AWES concept

5.3.2 Airborne element
- **5.3.2.1:** Refurbish/upgrade airborne element
- **5.3.2.2:** Make changes in operations and logistics according to new concept

5.3.3 Seaborne element
- **5.3.3.1:** Refurbish/upgrade airborne element
- **5.3.3.2:** Make changes in operations and logistics according to new concept

5.4 Decommission System

5.2.1 Airborne element
- **5.2.1.1:** Disconnect the airborne element
- **5.2.1.2:** Bring the airborne element to shore
- **5.2.1.3:** Recycle/ repurpose the airborne element

5.2.2 Seaborne element
- **5.2.2.1:** Reel in the mooring system (anchor and mooring line)
- **5.2.2.2:** Store the anchor in the (de)construction vessel to transport it back to shore
- **5.2.2.3:** Tow the seaborne element back to shore
- **5.2.2.4:** Recycle/ Repurpose the floater
- **5.2.2.5:** Recycle/ Repurpose the mooring system

Phase 1.0
Phase 2.0
Phase 3.0
Phase 4.0
Phase 5.0

4
Market Analysis

A market analysis is conducted to give a reference of competing energy sources which will be used to verify that the mission need statement has been successfully achieved. This requires some background on the cost aspects, as well as the sustainability aspects of other renewable sources. The future electricity demand expectations are discussed in section 4.1, after which the trends that are expected for competing renewable energy sources are shown in section 4.2. A sustainability analysis for conventional wind turbines is performed in section 4.3, and the potential that an airborne energy system has compared to competing energy sources in section 4.4. The chapter is summarised in a strengths, weaknesses, opportunities and threats chart which highlights the potential of an airborne wind energy system in the future electrical grid. This so-called SWOT analysis is shown in section 4.5

4.1. Electricity Demand Trends

The Paris Agreement, which has been signed by 175 countries, has set a milestone for 2050 where the goal is to have net-zero emissions. This milestone can only be reached if the electrification of industries that are now using fossil fuels sees a massive increase and therefore leads to a massive increase in electricity demand. The demand for electricity is anticipated to grow substantially, with a 40% increase from current levels by 2030, and more than two and a half times by 2050 [4]. However, emissions from electricity generation are expected to reach net zero in advanced economies by 2035 and globally by 2040. This transformation will primarily be driven by renewable energy sources, which are projected to increase from 29% in 2020 to 60% in 2030 and nearly 90% in 2050. The annual additions of solar PV and wind power will amount to 600 GW and 340 GW, respectively, from 2030 to 2050.

In the industrial sector, emissions are predicted to decrease by 20% by 2030 and 90% by 2050. The majority of emissions reductions in heavy industries by 2050, in the context of a Net Zero Emissions (NZE) scenario, will be facilitated by technologies that are currently unavailable in the market, many of which will rely on hydrogen or Carbon Capture, Utilisation, and Storage (CCUS). Beginning in 2030, all new industrial capacity additions will have near-zero emissions. By that year, there will be a monthly addition of 10 new and existing heavy industry plants equipped with CCUS, 3 new hydrogen-based industrial plants, and 2 GW of electrolyser capacity at industrial sites worldwide.

4.2. Competing Renewable Energy Systems

The main renewable electricity competitors for an airborne wind energy system are solar power and conventional wind turbines. These renewable sources are the energy sources that are expected to have the largest growth, and will therefore start to dominate the energy market in the future. Due to the limited area available onshore in the Netherlands and the limitations of the power transportation grid, there are currently no plans to build large-scale wind or solar power farms.

Solar Power

The solar power capacity in the Netherlands is expected to grow massively from about 10GW of the currently installed capacity to somewhere between 100 GW and 125 GW by 2050 depending on the chosen scenario [5]. The expected capacity is dependent on the chosen scale of generation, either distributed smaller-scale generation or utility-scale solar farms of

10 MW or more. There is no plan for larger scale solar farms with a capacity of 100 MW.

Wind Energy

Similar to solar power, the installed wind capacity in the Netherlands is expected to grow massively. There is currently 5 GW of installed onshore capacity which is expected to grow to between 10 GW and 20 GW installed capacity by 2050 [5]. The offshore capacity is currently 4 GW but is expected to grow faster than the onshore capacity. The expected capacity in 2050 is between 30 GW and 52 GW depending on the scenario. This highlights the focus on the offshore market which is due to the limited space on land for onshore wind energy growth.

Future Levelised Cost of Energy

It is important to get an insight into the future levelised cost of energy (LCoE) expectations to get a target cost to be competitive as an innovative energy method. Figure 4.1 shows the expected European baseload price prediction up to 2050. It is expected that this price will decrease to between 60 and 80 $\$/MWh$ after the late 2030s. Currently, offshore wind energy has an LCoE exceeding 200 $\$/MWh$, but it is expected that this will drop to below 100 $\$/MWh$ by 2025 and below 40 $\$/MWh$ by 2050 [6]. This will be the main competition to the airborne wind energy system so the goal is to design a system with a comparable LCoE.

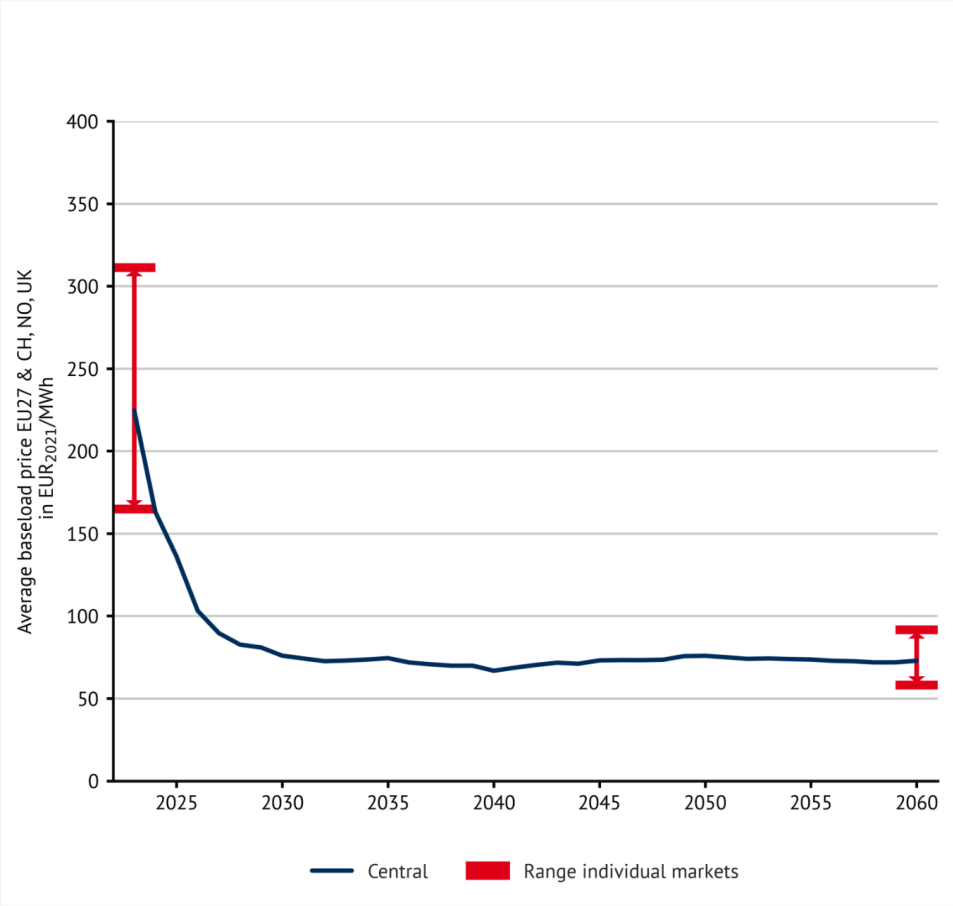

Figure 4.1: European Baseload Price Prediction [7]

4.3. Conventional Wind Turbines Sustainability Analysis

In order to verify that the airborne wind energy system is indeed more sustainable than a conventional wind turbine, some data on conventional turbines are required. The main materials

that are required for a wind turbine and their mass fractions are shown in table 4.1. This shows that 89% of the mass of wind turbines is made from steel [8] which is a recyclable material [9]. The main issue with recycling wind turbines is the turbine blades. The materials that are used for a typical rotor blade are shown in table 4.2 where it shows the large use of composites. Additionally, there is a lot of waste in the construction of rotor blades where a blade of 7 tons requires more than 4 tons of additional material. For offshore wind turbines, the materials used are responsible for 70% of climate change impacts [10].

Table 4.1: Turbine Material Fractions [8]

Material	Mass Fraction
Steel	89%
Glass fibre	6%
Copper	2%
Aluminium	1%
Adhesive	1%
Concrete	1%

Table 4.2: Rotor Blade Material Fractions [8]

Material	Mass Fraction
Glass fibre	58%
Resin	22%
Main Materials	8%
Hardener	7%
Others	5%

4.4. Airborne Wind Energy Potential

Due to the high maturity of the bottom fixed, conventional wind turbines, it is expected that it is difficult for an innovative system such as AWES to compete. Additionally, most of the area of the North Sea where bottom-fixed foundations are possible is either already in operation or has been planned. Floating offshore wind is less developed than bottom-fixed turbines, there are currently only pilot projects in the order of tens of megawatts. This is a potential market where an innovative technology such as airborne wind energy could compete if it can reach similar LCoE. It is expected that the floating offshore wind market will be 15% of the complete offshore wind energy market in Europe by 2050 [6], which accounts for 264 GW. This shows the massive growth of the market since there is less than 1 GW currently in operation.

The market for onshore wind energy surpasses that of offshore energy. According to a report by IRENA [11], it is projected that the total onshore capacity will reach 5,044 GW by 2050. While the current focus of this project does not lie primarily within the onshore market due to the competition from conventional wind turbines, there may be future opportunities for airborne wind to compete with traditional turbines in specific onshore markets. Furthermore, as offshore bottom-fixed wind turbines near the end of their operational life, there exists potential for airborne wind systems to reuse the existing foundations and infrastructure for their own use.

Floating airborne wind could have significant advantages compared to conventional wind turbines. It is expected that the material used can be significantly decreased due to the limited size of the airborne element compared to the turbine blades, and the replacement of a tower structure with a tether. Additionally, the materials that are used can be more sustainable and recyclable than conventional wind turbine blades since these are made of composites for which there is no large-scale recycling solution available.

4.5. SWOT Analysis

Figure 4.2 shows the strengths, weaknesses, opportunities and weaknesses of the airborne wind energy system. The comparison has been made with conventional wind turbines since that will be the main competition.

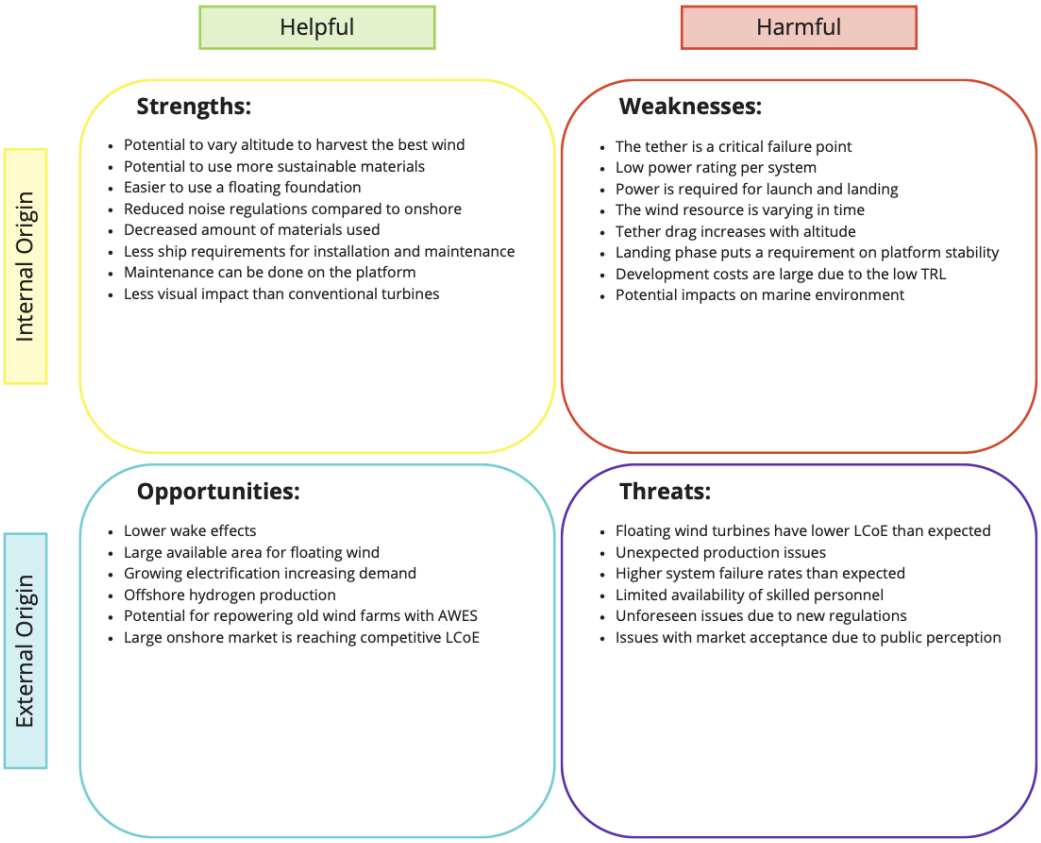

Figure 4.2: SWOT Analysis

5 Risk Assessment

Each design and concept needs to take possible dangers and accidents into account. This is done to ensure that the final product does not encounter any undue problems during its lifetime and to highlight potential barriers to different aspects of this concept. Section 5.1 identifies and categorises the risks while section 5.2 showcases strategies to mitigate the risks.

5.1. Identifying Risks

Given the concept of the system and the farm, a complete list of risks spanning across different aspects is presented along with a likelihood (L) and severity (S) level rated on a numbered scale between integers from and including 1 to 5. The five-point scale's description is outlined in table 5.1.

Table 5.1: Description of the five-point scale for likelihood and severity.

Scale	Likelihood	Severity
1	Improbable	Negligible
2	Remote	Low
3	Occasional	Moderate
4	Probable	Significant
5	Frequent	Catastrophic

The different risk types considered are divided between the farm (FL) and system (S). The system-level risks are further divided into the main elements of the airborne (A), seaborne (S) and tether (T) elements.
The risk type themselves include operational (O), budget (B), project management (M), safety (S), and technical (T) risks. The naming convention flows from the main level, FL or S, for the system level a further distinction is made between A, S, and T. After the first two letters are established, the specific type of risk (between O, B, M, S) is indicated. Then an integer index starts as more risks of the same type are listed. An example of a label could be SA-O-01 which indicates a system-level airborne operational risk that is first on the list.

5.1.1. System Level Risks

Based on the point system and the different types of risks possible for this AWES farm, an elaborate presentation of all the risks is available in tables 5.2 and 5.3.

Table 5.2: System Level Risk Register for Deep WattAir.

Risk ID	Description	S	L
SA-T-01	Airborne element falls/dives into the sea	5	3
SA-T-02	Due to collision with an object, the airborne element is destroyed	5	2
SA-T-03	Due to collision with an object, the airborne element is damaged	4	3
SA-T-04	The airborne element cannot land due to control system malfunction	5	2
SA-T-05	Corrosion of the airborne element	4	4
SA-T-06	Airborne element and component reliability has a low confidence level	4	4
SA-T-07	Airborne elements' structural reliability decreases due to wear	3	4

SA-T-08	Structural damage on the airborne element due to extreme weather	4	3
SA-T-09	Structural damage on the airborne element due to gusts	4	3
SA-O-10	Airborne element produces more wake than expected	3	3
SA-T-11	Moisture damaging the airborne elements' electrical components	4	4
SA-T-12	Lightning strike damages the airborne element	5	3
SA-O-13	The wake from one system affects next system's power generation level	3	4
SA-O-14	Data communication failure making system status monitoring impossible	3	3
SA-T-15	Single motor failure leading to decrease in thrust	3	4
SA-T-16	Multiple motor failures leading to critical decrease in thrust	5	3
SA-T-17	Rotor damage leading to decrease in thrust	3	5
SA-T-18	Multiple rotors damages leading to critical decrease in thrust	5	3
SA-T-19	Jammed control surfaces decreasing control	4	3
ST-T-01	The connection tether breaks	5	2
ST-T-02	The airborne element cannot land due to tether malfunction	5	2
ST-T-03	Creep in the tether decreasing structural rigidity	4	4
ST-T-04	Excess strain in tether leads to failure of electric cabling	5	2
ST-T-05	Tether damage leads to shorts in the electric cabling	5	2
ST-T-06	Structural damage on the tether due extreme weather	4	3
ST-T-07	Structural damage on the tether due to gusts	4	4
ST-T-08	Lightning strike damages the tether	4	1
SS-O-01	Birds nest on the seaborne element	1	5
SS-T-02	Collision with object damages the seaborne element	2	3
SS-S-03	Collision with maintenance boat could harm personnel	4	4
SS-T-04	Collision with external object destroys anchor lines	4	3
SS-T-05	The anchor(s) is not anchored correctly to the seabed and moves around	4	2
SS-T-06	The anchor line(s) fail	4	3
SS-T-07	Fishing nets damage the anchor(s)	4	3
SS-T-08	Structural damage on the seaborne element due to extreme weather	3	2
SS-T-09	Failure of the winch leading to the system being unable to land	5	3
SS-O-10	Damage to power connection making operation impossible	4	3
SS-S-11	Electrical damage on the seaborne element giving electrocution risk	4	3
SS-T-12	Overheating components leading to fire on the seaborne element	4	3
SS-T-13	Rising sea level increases tension in the mooring lines	4	2
SS-T-14	Lightning strike damages the seaborne element	4	4
SS-T-15	The seaborne elements' buoyancy is affected by damage	4	2
SS-T-16	Corrosion of the seaborne element	2	5
SS-T-17	The airborne element cannot land due to seaborne element instability	4	2
SS-T-18	Sea animals get attached to seaborne element	1	5

Table 5.3: Farm Level Risk Register for Deep WattAir.

Risk ID	Description	S	L
FL-T-01	Airborne element collides with another airborne element	5	2
FL-T-02	The connection tether get entangled with another connection tether	5	2
FL-T-03	Connection to the external grid is compromised	5	2

FL-T-04	Connection within the farm grid is compromised	5	3
FL-T-05	Changes in external suppliers affects component compatibility with other parts	4	3
FL-T-06	Power overload shorts farm or multiple systems	5	2
FL-T-07	Fishing nets damage the transmission lines	4	2
FL-O-01	No access to the wind farm for maintenance due to weather conditions	3	4
FL-O-02	Construction of farm disrupts underwater habitats	4	4
FL-O-03	Maintenance personnel unavailable due to widespread sickness	4	3
FL-O-04	Power yield lower than expected due to wind variability	4	3
FL-O-05	Farm affects bird migration patterns and paths during operations	3	5
FL-O-06	Farm affects sea-life migration patterns and paths during operations	3	5
FL-O-07	Wake from other farms affects power generation level	4	3
FL-O-08	Unexpected decrease in component lifetime increases maintenance effort	3	3
FL-O-09	Systems can not launch due to wave conditions	4	4
FL-O-10	Material shortages make certain components unavailable	4	4
FL-O-11	Political issues negatively affect operations of farm	4	2
FL-O-12	Global energy prices drop more than currently predicted	4	4
FL-O-13	Changes in external supplier components solicits re-training of maintenance personnel	3	3
FL-B-01	Changes in external suppliers increases prices	4	3
FL-B-02	Material shortages raise prices	4	2
FL-B-03	Labour wages increase due to inflation or legislation	4	3
FL-B-04	Maintenance costs increase due to fuel and shipping cost increases	3	3
FL-B-05	Increase in material and component costs by suppliers	4	3
FL-B-06	Subsidies (if solicited) fall through due to changes in legislation	5	1
FL-B-07	Exceeded cost budget	5	2
FL-B-08	Unexpected decrease in component lifetime increases maintenance cost	4	2
FL-M-01	Logistic delays due to unavailable replacement components for maintenance	3	2
FL-M-02	Breach in internal and external contracts	2	3
FL-M-03	Intellectual property contracts are breached	4	2
FL-M-04	Changes in external suppliers cause logistical complexities about transport and delays	3	2
FL-M-05	No access to the wind farm for maintenance due to unavailable vessels	4	2
FL-S-01	Personnel gets injured during maintenance procedures	4	3

5.2. Mitigating Risks

After laying out all the risks, the ones that are unacceptable due to a combination of their severity and likelihood are presented and mitigated in table 5.4.

Table 5.4: System Level Risk Mitigation for Deep WattAir.

Risk ID	Type	Mitigation Measure	S	L
SA-T-01	L	Have redundant control systems decreasing the likelihood of a crash	5	2
SA-T-02	S	Increase structural rigidity of the leading edge to decrease the severity of an impact	4	2
SA-T-03	S	Increase structural rigidity of the leading edge to decrease the severity of an impact	3	3
SA-T-04	S	Use the winch to reel in the system to decrease impact to be able to re-use parts	4	2
SA-T-05	L	Use corrosive resistant materials	4	2
SA-T-06	L	During development, test components on-shore until they break to understand the reliability	4	2
SA-T-07	L	Use condition-based maintenance to increase component reliability	3	3
SA-T-08	L	Land the system if bad weather is forecasted	3	3
SA-T-09	L	Use safety margins in the design to ensure the system will not be damaged	4	2
SA-T-11	L	Uses double seals to ensure that no moisture enters the airborne element	4	3
SA-T-12	L	Land the system if lightning is forecasted	5	1
SA-O-13	S/L	Take wake effects into account in the flight path planning	2	3
SA-T-15	S	Design the system to be able to operate with a single engine failure	2	4
SA-T-16	L	Land the system when a single engine fails and not operate until that is repaired	5	1
SA-T-17	S	Design the system to be able to operate with a rotor failure	2	4
SA-T-18	L	Land the system when a single rotor and not operate until that is repaired	5	1
SA-T-19	S	Have redundant control systems to land the system	2	3
ST-T-01	S	Glide the airborne element towards a centralised safe landing spot	3	2
ST-T-02	S	Land the airborne element at a centralised landing spot	3	2
ST-T-03	L	Monitor the tether health and replace if the creep becomes too large	4	2
ST-T-04	S	Coil the electric conductors such that they do not carry load	3	2
ST-T-05	S	Make the tether easily replaceable	3	2
ST-T-06	L	Land the system if bad weather is forecasted	4	2
ST-T-07	L	Use safety margins in the design to ensure the tether will not be damaged	4	2
SS-S-03	S	Uses safety equipment when near the AWES	2	4
SS-T-04	L	Restrict external parties access to the wind farm	4	2
SS-T-06	S	Have redundant anchoring to keep the AWES in place with a single failure	2	3
SS-T-07	L	Ensure no fishing within farm zone and monitor subsea components for entangled nets	4	2
SS-T-09	S	Glide the airborne element towards a centralised safe landing spot	3	3
SS-O-10	S	Glide the airborne element towards a centralised safe landing spot	3	3
SS-S-11	L	Check the seaborne element before personnel enters for maintenance	4	1
SS-T-12	S	Isolate the parts with the highest fire risk to contain the potential fire	3	3

SS-T-14	S	Include a lighting protection system to direct energy away from critical parts	2	4
SS-T-15	S	Ensure that the seaborne element can float with two out of three pylons	2	2

Table 5.5: Farm Level Risk Mitigation for Deep WattAir.

Risk ID	Type	Mitigation Measure	S	L
FL-T-01	L	Space farm appropriately and provide emergency landing pathways and platforms	5	1
FL-T-02	L	Space farm appropriately	5	1
FL-T-03	L	Install redundant connections and perform timely maintenance checks	5	1
FL-T-04	S/L	Install redundant connections and perform timely maintenance checks and design circuits where not all systems are in series	4	2
FL-T-05	L	Communication with suppliers for specific component requirements	4	2
FL-T-06	L	Implement and maintain breakers to ensure no overloads occur	5	1
FL-T-07	S/L	Ensure no fishing within farm zone and survey sub-sea components for entangled nets and include extra jacketing material around transmission lines to protect from damages	3	1
FL-O-01	S	Schedule maintenance checks accounted for delays of a week at least	2	4
FL-O-02	S	Scout construction grounds and safely move habitats to a safer zone if needed.	3	4
FL-O-03	S	Schedule maintenance checks accounted for delays and have extra people on standby	3	3
FL-O-04	L	More in-depth sensors and models to measure wind to improve confidence level	4	2
FL-O-05	L	Temporarily pause operations during peak migration times	3	4
FL-O-06	L	Temporarily pause operations during peak migration times	3	4
FL-O-07	S	Measure wake affects and design airborne elements accounting for that	3	3
FL-O-09	L	Control system on seaborne element and predict wave conditions beforehand	4	3
FL-O-10	S	Foresee material shortages and find suitable replacements preemptively	3	4
FL-O-12	S	Ensure farm is operating with a safety factor on the cost budget to stay competitive	3	4
FL-B-01	L	Perform appropriate research and negotiations to ensure the next best price	4	2
FL-B-03	S	Predict and account for changes due to inflation in future cost budgets	3	3
FL-B-05	S	Perform adequate supplier research for best market price and account for price increases	3	3
FL-B-07	L	Ensure farm is operating with a safety factor on the cost budget	5	1

FL-S-01	S/L	Ensure the correct use of safety equipment, timely maintenance training and have the appropriate insurances (for company and personnel)	3	2

5.2.1. Risk Map

The risk maps both before and after mitigation are presented below. As can be seen the unacceptable risks are those in the orange and red zones. Mitigation steps laid out most risks to the yellow zone.

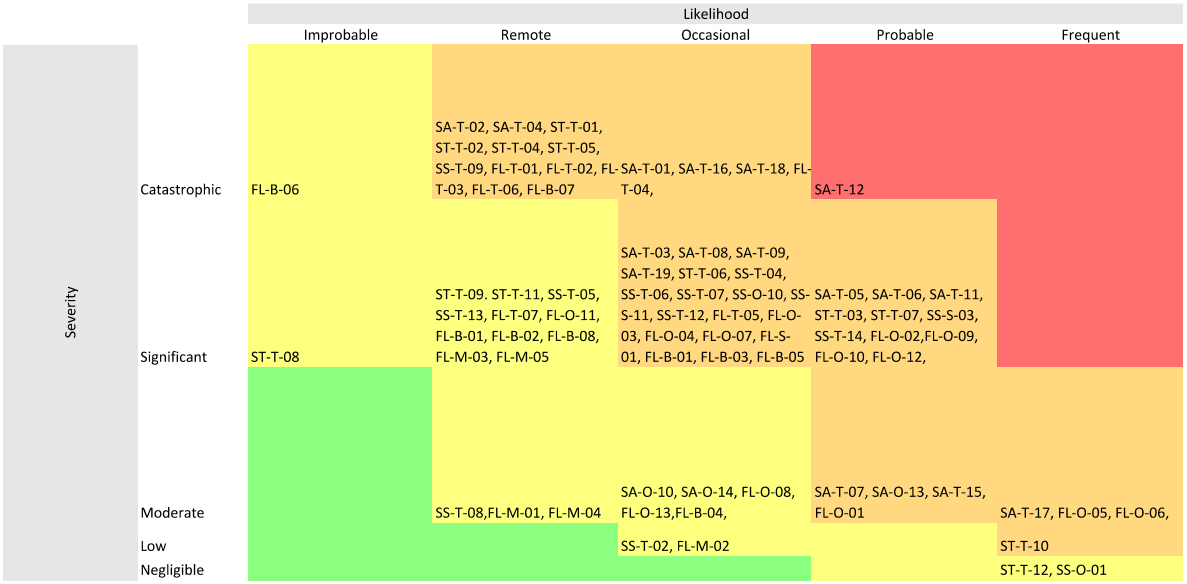

Figure 5.1: Risk map before mitigation

Severity	Likelihood: Improbable	Remote	Occasional	Probable	Frequent
Catastrophic	SA-T-12, SA-T-16, SA-T-18, FL-T-01, FL-T-02, FL-T-03, FL-T-06, FL-B-06, FL-B-07	SA-T-01			
Significant	ST-T-08, SS-S-11	SA-T-02, SA-T-04, SA-T-05, SA-T-06, SA-T-09, ST-T-03, ST-T-06, ST-T-07, SS-T-04, SS-T-07, SS-T-14, SS-T-16, SS-T-05, SS-T-13, FL-T-04, FL-T-04, FL-T-05, FL-O-04, FL-O-11, FL-B-02, FL-B-08, FL-M-03, FL-M-05, FL-B-01	SA-T-11, FL-O-09		
Moderate	FL-T-07	ST-T-01, SS-T-08, ST-T-02, ST-T-04, ST-T-05 ,FL-M-01, FL-M-04, FL-S-01	SA-T-03, SA-T-07, SA-T-08, SA-T-08, SA-O-10, SA-O-14, SS-T-09, SS-O-10, SS-T-12, FL-O-03, FL-O-06, FL-O-07, FL-O-08, FL-O-13, FL-B-04, FL-B-03, FL-B-05	FL-O-02, FL-O-05, FL-O-10, FL-O-12	
Low		SS-T-15	SA-O-13, SA-T-19, SS-T-02, SS-T-06, FL-M-02	SA-T-15, SA-T-17, SS-S-03, SS-T-14, FL-O-01	
Negligible					SS-T-17, SS-O-01

Figure 5.2: Risk map after mitigation

6 Material Analysis

An important part of any product is the choice of material. This chapter will provide an overview of the material property analysis in section 6.1. Then a corrosion resistance analysis is performed in section 6.2. Lastly, further recommendations for a more detailed analysis will be given in section 6.3.

6.1. Initial Material Analysis

In the preliminary design phase [3], an initial analysis of material properties was performed for a number of materials. These materials were analysed for bending stiffness mostly, due to the expected importance of such load cases for the airborne element. The geometry considered for this analysis was a simple rectangle with dimensions of 2 by 0.2 m under an applied moment of 1 MNm. This analysis also included an initial estimation of the cost per kg. The results are shown in table 6.1.

Table 6.1: An overview of the material properties and analysis criteria [3].

Material	σ_y [MPa]	ρ [kg/m^3]	E [GPa]	Cost [€/kg]	σ_z/σ_y [-]	E/ρ [m^2/s^2]
Al 2024-T6[1]	345	2780	73.1	2.11[2]	0.217	2.63E7
Al 7075-T6[1]	462	2810	71.7	2.11[2]	0.162	2.55E7
Titanium[1]	1050	4540	118	6.01[2]	0.071	2.60E7
Elektron-43[3]	195	1840	44.1	3.50[2]	0.385	2.40E7
CF-epoxy [12]	380	1540	83.0	55.00[4]	0.197	5.39E7
E-Glass-epoxy [12]	570	1970	21.5	1.90[4]	0.132	1.09E7

In addition to the above materials, another type of material to be considered is thermoplastics. Two thermoplastics considered are Poly-Ether-Ether-Ketone (PEEK) and Poly-Phenil-Sulphide (PPS) [13]. The material properties of both thermoplastics, reinforced with glass or carbon fibres, are shown in table 6.2.

Table 6.2: Material properties of reinforced PEEK and PPS[1]

Material	σ_y [MPa]	E [GPa]	ρ [kg/m^3]	Cost [€/kg]	σ_z/σ_y	E/ρ [m^2/s^2]
PEEK with 30% glass-fibre	150	11.9	1540	60 - 80 [13]	0.500	7.73E6
PEEK with 30% carbon-fibre	348	27.2	1450	60 - 80 [13]	0.216	1.88E7
PPS with 30% glass-fibre	151	13.3	1650	15 - 25 [13]	0.497	8.06E6
PPS with 30% carbon-fibre	178	24.1	1480	15 - 25 [13]	0.421	1.63E7

From this table, it can be seen that thermoplastics have a performance that is either similar or worse compared to most metals or thermosets, while they are significantly more expensive.

[1] Matweb [Cited 23 May 2023]
[2] Trading Economics [Cited 22 May 2023]
[3] Luxfer Mel Technologies [Cited 22 May 2023]
[4] Technica [Cited 23 May 2023]

This means that in terms of material properties, thermoplastics are less desirable as a material. One part where thermoplastics are more desirable is designing for recyclability, but most metals are also recyclable.

Another material analysis was performed for the tether. The materials considered for this were carbon fibre, Kevlar, and Dyneema. The results of this analysis are shown in table 6.3.

Table 6.3: Material properties for mechanical tether core [3].

Material	Ultimate Tensile Strength	E- Modulus	Strength to weight	Electrical Conductivity	Abrasion and Fatigue	Density
Carbon Fibre	3.5 GPa	125 - 181 GPa	1013	Conductive	Fails without showing signs	1.9 g/cm^3
Kevlar	3 GPa	70.5 - 112.4 GPa	993	Non-conductive	High resistance	1.44 g/cm^3
Dyneema	2 - 4 GPa	109 - 132 GPa	1390	Non-conductive	High resistance	0.97 g/cm^3

Analysis shows that Dyneema is considerably lighter than carbon fibre and Kevlar, stronger than Kevlar, and potentially as strong as carbon fibre. This makes Dyneema a strong candidate for the tether material

Lastly, the material needs to be analysed for use in the floater. Most existing floaters are constructed using steel [14], [15]. For this reason, it was decided to also use steel for the floater of the AWES. Four types of steel are considered, due to their use in maritime engineering [16]. These types are shown in table 6.4.

Table 6.4: Material properties for typical maritime steels [16]

Steel type	σ_y [MPa]	E [GPa]	ρ [kg/m^3]	Cost [€/kg]	E/ρ [m^2/s^2]
Mild 1020[5]	200	210	7870	0.47	2.69E7
Notch tough MS	200	210	7800	0.52	2.69E7
B quality	226	208	7850	0.54	2.67E7
Q1N	480	208	7750	2.82	2.67E7

This table shows that three of the four steels considered are very similar in performance with a similar cost. The only outlier here is the type Q1N, having a higher yield stress, but also a significantly higher cost.

6.2. Corrosion Analysis

Because the system will operate in a maritime environment, corrosion will be an important factor to consider. Because composites do not suffer from corrosion[6], the corrosion resistance of the metals in section 6.1 is investigated. First, the metals are analysed for general corrosion. Then, galvanic corrosion will be analysed, and lastly, pitting corrosion is looked into.

General corrosion

For aluminium, it was found from the data sheet of the Aluminum Association (AA) that the 2024-T6 alloy has a poor resistance to corrosion, whereas 7075-T6 has a fair resistance[7]. This means that, for maritime operating conditions, the aluminium will have to be protected

[5]Material properties of steel [Cited 13 June 2023]

[6]Composite corrosion [Cited 13 June 2023]

[7]AA Data Sheet [Cited 13 June 2023]

at the joints at a minimum. This can be done by applying for example a thin layer of pure aluminium or a resin coating.

According to *Timet*[8], titanium does not experience corrosion at all when exposed to seawater, which makes titanium an excellent candidate in terms of corrosion resistance.

Compared to titanium, magnesium is on the other side of the corrosion resistance spectrum. Most magnesium alloys have a corrosion rate in the order of hundreds of metres per year [17], making it an undesirable material when designing for corrosion resistance.

Finally, steel has either a similar performance as aluminium, for mild steel, or a significantly better performance [18]. This means that steel is indeed a good material choice for the floater.

Galvanic corrosion
Another aspect that should be discussed is galvanic corrosion, which is corrosion of the metal due to contact with another metal (or other conductive materials). These metals all have an electric potential, and if two different metals are connected, either directly or indirectly through water, the material with the lower potential will corrode. Table 6.5 shows the approximate electric potentials of the metals considered.

Table 6.5: Electric potential of metals in maritime conditions[9]

Metal	Electric Potential [mV]
Aluminium	-750
Titanium	-150
Magnesium	-1600
Steel	-100

As can be seen in table 9, magnesium has the lowest electric potential of the metals considered. This makes it unsuitable as the main material, but it can be used to reduce the corrosion rates of another metal, for example on the floater.

What also needs to be taken into account is that, should metal be in contact with a composite, and not properly treated, the galvanic corrosion process will be accelerated [18].

Pitting corrosion
The final type of corrosion to be investigated is pitting corrosion. Pitting corrosion is a very local form of corrosion, which will form pits on the surface of the material, potentially going all the way through.

For aluminium, it was found that the pitting rate can be expressed as an equation in terms of time t, shown in equation (6.1)[9]:

$$v = K\sqrt[3]{t} \tag{6.1}$$

In this equation, v is the pitting rate, while K is a constant dependent on the exact type of aluminium. From this relation, it can be seen that the pitting rate slows down over time, with most pits not reaching even one mm in depth[9]. This makes it so that aluminium can be a suitable material for an AWES in terms of corrosion resistance, provided a suitable skin thickness is chosen and any defect is caught early on.

[8] *Timet* titanium corrosion data sheet [Cited 13 June 2023]
[9] Aluminium corrosion in marine environment [Cited 13 June 2023]

Titanium was found to not suffer from pit corrosion at temperatures below 100 $^{\circ}$C[10], again making it a good prospect for material choice in corrosion performance.

The pitting corrosion of magnesium is not a well-studied subject, due to the fact that, usually, other types of corrosion are the critical failure cause [17]. However, one study did perform a pitting corrosion analysis for magnesium immersed in saline solutions. This study showed pits of almost one mm deep after just several hours [19]. This means that magnesium is again not the preferred choice of material.

The resistance of steel to pitting corrosion in maritime environments is estimated to be of the order of μm per year [20]. This means that pitting corrosion for steel is negligible for the expected operating time of the farm.

Conclusions
From this corrosion analysis, it can be seen that titanium and steel are very resistant to multiple types of corrosion, aluminium can be resistant, but protection is recommended, and magnesium is not a viable option in terms of corrosion resistance.

6.3. Further Material Analysis Recommendations

The analysis performed in this chapter is done for what the team considers to be the most critical in operation. Next to that, the analysis is also at a qualitative level, and for a more detailed design, a more thorough analysis is recommended before a material is either selected or discarded. This analysis should then also include stress concentration & crack propagation characteristics, fatigue performance, and creep analysis.

Corrosion will also need to be investigated in more detail because the current analysis is qualitative, and based on data for maritime materials, which aluminium 7075-T6 is not. A further look into protective coating is recommended for the aluminium and potentially the steel, as well as sacrificial metals to slow galvanic corrosion.

[10] Pit corrosion titanium [Cited 14 June 2023]

Part 2

Single System Design

In the second part, the design procedure of the single system will be detailed encompassing the power generation, the sizing and the design of the single system. The different power generation relations and the flight path will be explored. Which influences the design of the airborne element including the main wing, rotors, tail and tether. Furthermore the electronics and the power losses of a single system are laid out. Lastly the seaborne element is designed using stability and buoyancy relations.

7
Power Generation

The chapter is introducing the driving formulas that give the base of the design. The aim of the system is to capture wind energy, therefore the most significant equations regard the power generation. First, the wind patterns and magnitudes are analysed in section 7.1. Secondly, the power generation formula by Trevisi [21] is stated alongside the relation for optimal velocity for cross-wind operations in section 7.2. The chapter is concluded by expanding on the power generation formula by modelling the flight path in section 7.3 to provide a more accurate relation for the surface.

7.1. Wind Analysis

Previously, in the midterm report [3], a detailed analysis was performed on the wind characteristics within the North Sea. This analysis was performed utilising data provided by the Royal Netherlands Meteorological Institute for the Meteomast IJmuiden [22]. The mast is located at a longitude 52.85°N and latitude 3.44°E, 82 kilometres from the Dutch shore[1]. Within this section, a summary will be provided for the results found previously and additional material will be provided.

Firstly, two important figures were derived. The first one is the histogram for the wind velocities at 10 m and 200 m. The second is the wind shear profile from 10 to 200 meters. Besides that, it was found that the predominant wind direction is southwest.

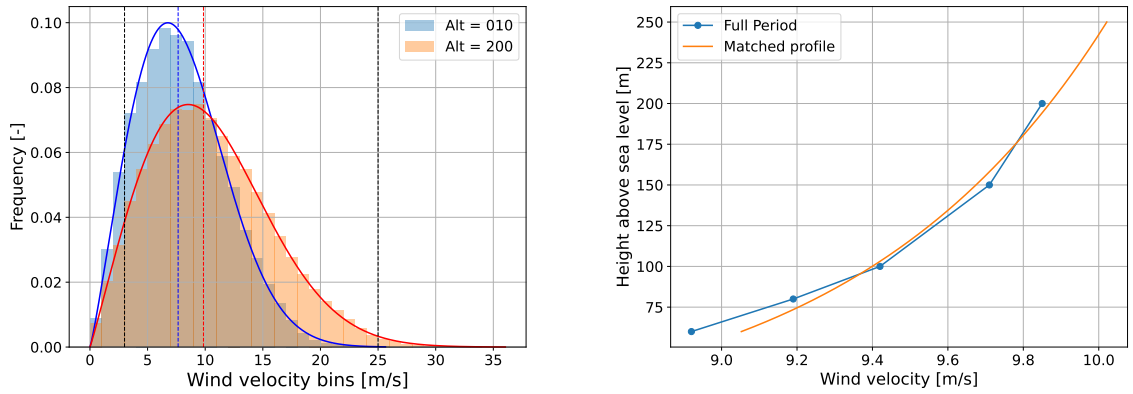

(a) Histogram for the wind velocities at 10 and 200 m measured once an hour from 2004 to 2013

(b) Wind shear profile from 10 to 200 m

Figure 7.1: Wind analysis results for a period from 2004 to 2013 at the Meteomast IJmuiden [3].

7.1.1. Frequency of occurrence of wind velocities at 10 and 200 m

From figure 7.1a a range of conclusions could be made. Firstly, at higher altitudes, the wind velocities reach a higher magnitude and are also more constant around these velocities. For the full measured period, the mean velocity was 7.65 m/s at 10 m and 9.85 m/s at 200 m altitude. Besides that, when considering the operational window of the aircraft being within wind speeds of 4 to 25 m/s, the frequency of operation could be observed purely based on

[1] Site Studies Wind Farm Zone Borssele [Cited 18 June 2023]

wind velocities. At 10 meters this percentage is 90.7%, at an altitude of 200 m the percentage value increase to 93.5% of the time during the full measured period.

The reason why these values are important is that they provided the foundation for the calculation of the capacity factor. The capacity factor is one of the most important figures since it describes how much the system is actually generating in comparison to the maximum theoretical output. It must be noted that, for that calculation, wind velocity isn't the only important value of the capacity factor and that the capacity factor can be misleading if its background isn't fully understood. For the exact calculation of the capacity factor, which relied on figure 7.1a, the numerical values on said plot were used.

7.1.2. Altitude Dependence

Within figure 7.1b it can be observed that the wind velocity is a function of the altitude. The result observed in the plot was created using the median velocities throughout the full period for an altitude of 10, 20, 40, 60, 80, 100, 150, and 200 m. Although the result of this profile looked very promising a key shortcoming was found. The shear profile observed only provides information from 10 up to 200 m, whereas the aircraft could fly at higher altitudes if deemed feasible and economical. For this reason, utilising the select values used to construct the plot an extrapolation was performed to consult the velocities at higher altitudes.

Typically for this extrapolation to higher altitudes, it was observed in the literature that the power law would be utilised for altitudes above the blending height (60 m) [23]. This extrapolation is done using equation (7.1) where h_{blend} is the blend height and V_{blend} is the wind velocity at the blend height.

$$V = V_{blend} \left(\frac{h}{h_{blend}} \right)^{\alpha} \tag{7.1}$$

However, when implementing this equation (with the data available above 60 m) to match and extrapolate the wind velocities it was found that at higher altitudes the velocities rose at a very quick rate. This rate didn't really match the trends observed at measured altitudes. For this reason, it was chosen to match the observed data with a generic exponential function equation (7.2).

$$h_{alt} = \beta e^{V_w ind * \alpha} \tag{7.2}$$

The approximation which was then found utilising an exponential regression script can be observed in equation (7.3) rewritten as a function of altitude. It can be utilised from 10 meters to 300 meters and the implementation of the regression can be observed in figure 7.1b. It must be noted that above 200 meters the velocities are overestimated using the regression.

$$V_{wind} = \frac{1}{1.473} \cdot \log \left(\frac{h_{altitude}}{9.709 \cdot 10^{-5}} \right) \tag{7.3}$$

7.2. Trevisi's Power Formula

Now that the approximate wind speed has been analysed, a power estimation has to be made. To do this, the power formula derived by Trevisi Trevisi [21] is used.

First, Trevisi's assumptions are listed:

- The external forces are in equilibrium, meaning steady flight.
- The inertia forces are negligible

- The tether is straight
- The equation represents only the power generation when operated and disregards their operational phases.

Trevisi's paper [21] provides an analytic solution to the power generation of a simplified case and is displayed in equation (7.4). It is utilised as a base equation for power generation, making it the most significant formula of the project. It incorporates the parameters of the design such as the aerodynamic coefficients C_L and C_D, the position of the aircraft in terms of altitude h, flight inclination θ and flight side angle ψ, mass m and wing surface area S. It also uses the wind speed V_{wind} and air density ρ as environmental parameters.

$$P_{FG} = \frac{1}{2}\rho S V_{wind}(h)^3 \gamma_t C_D \left[(1+\gamma_t)^2 + G_e^2\right]^{\frac{3}{2}} \left[\frac{\cos\phi\cos\psi}{1+\gamma_t}\right]^3 \tag{7.4}$$

$$\text{with} \quad \gamma_t = \frac{C_{D_{rotor}}}{C_D} \qquad G_e = \frac{C_L}{C_D} \qquad \phi = \theta + \Delta$$

$$\text{For } \Delta: \quad \Delta^3(\sin\theta+\cos\theta)^2 - 2\Delta^2(\sin\theta+\cos\theta)(\cos\theta) + \Delta(\cos\theta)^2 - \frac{M^*}{Q^*} = 0$$

$$M^* = \frac{mg}{\cos\theta(\tan(\theta)^2+1)} \qquad Q^* = \frac{1}{2}\frac{\rho S C_D V_{wind}(h)^2((1+\gamma_t)^2+G_e^2)^{\frac{3}{2}}}{(1+\gamma_t)^2}$$

It is important to note that the theoretical limit to harvest wind power in open airspace has been derived and is known as Betz's law [24]. The limit of harvested power is $\frac{16}{27}$ of the power of the wind available. It can be used to test if the power production is theoretically possible.

For the optimisation of the power equation above, the following equation (equation (7.5)), needs to be maximised.

$$\left[(1+\gamma_t)^2 + G_e^2\right]^{\frac{3}{2}} \left[\frac{\cos\phi\cos\psi}{1+\gamma_t}\right]^3 \tag{7.5}$$

Equation (7.6) expands on γ_t and G_e as a function of the lift and drag coefficients and the flight side angle,ψ, drops as this changes over the flight path.

$$\left[\left((1+\frac{C_{D_{rotor}}}{C_D}\right)^2 + \left(\frac{C_L}{C_D}\right)^2\right]^{\frac{3}{2}} \left[\frac{\cos\phi}{1+\left(\frac{C_{D_{rotor}}}{C_D}\right)^2}\right]^3 \tag{7.6}$$

The lift coefficient, C_L, will be designed at a constant for the power generation, which is as determined as follows, [25].

$$C_L = \frac{C_{L_{max}}}{1.25} \tag{7.7}$$

The drag coefficient is the sum of the airfoil, tether and rotor drag coefficient. The rotor drag is dependent on the nominal velocity, V_n, and is shown in equation (7.8), [26].

$$V_n = \frac{2C_L\sqrt{1+\left(\frac{C_D}{C_L}\right)^2}}{3C_D} V_{wind} \tag{7.8}$$

7.2.1. Expanding on the Power Formula

The first consideration taken into account to expand on the power generation is the variation of parameters along the flight path in equation (7.4). Important to note here is that equation (7.4) has been derived for steady and straight flight, therefore, its accuracy is higher for straight sections but during the turns it is questionable. Therefore, to give a more accurate relation between the surface area and power, the following equations are used.

First, the requirement for power generation is recognised, as the airborne element needs to generate power to satisfy the LCoE requirement. Therefore, 1 MW is a fixed value on the average power. The average power is expressed by integrating the flight path over time and dividing by the period shown in equation (7.9)

$$P_{ave} = \frac{1}{T} \int P dt \tag{7.9}$$

The parameters to find therefore are the power as a function of time and the period. Equation (7.4) is rewritten in equation (7.10) with V_n expressed as equation (7.11) [21].

$$P(t) = \frac{1}{2} \rho S V_w^3 \gamma_t C_D \left[(1+\gamma_t)^2 + G_e^2 \right]^{\frac{3}{2}} \left[\frac{\cos\phi \cos\psi}{1+\gamma_t} \right]^3 \tag{7.10}$$

$$V_n^2 = V_w^2 \left[(1+\gamma_t)^2 + G_e^2 \right] \left[\frac{\cos\phi \cos\psi}{1+\gamma_t} \right]^2 \tag{7.11}$$

For the case of simplicity, all the parts that are considered constant over the flight path are collected as a term in equation (7.12)

$$k_1 = \frac{1}{2} \rho S \gamma_t C_D \left[(1+\gamma_t)^2 + G_e^2 \right]^{\frac{3}{2}} \left[\frac{1}{1+\gamma_t} \right]^3 \tag{7.12}$$

The time-dependent power generation equation can then be rewritten as shown in equation (7.13). This formula is used to express the power generation over time; however, the time dependence of the variables V_a, ϕ, and ψ has to be set up in order to conduct the analysis. The relations are set up by modelling the flight path in section 7.3.

$$P(t) = k_1 V_{wind}(t)^3 (\cos\phi(t) \cos\psi(t)) \tag{7.13}$$

7.3. Flight Path Modelling

First, the assumptions are stated.

Assumptions

- The flight path is appropriately approximated by to a two-dimensional section of the airspace.
- Conservation of energy of the airborne system is satisfied as the losses due that non conservative forces, mainly drag, are matched by the energy extracted from the wind. The assumption is mainly based on that no external forces are used to maintain the same flight path.
- Trevisi's assumptions are applicable to the power generation over the flight path.
- No bank angle is experienced during the flight.

The flight path is modelled by straight parts and circular turns. The parameterisation and modelling of the flight path is demonstrated on figure 7.2. As can be seen, the parameters of the flight path are the angle of incline of the straight sections, ω, and the radius of the circular sections, R. Two spatial variables are utilised in the modelling: h for the straight sections and θ_t for the circular ones. h is zero at the middle and is positive upwards while θ_t is zero at the horizontal angle and is positive upwards.

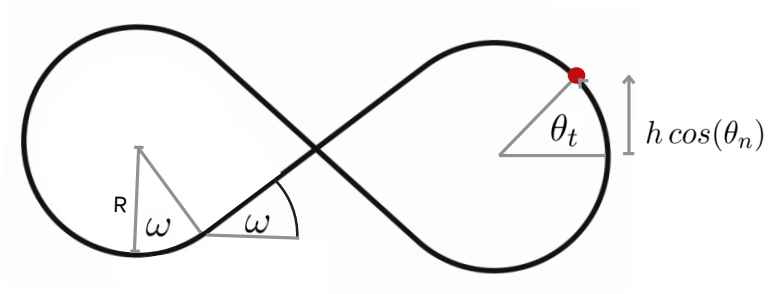

Figure 7.2: Flight Path Modelling

Firstly, certain equations can be derived from the law of conservation of energy. The datum point states a nominal velocity V_n, found by equation (7.11), which can be used with the combination of the altitude difference to find V_a. Note that the sin of the inclination is included to relate h to the altitude as the entire flight path is tilted by the inclination angle.

$$\sum E = m\,g\,h\,cos(\theta_n) + \frac{1}{2} m\,V_n^2 \qquad (7.14)$$

$$V_a = (V_n^2 - 2g\,h\,cos(\theta))^{0.5} \qquad (7.15)$$

$$V_a = (V_n^2 - 2g\,R\,sin(\theta_t)\,cos(\theta))^{0.5} \qquad (7.16)$$

For the straights, the following relations exist. With the altitude at nominal velocity, alt_n and the nominal inclination of the tether, θ_n, which is also the defined datum.

$$\psi(h) = \text{arcsin}\left[\frac{\cos(\omega)h}{l_{tether}}\right] \qquad (7.17)$$

$$\theta(h) = arcsin\left[\frac{alt_n + h\,cos(\theta_n)}{l_{tether}}\right] \qquad (7.18)$$

For the turns, the following relations exist.

$$\psi(\theta_t) = arcsin\left[\frac{R(cos(\theta_t) + cotan(\omega))}{l_{tether}}\right] \qquad (7.19)$$

$$\theta(\theta_t) = arcsin\left[\frac{alt_n + Rsin(\theta_t)cos(\theta_n)}{l_{tether}}\right] \qquad (7.20)$$

Relating time to the spatial variables to support the time integration of the power generated is expressed for the straight lines on equation (7.21) and equation (7.22).

$$dt = \frac{dt}{dh} dh \qquad (7.21)$$

$$\frac{dt}{dh} = \frac{1}{-sin(\omega)V_a} \qquad (7.22)$$

For the turns equation (7.23) and equation (7.24) state the substitution.

$$dt = \frac{dt}{d\theta_t} d\theta_t \qquad (7.23)$$

$$\frac{dt}{d\theta_t} = \frac{R}{V_a} \qquad (7.24)$$

The integrals for the power generation equation can be put together to showcase the power generated in the time taken for one complete figure eight loop.

For the straight sectors,

$$\int Pdt = 2k_1 \int_{-Rsin(\omega)}^{Rsin(\omega)} \frac{V_{wind}(h)^3}{sin(\omega)} (V_n^2 - 2g\,h\,sin(\theta))^{\frac{-1}{2}} (cos(\psi)cos(\phi) - \gamma_{out}) dh \tag{7.25}$$

and for the turns,

$$\int Pdt = 2k_1 \int_{-\pi/2-\omega}^{\pi/2+\omega} V_{wind}(h)^3\, R\, (V_n^2 - 2g\,R\,sin(\theta_t)\,sin(\theta))^{\frac{-1}{2}} (cos(\psi)cos(\phi) - \gamma_{out}) d\theta_t \tag{7.26}$$

The time of the sectors is computed by the very simple $T = \int dt$. For the straight segment, it is given by

$$T_{straight} = \int_{-Rsin(\omega)}^{Rsin(\omega)} \frac{1}{sin(\omega)(V_n^2 - 2g\,h\,cos(\theta))^{\frac{1}{2}}} dh \tag{7.27}$$

and for the circular parts it is given by

$$T_{turns} = \int_{-\pi/2-\omega}^{\pi/2+\omega} \frac{R}{(V_n^2 - 2g\,R\,sin(\theta_t)\,cos(\theta))^{\frac{1}{2}}} d\theta_t \tag{7.28}$$

where V_a for straights and turns have been defined in equation (7.15) and equation (7.16) respectively.

The surface area is one of the main characteristics of the craft and can be extracted from equation (7.10). As the average power P_{ave} is set by the requirements, the surface area can be found by equation (7.29).

$$S = \frac{P_{ave}}{\frac{1}{T}\int_0^T \frac{P(t)}{S} dt} \tag{7.29}$$

As the integration to get the period and the power depend on the flight parameters, the surface area is also a function of these parameters. Therefore ω and R can be optimised to get the minimum surface area. However, in these calculations, it is assumed that there is no loss in the generated power and negligible additional wing loads due to the turns which is a very strong assumption and leads to an optimal R of close to zero which is not representative. Therefore, the aim is to set R as high as the operations of the airborne element allow. This allows a higher integrity of the assumptions as the extra loads at the turns are disregarded in the calculations. Either the altitude or the nominal velocity determines R by the relations expressed in equation (7.30). The minimum altitude is set by either half of the nominal altitude or based on the maximum height difference to avoid stall speed, depending on which one is more pressing.

$$R = min\left[\frac{alt_n}{2cos(\theta)}, \frac{V_n^2 - V_{stall}^2}{2g\,cos(\theta)}\right] \tag{7.30}$$

The ω can be optimised in this case. The rest of the relations and the tool needs to be set up to conclude the optimum numerically. The result of the optimisation is described in section 10.6.

8

Airborne System & Tether Sizing Relations

To design the optimal sizing for a rigid-wing fly-gen airborne wind energy system, a code sizing tool will be made. To make this sizing tool, relations have to be set up for different aspects of the design, and the interactions between these subsystems. This chapter starts with relations for rotor sizing in section 8.1, then continues with the main wing relations both in aerodynamic aspects and structural aspects in section 8.2 and section 8.3 respectively. Additionally, the sizing relations for the tether are defined in section 8.4. The tail aerodynamic relations are defined in section 8.5 and the tail boom structural relations are shown in section 8.6. The mass of the electrical system is estimated in section 8.7. Finally, the material selection for each subsystem is shown in section 8.8.

8.1. Rotor Relations

The rotors have two distinct functions for which they have to be sized. The first function is to harvest the energy in the wind to generate power, sized in section 8.1.1. The second function is to provide thrust for vertical take-off and landing, sized in section 8.1.2. The required rotor size for each of these functions is calculated and the largest required size is then used.

8.1.1. Rotor Power Generation Phase Sizing

The rotors are the components that are harvesting the wind energy. The objective is to harvest this energy while minimising the drag penalty and the influence on control surfaces. The theoretical limit of wind power harvesting is the Betz limit which is given as a fraction of the incoming wind velocity and is defined as $\frac{16}{27}$ [24]. Therefore, for an airborne fly-gen concept, potential power generation is a function of apparent wind velocity as defined in chapter 7.

The area of a single rotor is calculated using equation (8.1) which leads to a diameter of the rotor calculated by equation (8.2) [26]. The power coefficient C_p is assumed to be 0.2. This is because an optimised wind turbine blade has a C_p of 0.35-0.45 [1]. Thus, to be conservative with the estimation, a lower number was used.

$$A_{rotor} = \frac{2P_{max}}{N_{rotors}\rho V_n^3 C_P} \tag{8.1}$$

$$d_{rotor} = \sqrt{\frac{4A_{rotor}}{\pi}} \tag{8.2}$$

The airborne element will be designed to generate 1 MW of power, which will be generated by multiple rotors. The number of rotors is variable and will depend on the capabilities of the electric motor/generators and the practical limits of the rotor radius. The drag of the rotors is an important variable in the aerodynamic design of the airborne element and is calculated using equation (8.3) [26].

$$C_{D_{rotor}} = \frac{P}{\frac{1}{2}\rho S V_n^3} \tag{8.3}$$

Where S is the surface area of the airborne element.

[1] Understanding Coefficient of Power (Cp) and Betz Limit [Cited 24 May 2023]

8.1.2. Rotor Take-off and Landing Sizing

The airborne element will use a vertical take-off and landing method. During this phase, the airborne element will draw power for the grid to drive the rotors to provide take-off thrust. To estimate the rotor size, it is assumed that the disk loading (D_L) is the same as the one from Makani data[14]. The disk loading is defined as mass over the total rotor area and is the average pressure change over the actuator disk [27], as shown in equation (8.4). Makani has a total airborne mass of 1732 kg and 8 rotors with a diameter of 2.3 m [14].

$$D_L = \frac{m}{N_{rotors}\frac{1}{4}\pi d^2} \tag{8.4}$$

Resulting in a disk loading, D_L, of 52 kg/m^2.

Using this disk loading and the mass of the airborne element, the total required rotor area can be calculated. Using this total area and the design requirement where the airborne element has to be able to land with 2 engines inoperable, the required rotor radius for take-off can be calculated.

8.2. Main Wing Aerodynamic Relations

This section discusses the aerodynamic design of the main wing(s). First, the airfoil is selected on the basis of the optimisation of the lift and drag coefficient. Using the selected airfoil, the effect of stacking multiple wings is analysed. Lastly, the sizing relations for the main wings are established.

8.2.1. Airfoil Selection

In order to maximise the parameters mentioned in chapter 10,equation (7.6). As seen in equation (7.7), an airfoil with a high maximum lift coefficient should be selected, for a higher designed lift coefficient. Therefore, a multi-element airfoil is chosen to increase the maximum lift coefficient. An optimal airfoil for rigid wings in AWES, [25], has been selected and is displayed in figure 8.1.

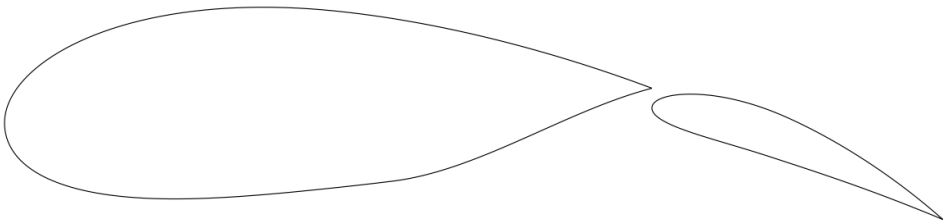

Figure 8.1: Cross section of the selected airfoil design [25]

8.2.2. Effect of stacking wings

For the airborne element, a configuration with stacked wings is possible. Therefore, the interaction should be looked at. Due to the stacking of airfoils, the lift coefficient is estimated to have a loss of 20%, [28]. As seen in Equation (8.5), the influence of multiple wings is estimated. A decrease in C_L causes a decrease in the lift-induced drag, however, the parasitic drag is estimated to increase by 50% per stacked wing, [29], as can be seen in Equation (8.6).

$$C_L = C_{L_{airfoil}} \cdot 0.8^{N_{wings}-1} \tag{8.5}$$

$$C_{d_0} = C_{d_{0_{airfoil}}} \cdot 1.5^{N_{wings}-1} \tag{8.6}$$

The parasitic and lift-induced drag are summed to calculate the total airfoil drag coefficient, equation (8.7).

$$C_{D_{airfoil}} = C_{d_0} + \frac{C_L^2}{\pi ARe} \tag{8.7}$$

The changes in lift coefficient and drag coefficient due to the angle of attack per stacking option of the wing are visualised in figure 8.2 and figure 8.3 respectively.

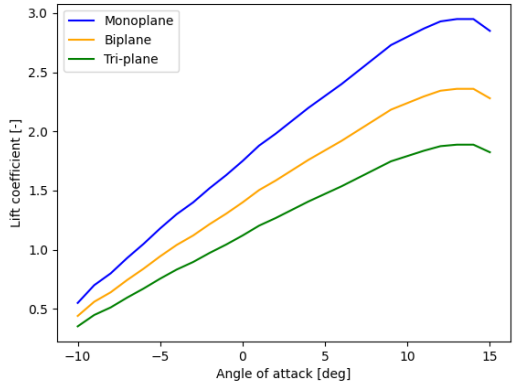

Figure 8.2: α vs C_L

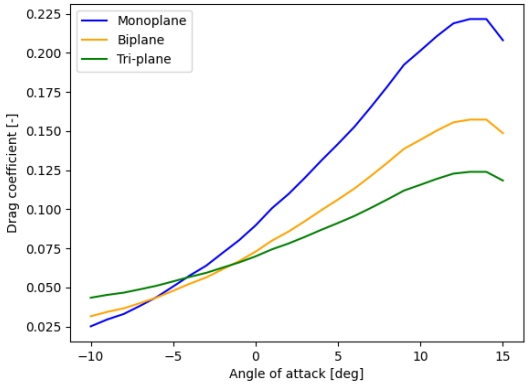

Figure 8.3: α vs C_D

8.2.3. Effects of the flight path on the airfoil characteristics

Along the flight path, the angle of attack of the incoming air, α, changes. This results in a change in the lift coefficient, as well as the drag coefficient. Thus, the power optimisation is dependent on α, this is visualised in figure 8.4. The maximum, i.e. the most optimal, angle of attack is denoted with 'x', which occurs for the airfoil drag coefficient at a lower angle of attack than for the total drag coefficient.

Optimal power generation increases with the stacking of wings. It is clear that optimal power generation occurs at the maximum lift coefficient; however, during flight, it is not optimal to fly at $C_{L_{max}}$. Note that the drag coefficient of the pylons needed to hold the stacked wings is not taken into account.

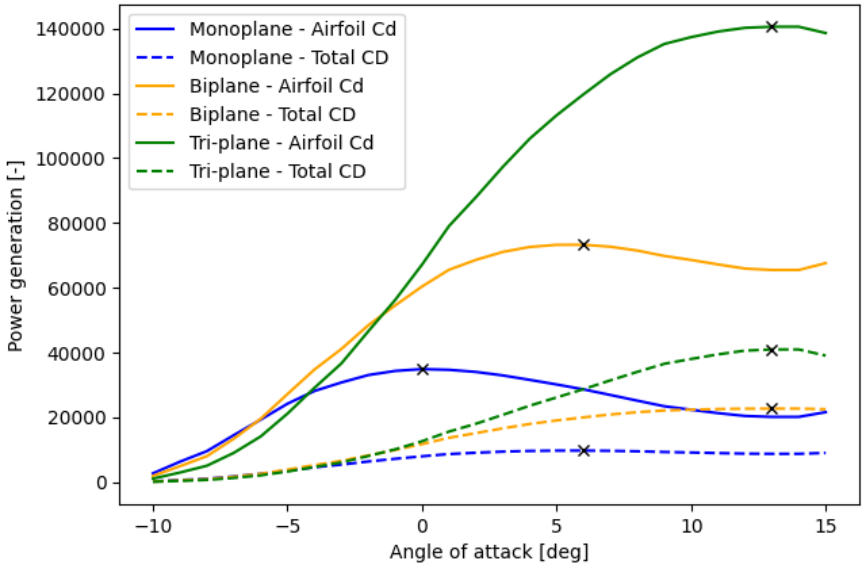

Figure 8.4: α vs Power optimisation graph

8.2.4. Main Wing Sizing

The geometry of the wing can be calculated as followed. Depending on the number of wings, (monoplane, biplane, triplane, etc.), the area per wing can be calculated. The total surface area, A, is the sum of the surface area of the main wing(s) and the horizontal tail. With the given aspect ratio, AR, the wingspan, b, and chord, c, of the main wing(s), can be calculated.

$$S = N_{wings} S_{wing} + S_{tail_h} \tag{8.8}$$

$$AR = \frac{b^2}{S_{wing}} = \frac{b}{c} \tag{8.9}$$

The airfoil mentioned above, figure 8.1, has a maximum thickness to chord ratio, $\frac{t}{c}$, of 29%.

8.3. Main Wing Structural Relations

A model for the analysis of the wings is established with the use of the calculations obtained from MIT[2]. Alongside, a few assumptions are made to simplify the calculations:

Assumptions

- The dimensions of the wings are constant over the wingspan
- All stacked wings bend at the same rate
- The lift can be approximated as a uniform distribution for a constant chord
- Material properties are constant over the wing
- The thin-walled approximation can be applied to the wing
- The weight of the rotors and wings is negligible compared to the lift
- The mass of the wing is split into the mass of the skin and the mass of the wing box

Using these assumptions, a simplified model can be made to perform the analysis, shown in figure 8.5.

[2]MIT Wing Bending Calculations [Cited 5 June 2023]

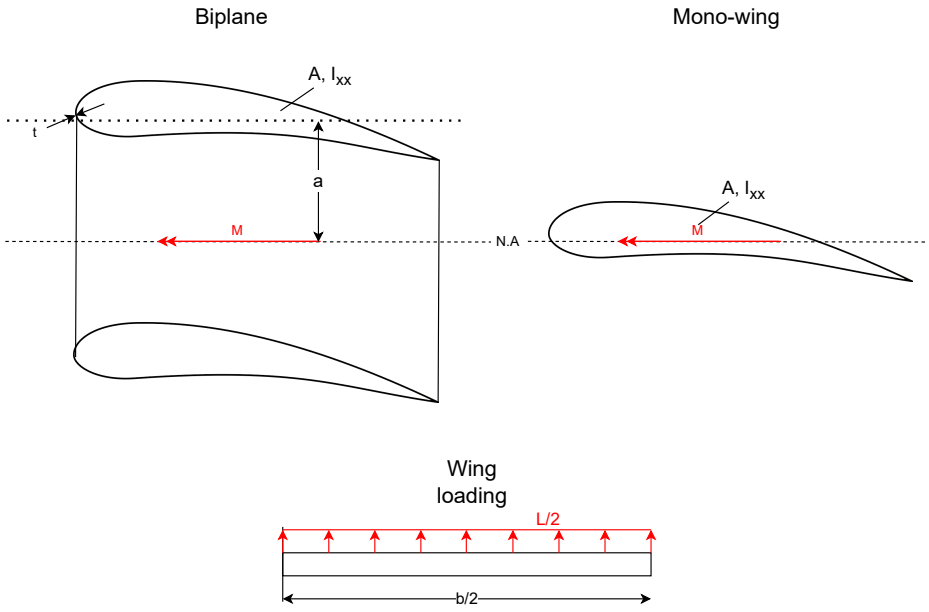

Figure 8.5: A simplified model for wing analysis.

From the model, it is established that, for most airfoils, the cross-sectional area A and the area moment of inertia I can be estimated using equation (8.10) and equation (8.11):

$$A \simeq K_A ct = K_A c^2 \tau \tag{8.10}$$

$$I \simeq K_I ct(t^2 + h^2) = K_I c^4 \tau(\tau^2 + \varepsilon^2) \tag{8.11}$$

where c is the chord, t is the max thickness of the airfoil, $\tau = t/c$ the thickness to chord ratio, h is the max camber, $\varepsilon = h/c$ the camber to chord ratio, $K_A \simeq 0.60$, and $K_I \simeq 0.036$. These equations are applicable to solid airfoils.

To approximate the I for a hollow airfoil, using the thin-walled approximation, equation (8.13) can be derived from equation (8.11):

$$I_h = K_I \tau(\tau^2 + \varepsilon^2)(c^4 - (c - 2t_{skin})^4) \tag{8.12}$$

$$I_h \simeq 8K_I c^3 t_{skin} \tau(\tau^2 + \varepsilon^2) \tag{8.13}$$

where t_{skin} is the thickness of the skin. To calculate the cross-sectional area, the same method can be used on equation (8.10) to get equation (8.15):

$$A_h = K_A \tau(c^2 - (c - t_{skin})^2) \tag{8.14}$$

$$A_h \simeq 4K_A \tau c t_{skin} \tag{8.15}$$

Using this area, the mass can be estimated using equation (8.16)

$$m_{skin} = \rho A b = 4\rho K_A \tau c t_{skin} b \tag{8.16}$$

However, this mass is not taking into account the wing box. To do this, the wing is analysed for bending resistance and the equivalent skin thickness, t_e, of the wing without a wing box is found. From here, the mass of the total wing, m_{tot} is calculated for t_e using equation (8.16). This is done by combining equations (8.17) to (8.19),

$$\sigma_{z,max} = \frac{M y_{max}}{I_{xx}} = SF\sigma_y \tag{8.17}$$

$$M = \frac{Lb}{8} \tag{8.18}$$

$$y_{max} = \begin{cases} \frac{c\tau}{2} & \text{if mono-wing,} \\ a + \frac{c\tau}{2} & \text{if biplane} \end{cases} \tag{8.19}$$

Together with equations (8.13) and (8.15), and using the parallel axis theorem. Then equation (8.20) will give the mass fraction of the skin with respect to the total mass of the wing:

$$\frac{m_{skin}}{m_{tot}} = \frac{t_{skin}}{t_e} = \begin{cases} \frac{128 SF\sigma_y K_I c^2(\tau^2+\varepsilon^2)}{Lb} t_{skin} & \text{if mono-wing,} \\ \frac{64 c\tau S_F \sigma_y (2K_I c^2(\tau^2+\varepsilon^2) + K_A a^2)}{Lb(a+\frac{c\tau}{2})} t_{skin} & \text{if biplane} \end{cases} \tag{8.20}$$

with S_F a safety factor as a design variable, σ_y the yield strength of the selected material, L the lift generated by the wing, b the wingspan, and a, the distance from the chord line of the wing to the neutral axis. From this, the mass fraction of the wing box can be found with equation (8.21):

$$\frac{m_{wb}}{m_{tot}} = 1 - \frac{m_{skin}}{m_{tot}} \tag{8.21}$$

From here the mass of the wing box can be estimated by multiplying it by the total mass. These methods can also be applied to the calculations of the horizontal tail wing.

8.4. Tether Relations

The tether is both a load-carrying component, as well an electric conductor. This section will show the sizing relations for both, it starts with the load-carrying part and follows with the conducting.

8.4.1. Tether Load Carrying Sizing

The tether connects the airborne element with the seaborne element, causing a force on the airborne element. The tension in the tether will be calculated with Equation (8.22), [21], with a safety factor of 30 %, [14].

$$F_T = \frac{2}{9}\rho A V_{wind}^2 \cos^2(\theta) C_L \frac{C_L}{C_D} \cdot \text{Safety factor} \tag{8.22}$$

The diameter of the structural part of the tether can be calculated, equation (8.23), which includes the yield strength of the material [30].

$$d_{tether_{structural}} = \sqrt{\frac{4F_T}{\pi\sigma}} \tag{8.23}$$

8.4.2. Tether Conductor Sizing

First, the assumptions are stated.

Assumptions

- The tether conductor voltage is 4000 V
- The total electrical cable diameter is twice the conductor diameter
- The insulation material of the conductor cable is polyethylene
- The conductor temperature is 20 $^{\circ}C$
- The conductor material is uniform
- The tether efficiency will be designed to be 98%

The tether conductor size depends on the thermal limit of the conductor, which is the maximum heat that can be generated in the conductor. The heat generated in a conductor is directly proportional to the Ohmic power loss. Determining the thermal limit of a conductor is a complex problem which depends on the heat dissipation of the conductor. This analysis is deemed too complex for a preliminary design, so an assumption for the maximum heat losses is made. Bauer and Kennel [31] uses a tether efficiency η_{te} of 98%, which means that 2% of the power is lost to heat generation. This value will also be used in this analysis, however, it must be noted that the tether efficiency dictates tether mass and diameter. This means that there is a trade-off between heat losses, gravity losses and drag losses of the tether where an optimum power can be found.

For the conductor sizing, an equation for conductor area must be derived. For this, firstly the definition of power loss is used. Equation (8.24) shows two definitions of power loss which can be equated to each other.

$$P_{loss} = (1 - \eta_{tether})P_{tether} = I^2 R_{tether} \quad \rightarrow \quad R_{tether} = \frac{(1 - \eta_{tether})P_{tether}}{I^2} \tag{8.24}$$

Next, a different expression for the tether resistance can be derived. Assuming that the tether conductor consists of an even number of parallel conducting wires of which half consists of positive wires and half consists of negative wires. Then, the total resistance of the tether can be expressed by equation (8.25) [31].

$$R_{tether} = 4\frac{R_{cw}}{n_c} \tag{8.25}$$

Here, R_{cw} is the resistance of one conducting wire. This resistance is a function of the wire material resistivity ρ_{alu} and the geometry of the wire (length L_{cw} and cross-sectional area A_{cw}). This relation is shown in equation (8.26).

$$R_{cw} = \rho_{alu}\frac{L_{cw}}{A_{cw}} \tag{8.26}$$

Then substitution of equation (8.26) into equation (8.25) results in equation (8.27)

$$R_{tether} = 4\frac{\rho_{alu}L_{cw}}{n_c A_{cw}} \tag{8.27}$$

Equating equation (8.27) to equation (8.25) and rewriting results in an equation for total conductor area equation (8.28), where the total conductor area is the conductor area of a single wire multiplied by the number of wires.

$$A_{conductor} = n_c A_{cw} = 4\frac{\rho_{Al} L_{cw} I^2}{(1-\eta_{te}) P_{tether}} \tag{8.28}$$

Here, η_{te} is the tether conduction efficiency and ρ_{alu} is the resistivity of aluminium. The current I can then be determined using equation (8.29), using the assumed tether voltage of 4000 V from chapter 11.

$$I = \frac{P_{tether}}{V} \tag{8.29}$$

As discussed in section 11.2, the power transmitted in the tether is not the same as the power generated by the generators. There are losses in both the generators and the motor controllers induce losses. The effect of this is shown in equation (8.30).

$$P_{tether} = P_{peak} \eta_{motor} \eta_{controller} \tag{8.30}$$

The values for η_{motor} and $\eta_{controller}$ are discussed in section 11.2. The conductor length can be determined using equation (8.31). In this equation, $coiling$ is a scaling factor which takes into account the additional length of the conductors compared to the tether length due to coiling. Coiling is required since the conductors should never be subject to tension to avoid the risk of them breaking. This means that when the structural tether elongates due to strain, the coiled conductors should be able to elongate as well. The coiling factor is determined by finding the maximum possible strain of the tether. For the chosen tether material (Dyneema), it was found that the strain at the ultimate load is approximately 0.037 [3]. To be conservative, a coiling factor of 1.04 is chosen, which means the structural tether will fail before strain can affect the conductors.

$$L_{cw} = L \cdot coiling \tag{8.31}$$

Now, an estimate for the total conductor area can be found from the peak power of the flight path. Next, the number of electrical cables around the structural tether and their diameter must be determined. For this, equation (8.32) and equation (8.33) [31] are used. These equations are trigonometric relations of the distance between a variable amount of wires around a structural core, which can be seen in figure 8.6.

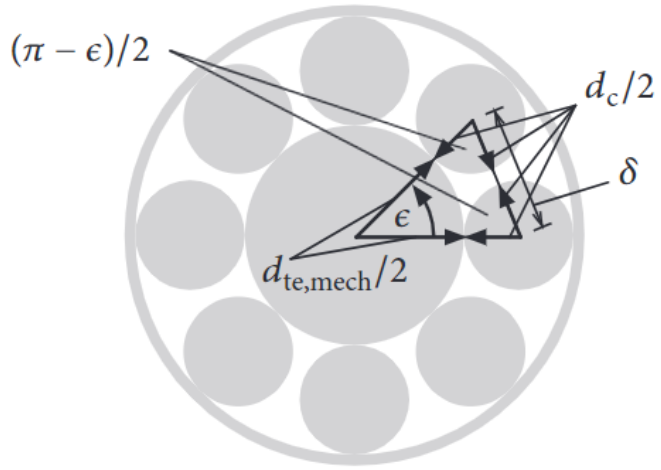

Figure 8.6: Trigonometry of the distance between conductor wires around a structural tether [31]

It can be seen that the minimum distance between the conducting wires will be equal to the diameter of the conducting wires. Otherwise, they will overlap. It is desirable to space the tether conductors as efficiently as possible, in order to get the smallest tether diameter and thus the smallest tether drag. For this reason, the cable distance δ should be as close to the electrical cable diameter d_c as possible. To find this, the cable diameter and cable angle ϵ are calculated for a range of numbers of cables n_c. Then, equation (8.32) is used with these values to calculate the cable distance and the maximum number of cables is determined for which the cable distance is still bigger than the cable diameter.

$$\frac{\delta}{\sin(\epsilon)} = \frac{d_{te,mech}/2 + d_c/2}{\sin((\pi - \epsilon)/2)} \tag{8.32}$$

To determine the cable angle, equation (8.33) is used. It just divides the total circular angle by the number of cables to find the angle between two cables.

$$\epsilon = \frac{2\pi}{n_c} \tag{8.33}$$

The diameter of a single conductor cable is calculated using equation (8.34) and equation (8.35). Equation (8.34) uses the total tether conductor area of equation (8.28) and divides it over the number of conductors. This circular area is then converted to diameter. Then, equation (8.35) takes into account that the conducting wires also have an insulating layer. It is assumed that this layer doubles the diameter of the conductor wire. This is a conservative assumption, which is deemed acceptable at this stage. In a more detailed stage of development, the minimum thickness of the insulation layer should be investigated.

$$d_{core} = 2\sqrt{\frac{A_{conductor}}{n_c \cdot \pi}} \tag{8.34}$$

$$d_{electrical} = 2d_{core} \tag{8.35}$$

With this method, a minimum conduction wire diameter can be found, which can now be used to find the total tether diameter.

8.4.3. Tether Mass Calculation

After the size of the tether conductors is determined, the mass can be calculated by using the density of the conductor and insulator materials. The conductor material is aluminium.

The insulating material is assumed to be polyethylene. Equation (8.36) can then be used to calculate the tether conductor mass.

$$m_{te,c} = L_{cw}(\rho_{Al} A_{conductor} + \rho_{PE}(A_{cables} - A_{conductor})) \tag{8.36}$$

Here, L_{cw} is the conductor wire length (equation (8.31)), ρ_{alu} is the density of aluminium, ρ_{PE} is the density of polyethylene, $A_{conductor}$ is the total conductor core area (equation (8.28)) and A_{cables} is the total area of the conductor cables. $A_{conductors}$ can be determined from the conductor wire diameter d_c and the number of conductors n_c.

Then, the tether conductor mass can be added to the structural tether mass to find the total tether mass.

8.5. Aerodynamic Tail Sizing Relations

The tail consists of two parts, the horizontal tail and the vertical tail(s). Depending on the configuration of the tail, (conventional, boom tail, T-tail, etc), the geometry can differ. The area of both horizontal and vertical, A_{tail_h} and A_{tail_v}, respectively, is assumed to be a percentage of the area of the main wing.

$$S_{tail_h} = 20\% \text{ of } S_{wing} \tag{8.37}$$

$$S_{tail_v} = \frac{16\% \text{ of } S_{wing}}{N_{tails_v}} \tag{8.38}$$

To calculate the length between the main wing(s) and the tail, Equations (8.39) and (8.40) are used [32]. Using an estimation of the volume coefficients the required length of the tail is estimated. This will be the largest distance that is calculated for l_{tail_h} and l_{tail_v}.

$$V_h = \frac{S_{tail_h} l_{tail_h}}{S_{wing} c} \tag{8.39}$$

$$V_v = \frac{A_{tail_v} l_{tail_v}}{A_{wing} b} \tag{8.40}$$

To estimate the geometry of the tail, Equations (8.41) and (8.42), are used. It is estimated that the chord of the horizontal tail is equal to the chord of the vertical tail, $c_{tail_h} = c_{tail_v}$, for each possible tail configuration. With the aspect ratio of the horizontal tail being half of the aspect ratio of the wing, [32], the sizing can be calculated.

$$AR_{tail_h} = \frac{b_{tail_h}^2}{S_{tail_h}} = \frac{b_{tail_h}}{c_{tail_h}} \tag{8.41}$$

$$AR_{tail_v} = \frac{b_{tail_v}^2}{S_{tail_v}} = \frac{b_{tail_v}}{c_{tail_v}} \tag{8.42}$$

8.6. Tail Boom Sizing Relations

Another important structural component is the connection between the main wing and the tail, here called the tail boom. For this analysis, some simplifying assumptions need to be made as well:

Assumptions

- The main wing structure is a rigid connection
- Bending, angular tip deflection and buckling are the limiting factors
- The weight of the boom(s) is/are negligible
- The tail boom has a circular, hollow cross-section
- The thin-walled approximation can be applied
- The lift generated by the horizontal tail is distributed evenly over the number of booms
- The length of the tail boom is a function of the main wing surface area
- The top section of the tail boom can be approximated as a thin plate

With these assumptions, a simplified representation can be made of the tail boom, shown in figure 8.7

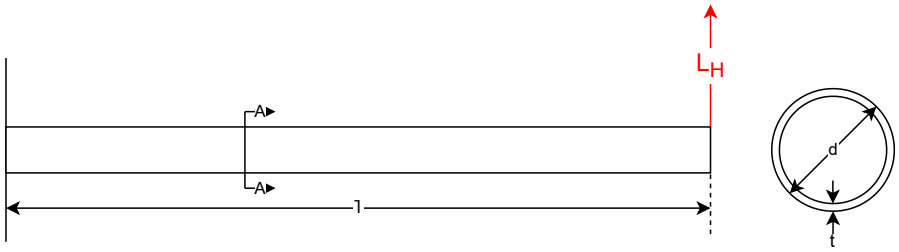

Figure 8.7: A simplified representation of the tail boom.

with L_H the lift generated by the horizontal tail, l the length of the boom, d the diameter of the boom, and t the wall thickness. As stated in the assumptions, the limiting cases are bending, angular tip deflection, and buckling. The angular deflection is calculated using equation (8.43):

$$\theta_{max} = \frac{L_H l^2}{2EI_{xx}} \tag{8.43}$$

Using equations (8.17) and (8.43) allows for the derivation of the diameter as a function of the thickness, as shown in equations (8.44) to (8.51):

$$k_1 = \frac{L_H l^2}{2E\pi\theta_{max}} \tag{8.44}$$

$$k_2 = \frac{L_H l}{2SF\sigma_y} \tag{8.45}$$

$$I_{xx,1} \geq k_1 \tag{8.46}$$

$$\frac{I_{xx,2}}{d} \geq k_2 \tag{8.47}$$

$$I_{xx} = \frac{\pi d^3 t}{8} \tag{8.48}$$

$$d_1 \geq \sqrt[3]{\frac{8k_1}{\pi t}} \tag{8.49}$$

$$d_2 \geq \sqrt{\frac{8k_2}{\pi t}} \tag{8.50}$$

$$d = \max(d_1, d_2) \tag{8.51}$$

As can be seen from equation (8.51), the maximum diameter is selected for the final diameter. This is because the maximum d will allow for both the bending and the angular deflection resistance.

The buckling of the boom is also considered. By assuming that the top of the tail boom can be approximated as a thin plate, equation (8.52) can be used [33]:

$$\sigma_{cr} = \frac{\pi^2 kE}{9}\left(\frac{t}{b}\right)^2 \tag{8.52}$$

σ_{cr} can be set to be equal to the maximum bending stress the airborne element experiences, while b can be set as a fraction of the total diameter:

$$\sigma_{cr} = SF\sigma_y \tag{8.53}$$

$$b = \frac{d\phi}{2} \tag{8.54}$$

$$k(d) = 1.065\left(\frac{\phi}{L}\right)^2 d^2 + 0.608 + 1.064\left(\frac{L}{\phi}\right)^2 \frac{1}{d^2} \tag{8.55}$$

Equation (8.55) is found for the clamping case where three sides are fixed and the last one is free [33]. By solving equation (8.52) for t, equation (8.56) for the thickness as a function of the diameter can be found:

$$t = \frac{3}{2\pi}\phi d\sqrt{\frac{SF\sigma_y}{Ek(d)}} \tag{8.56}$$

Equation (8.51) is then substituted into equation (8.56) and solved for t, after which the diameter d can be found.

After optimising the dimensions for the boom, its mass can be calculated using equation (8.57):

$$m = \pi\rho t l d \tag{8.57}$$

Torsion

Should there be only one boom, torsion will also need to be taken into account, due to the force generated by the vertical tail. A simple overview of the model used for analysis is given in figure 8.8.

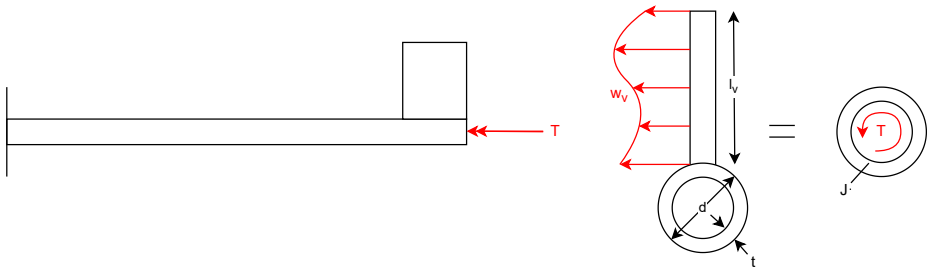

Figure 8.8: A simplified model for torsion analysis in the tail.

Where T is the torsion generated by the vertical tail, w_v is the lift distribution of the vertical tail, and L_v is the length of the vertical tail.

This torsion will cause shear stress and rotation in the tail boom. The shear stress and rotation generated due to that torsion are given in equations (8.58) and (8.59):

$$\tau_s = \frac{T\rho}{J} \tag{8.58}$$

$$\frac{d\theta}{dz} = \frac{T}{GJ} \tag{8.59}$$

Where τ_s is the shear stress, ρ the radius at which the stress is calculated, J is the polar moment of inertia, $\frac{d\theta}{dz}$ the angular twist per unit length, and G is the shear modulus of the material. The torsion and polar moment of inertia are calculated using equations (8.60) and (8.61):

$$T = w_v L_v a \tag{8.60}$$

$$J = \frac{\pi t d^3}{4} \tag{8.61}$$

8.7. Airborne Element Electronics Mass Estimation

Next to the tether conductor mass, the mass of the electronic components of the airborne elements must be estimated. The most important electronic components are the motor/generator. To estimate their mass, existing motors were investigated.

Assumptions

- The motor/generators make up 50% of the total electronics mass of the airborne element
- The produced power has a power factor of 1

Three companies have been found that produce the type of motor selected: Yasa[3], Emrax[4] and Beyond[5]. The continuous peak power and mass of each model produced by each company were collected to determine an average power-to-mass ratio. With this ratio, a motor mass estimation can be made using the peak power that the engines need to produce. This relation is shown in equation (8.62).

$$m_{\text{motors}} = 0.0003 P_{peak} \tag{8.62}$$

Besides the motor/generators, there are a lot of other electrical components. They include wiring, motor controllers, cooling radiators and pumps, computers for the control system, actuators for the control surfaces, converter and storage (voltage regulation) for the low-voltage network, GPS, communication antennas, sensors like pitot tubes and accelerometers and lights. The design lacks detail at this stage to determine the mass of all these components. For this reason, an order of magnitude estimation is made. It is assumed that the mass of all other electronic components is equal to the mass of the motor/generator because these are heavy components. In a later design stage, the electronics mass can then be iterated when a more detailed design is available. With this assumption, the following equation for the electronic mass of the airborne system can be defined:

$$m_{\text{ab,el}} = 2 m_{\text{motors}} \tag{8.63}$$

Combining equation (8.62) and equation (8.63) gives a relation between electronics mass and peak power.

8.8. Material Selection for Components

Now that analysis of different material properties and structures has been performed, a selection of materials can be made for the different components. An overview of the main materials used for the components, and the justification, is shown in table 8.1.

[3] yasa.com [Cited 8 June 2023]
[4] emrax.com [Cited 8 June 2023]
[5] beyondmotors.io [Cited 8 June 2023]

Table 8.1: An overview of the main materials selected for system components.

Section	Material	Justification
Wings (Main & Tail)	Aluminium 7075-T6	Reasonable corrosion resistance, relatively cheap, small mass
Struts (if applicable)	PPS 30% CF	light, strong, mostly in tension/compression
Rotors	Aluminium	Used in most aerospace engineering cases
Tether	Dyneema	Very strong in tension, light
Fuselage	Aluminium 7075-T6	Reasonable corrosion resistance, relatively cheap, small mass
Nacelle of rotor	Carbon Fibre-epoxy	Used by modern propeller aircraft

9
Airborne Design Code

This chapter introduces the calculation tool used in the design process in section 9.1 and its verification and validation in section 9.2. The calculation tool follows a systematic approach, selecting an airfoil and approximating drag based on mass and velocity. Subsequently, it iterates to compute attributes of the subsystem for better convergence. In V & V, unit tests have been conducted, covering various aspects of the code's functionality. Validation is performed by comparing results with existing AWES, namely Makani and Ampyx. Challenges in mass and rotor sizing require further some refinement and readjustment. The accuracy of the calculation tool can be improved by incorporating comparable aircraft data and refining rotor sizing using data from drone technology. Overall, the calculation tool enhances the design process as well as its accuracy and reliability.

9.1. Calculation Tool Description

The structure of the report on the single system design reflects the structure of the code with a small exception. First, the airfoil is chosen to provide lift and drag coefficients of the wing. The drag of the other components is found by approximating the mass and nominal velocity of the craft. Once these attributes are given the surface area and nominal velocity are computed based on the power formula. Then the mass and drag coefficient are computed by sizing each subsystem, which gives the option to reiterate with more accurate results. The process is repeated until convergence and is presented on figure 9.1.

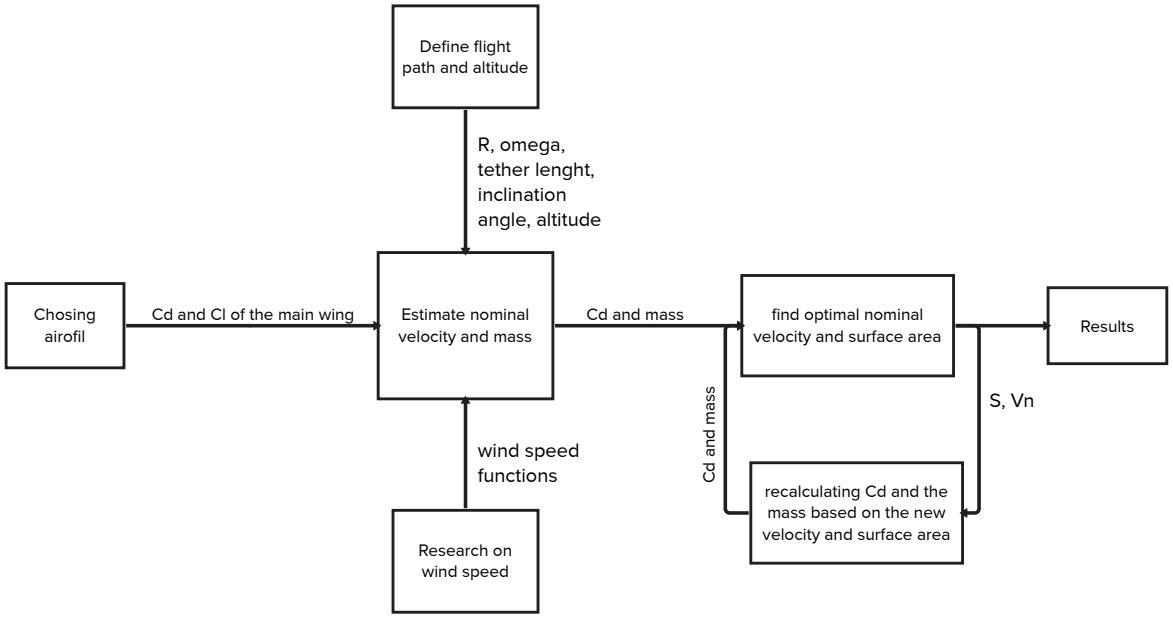

Figure 9.1: Code Structure

The architecture of the code complies with the object oriented standards. The main object is the airborne system that has the objects tether, rotor, tail boom, tail, operations and wind as properties. The rotor also includes the nacelle as its own object and all of them are cross-linked via the airborne object. Each subsystem is sized in its own class and their computations. The

airborne class computes the surface area and velocity, sums the mass aerodynamic values of each subsystem, and has methods to optimise the flight path. Various loss functions are used to check convergence with bounds on the iterations to avoid infinite loops. Every property that is not a parameter and is not defined only by parameters, is updated every time they are called. Resulting in coherence of the values and a non-linear computational architecture.

9.2. Code Verification & Validation

The code will be verified by using unit tests. The tests and their results are shown in section 9.2.1. The validation process based on existing AWES is discussed in section 9.2.2.

9.2.1. Sizing Tool Unit Tests

Due to the time constraint, the verification and validation of the 600-line-long code is incomplete. The unit tests do not cover every part of it, however, two scripts of calculations were concurrently established by two members to increase certainty. Having stated this, 50 unit tests are utilised accompanied by the derivations and references of the implemented relations to support. The unit tests and their results are presented in table 9.1.

Table 9.1: Table of Unit Tests

Unit test id	Description	Justification	Result
operations-01	g is almost equal 9.81 m/s^2	correct value of g is fundamental	pass
operations-02	altitude must be higher than 100 m	operability falls apart below 100 meters	pass
operations-03	R is greater than 20 m	so that the turn are not high loading	pass
operations-04	omega is greater than 20 degrees	so that the parameterised flight path assumptions of small angles are valid	pass
material-01	Aluminium density is 2810 kg/m^3	checks the correct values	pass
material-02	aluminium E is 71.7 GPa		pass
material-03	aluminium yield strength is 462 MPa		pass
material-04	carbon fibre density is 1540 kg/m^3		pass
material-05	material definition results in the right properties	checks if setting the values are correct	pass
tether-01	tether length is greater than the nominal altitude	as the inclination angle has to be higher than 90 degrees, tether length also has to be higher than the altitude	pass
tether-02	tether diameter is greater than 1 cm	below 1 cm the diameter is highly unrealistic	pass
tether-03	cross sectional area of the cable is smaller than of the entire tether	the cables are inside the tether, therefore this relation should hold	pass

Table 9.1: Table of Unit Tests

Unit test id	Description	Justification	Result
tether-04	length of cable is higher than of the tether	the cable is twisted around the tether, therefore its length should also be higher	pass
tether-05	structural diameter must be at least half of the cable diameter	so the cables can be stacked around the structural component	pass
			pass
nacelle-01	the length is higher than the height	so that the nacelle is elongated	pass
nacelle-02	the length is higher than the width		pass
			pass
wing-01	surface area is almost equals to wing span times chord length	constant c is assumed so it should hold	pass
wing-02	chord length is higher than thickness of the airfoil	because airfoils have elongated shapes	pass
wing-03	lift is higher than the weight	because the tether is pulling down the system as well	pass
wing-04	mass of the wing should be positive	sanity check on the sign of the mass	pass
wing-05	mass of the wing box shall be positive	checks if calculated equivalent thickness is positive	pass
wing-06	cross sectional area is lower than the chord times airfoil thickness	the airfoil has to fit into a rectangle with dimension of the chord and airfoil thickness	pass
wing-07	position of its centre of mass should be within the chord length	because the leading edge is the most forward position of the aircraft	pass
tail-01	horizontal tail surface area is larger than the vertical	because a larger contribution is required to the pitching moment.	pass
tail-02	airfoil thickness of horizontal tail plane is lower than its chord length	because the airfoil is elongated	pass
tail-03	airfoil thickness of vertical tail plane is lower than its chord length		pass
tail-04	tail mass is lower than the wing mass	sanity check on magnitudes	pass
tail-05	tail length is lower than main wing span		pass
			pass
boom-01	thickness of the skin is larger than 1 mm	production limits	pass
boom-02	boom diameter is less than thickness of the main wing	sanity check on magnitudes	pass

Table 9.1: Table of Unit Tests

Unit test id	Description	Justification	Result
boom-03	boom cross sectional area of the structure is lower than of the wing		failed and got fixed
boom-04	boom mass is lower than wing mass		pass
			pass
strut-01	strut cross sectional area should be less than of the boom	the struts should be a smaller element than the boom	pass
strut-02	strut height should be greater than the diameter of the rotors	so the rotors do not collide	pass
strut-03	mass of a strut should be less than of the boom	the strut has to be lighter than the boom	pass
			pass
airborne-01	the entire mass is greater than of the wing	as every component have to be positive	pass
airborne-02	glide ratio is greater than 1	as if not met the design is unrealistic as cl should be greater than cd	pass
airborne-03	glide ratio is lower than 50	it would be unrealistic to achieve a glide ratio of a glider	pass
airborne-04	position of centre of gravity is positive	as we measure from the leading edge no component can have a negative x position	pass
airborne-05	surface area is greater than the weight over dynamic pressure	because more excess lift has to be generated to generate power.	pass
airborne-06	delta is positive	delta accounts for an extra pitch angle to match affects of weight, which has to be positive	pass
airborne-07	delta is lower than 90 degrees	as that would stall the aircraft	pass
airborne-08	γ_t is lower than 1	so that the cd of the rotors is lower than of the entire system	pass
airborne-09	mach number of the flight is lower than 0.3	so incompressible assumptions are valid	pass
airborne-10	γ_{out} is greater than or equal to 0	otherwise it would not be a loss term	pass
airborne-11	γ_{out} is lower than 1	otherwise the system would consume power instead of generating it	pass
			pass
altitude_set-01	setting altitude changes the property of operations instance	so setting altitude works properly	pass
altitude_set-02	altitude of the operations assigned to the instances such as boom, wing, tail, tether, rotor, airborne and strut changes as well		pass
			pass

Table 9.1: Table of Unit Tests

Unit test id	Description	Justification	Result
omega_set-01	setting omega changes the property of operations instance the changes carry through the same instance carried through properties	so setting omega works properly	pass
omega_set-02			pass

9.2.2. Sizing Tool Validation

Validation can be done by comparison to existing AWESs like Makani, Ampyx and KiteKraft. Makani en Ampyx have a mono-plane design, meaning that the calculations for a mono-plane can be validated, KiteKraft on the other hand has a biplane design, which makes use of different sizing calculations.

The Makani M600 was designed to generate 600 kW, however, the M600 only generated 40 kW when in operation[14]. For their rated power, airfoil characteristics and flight performance. The code resulted in an overestimation of the mass of the airborne element and the rotor diameter. Note, the mass estimation is different for mono-plane (Makani) and biplane (Deep WattAir).

Ampyx and KiteKraft have not released any data on their prototypes needed for validation. Two sub-systems, mass and rotor sizing, deviated heavily compared to the other values, such as sizing, therefore, it is needed that both sub-systems are re-iterated.

The mass of each sub-part, such as wings, empennage, and structures, can be validated with the use of comparable aircraft component mass and sizing. Relations between the sizing and the mass of each sub-part combined with the materials and structural forces should give a more accurate representation in the code.

Due to the limited knowledge and values for rotor sizing for power generation and vertical take-off and landing, the calculations are preliminary. The rotor sizing can be validated with the use of the rotors of drones. Implementing the found relations in the code should result in a more accurate estimation.

10 Airborne & Tether Design

The Deep WattAir single system consists of the airborne element, tether, and seaborne element. First, the airborne and tether are designed with the 'airborne design code', chapter 9. Note, all values are preliminary due to inaccuracies and simplification in equations.

The parameters that were used as inputs for the design are shown in section 10.1. These inputs then give a configuration sizing which is discussed in section 10.2 after which the specifications are given in section 10.3. With these specs, a hardware diagram is made which is shown in section 10.4. Using this airborne design, the generated power is plotted in section 10.5. Due to the varying velocity, the power generation is fluctuating which is shown in section 10.6. The cut-in and cut-out velocities are calculated in section 10.7. Finally, the take-off phase is modelled in section 10.8.

10.1. Airborne Element Design Parameters

The airborne element and the tether are designed based on design inputs. In table 10.1 the inputs for the single system are given.

Table 10.1: Inputs for airborne design

Input parameters	Value	Unit
Power	1	MW
Altitude	200	m
Flight inclination	30	deg
Number of rotors	8	-
Material properties		
Main wing aspect ratio	17	-
Maximum lift coefficient	2.95	-
Zero-lift drag coefficient	0.018	-

10.2. Airborne Element Configuration

The configuration of the airborne element consists of the shape, number of elements, and overall design. A comparison of the mass and the aerodynamic changes due to the number of wings and vertical tails was performed. This concluded that the most optimal power generation will happen with 2 main wings and 2 vertical tails. Therefore, the biplane concept with a boom tail was designed. Given the input of 8 rotors, it was found that placing 4 rotors on each side and stacking 2 wings above each other, gave the least flow interference and is thus most optimal. For structural reasons, struts are placed between the wings, at the rotors and at the tail connection, with 10 struts in total. In figure 10.1, the side, front and top views are shown.

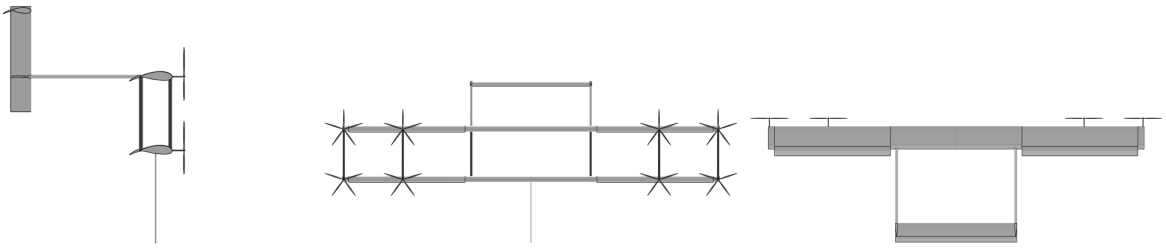

(a) Side view **(b)** Front view **(c)** Top view

Figure 10.1: CATIA drawing of the airborne element and tether

10.3. Airborne Element and Tether Specifications

Given the configuration, the specifications of the single system can be established. The specification, meaning the exact values of the design are split up in forces and sizing of the airborne element and the tether.

Forces acting on the airborne element and tether

The main forces acting on the airborne element are lift, drag and tether tension.

Table 10.2: Force parameters

Parameter	Value	Unit
Lift force	807	kN
Drag force	71	kN
Maximum tether force	69	kN

Sizing of the airborne element and tether

Given the inputs and the equations described in the chapters above, the sizing of the airborne element and the tether can be calculated. In tables 10.3 to 10.8, the sizing of the main wing, tails, boom, rotor, tether and struts are shown.

Table 10.3: Main wing parameters

Parameter	Value	Unit
Aspect ratio	17	-
Surface area	53.6	m^2
Wingspan	30	m
Chord	1.8	m
Wing thickness	0.52	m

Table 10.4: Horizontal tail parameters

Parameter	Value	Unit
Aspect ratio	8.5	-
Surface area	10.7	m^2
Wingspan	9.5	m
Chord	1.1	m
Wing thickness	0.33	m

Table 10.5: Vertical tail parameters

Parameter	Value	Unit
Aspect ratio	1.3	-
Surface area	8.6	m^2
Wingspan	3.8	m
Chord	1.1	m
Wing thickness	0.11	m

Table 10.6: Boom parameters

Parameter	Value	Unit
Boom length	6.2	m
Boom diameter	0.2	m

Table 10.7: Rotor and tether parameters

Parameter	Value	Unit
Rotor diameter	3.2	m
Tether diameter	0.037	m

Table 10.8: Strut parameters

Parameter	Value	Unit
Strut diameter	0.18	m
Strut height	4	m

Mass estimations of the airborne element and tether

The preliminary estimation of the mass is shown in the table below.

Table 10.9: Mass of the airborne element and tether

Element	Value	
Airborne element	2313	kg
Tether	375	kg

10.4. Airborne Element Hardware Diagrams

In the airborne element, electrical components are present. The hardware components; flaps, computer, motor controller, motor for rotors, etc.

The location of the hardware in the airborne element is shown in figure 10.2.

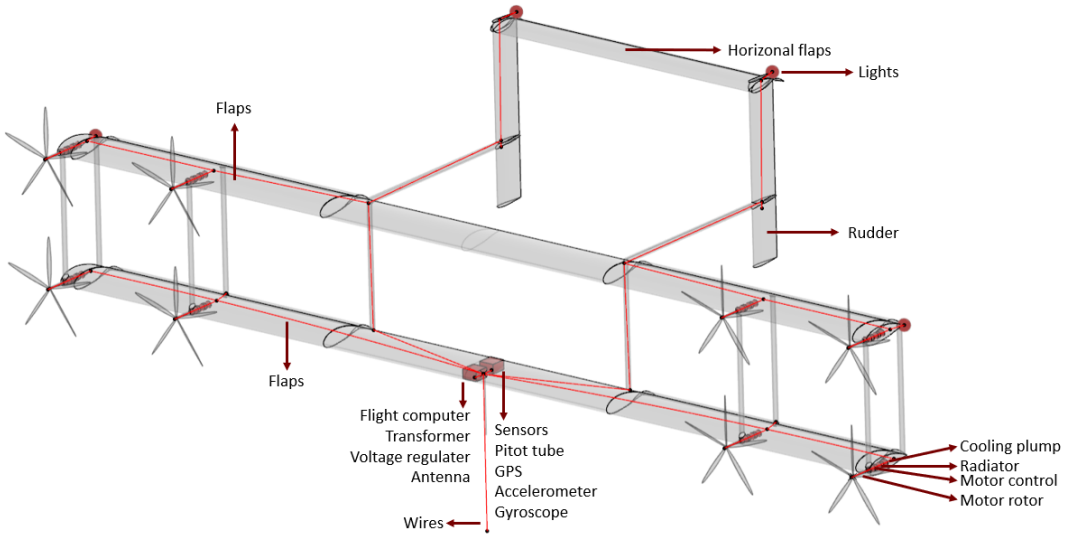

Figure 10.2: Hardware of the airborne element (components not on scale)

10.5. Analysis at Changing Wind Speed

The average power generated, calculated with equation (7.4), is dependent on the wind velocity. At the designed wind velocity of 9.8 m/s at an altitude of 200 m, the average power is 1 MW. The power generated is capped after the design wind speed at 1 MW, due to the fact that the rotors cannot generate more than 1 MW. The capped power generation curve is shown in figure 10.3a. Note, the kink in the curve at 7 m/s is caused by a kink in Δ (angle to counteract the gravity loss), shown in figure 10.3b.

Due to the power equation, it is clear that given the capped power, the lift coefficient of the airborne element can be decreased, which can be done by angling the flaps.

The figure 10.3c shows the change needed in lift coefficient, C_L, for the capped power. Given the changes, multiple different parameters change accordingly; including the drag coefficient C_D, where the $C_{D_{airfoil}}$ and $C_{D_{rotor}}$ change and the tension force in the tether, figure 10.3d and 10.3e respectively.

The tension force in the tether is maximum at the designed wind speed, due to the higher lift coefficient. For safety, the structural part of the tether is designed with a 30% increase in tension force, given a maximum force of 68.5 kN.

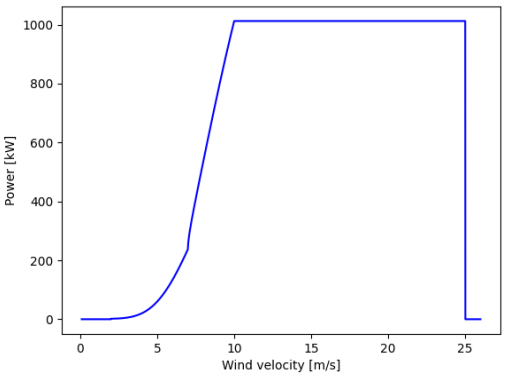

(a) Power generated vs wind velocity

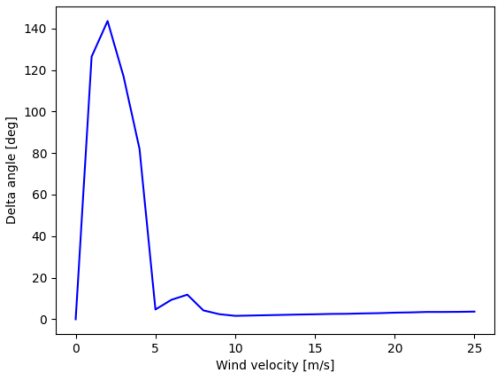

(b) Delta angle vs wind velocity

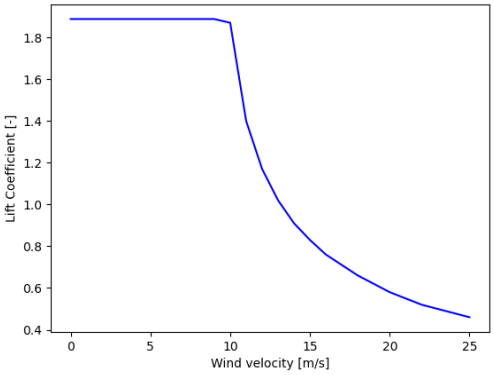

(c) Lift coefficient vs wind velocity

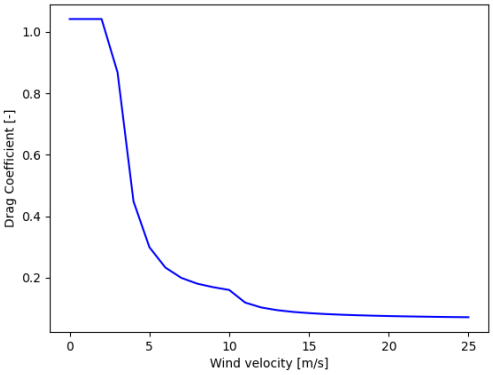

(d) Drag coefficient vs wind velocity

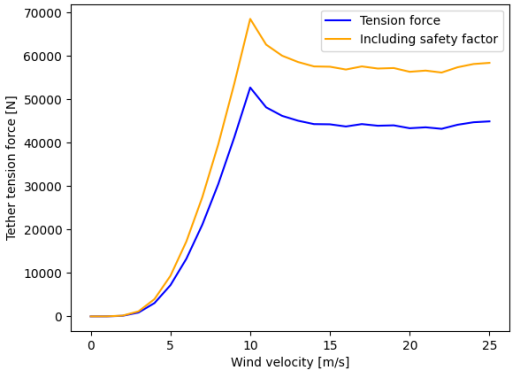

(e) Tether tension force vs wind velocity

Figure 10.3: Changes in parameters due to changes in wind velocity

10.6. Power Generation Variation over Flight Path

The power over the flight path can be analysed by utilising the relations explored in section 7.3. The resulting power curve of one cycle, starting with the right circular section, is displayed in figure 10.4. The figure shows that the power generation is higher at lower altitudes where the velocity is higher but these segments take less time resulting in an extra loss of average power with respect to the average taken spatially.

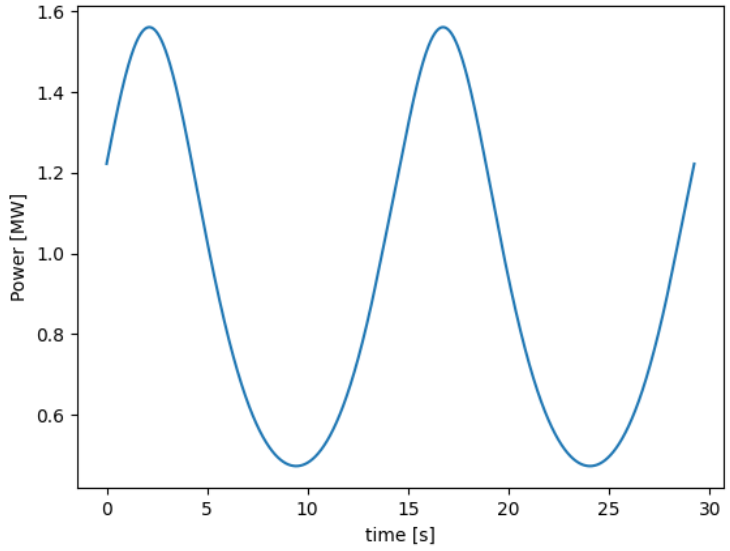

Figure 10.4: Power over the flight path

In addition to that the flight path can be optimised. As mentioned before in section 7.3, R is set as large as possible, while ω can be optimised to achieve minimal required surface area. figure 10.5 shows that ω for our design is optimal with little change around from 68 to 76 degrees. The results comply with intuition increasing omega makes the flight path wider and therefore less efficient because of the decreased angle with respect to the wind. On the other side it is beneficial to spend more time in the middle section which can be achieved by decreasing ω.

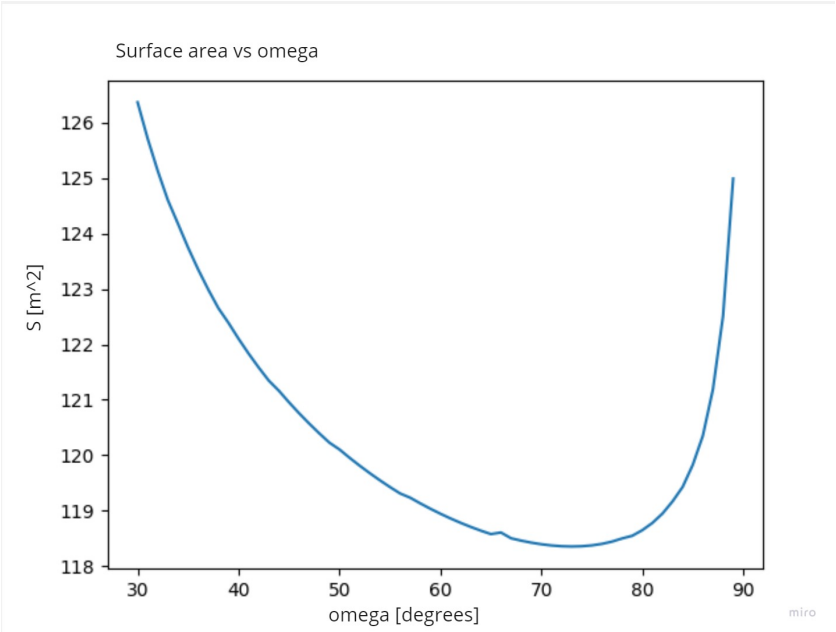

Figure 10.5: Surface area vs ω

10.7. Cut-in and Cut-out Speed

The airborne element cannot fly at all wind speeds, this is at too low or too high speeds. In order to determine the cut-in speed, V_{cut-in}, meaning the minimum wind velocity at which the airborne element is able to fly, the airborne element needs to generate more lift than weight. From figure 10.6, the cut-in speed can be estimated, with the use of Equations (10.1) and (10.2).

The cut-out speed of the system, $V_{cut-out}$, meaning the maximum wind velocity the airborne element is able to fly at is 25 m/s

$$L = W = \frac{1}{2}\rho S V_a^2 C_L \qquad (10.1)$$

$$D = \frac{1}{2}\rho S V_a^2 C_D \qquad (10.2)$$

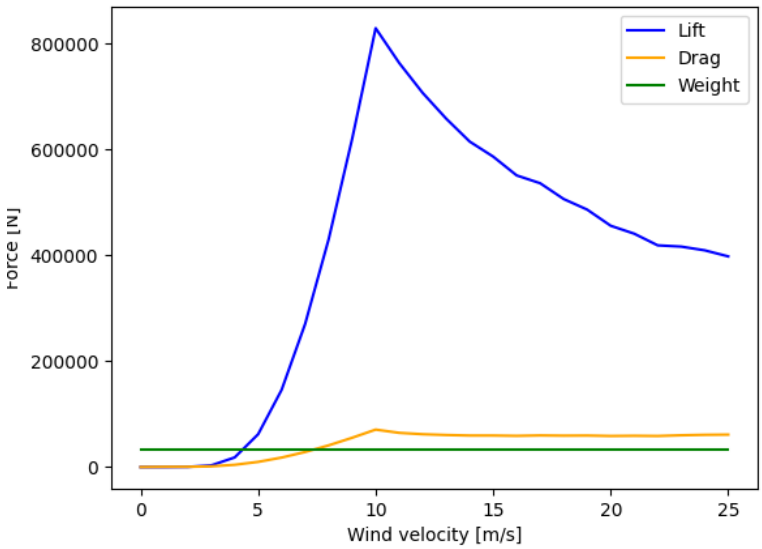

Figure 10.6: Lift, Drag and Weight vs wind speed

10.8. Take-off Phase Estimation

The determination of the thrust is a vital part to ensure the rotors can be sized. Within this section the simplified model to determine the thrust will be provided together with the considerations which are made for simulation.

10.8.1. Model

To ensure the airborne energy unit reaches altitude a vertical take-off and landing system (VTOL) will be made use of. Here thrust will be utilised generated by the rotors (+ motors) to reach operational altitude or return to the station. To ensure the system is able to take-off and land the systems should be sized to ensure sufficient thrust can be provided in a given case in a requested time utilising a set procedure. To analyse the take-off and landing procedure first a simplified 2d free diagram is constructed where only the vertical forces are considered. These vertical forces include the thrust, drag and weight. The diagram can be observed in figure 10.7.

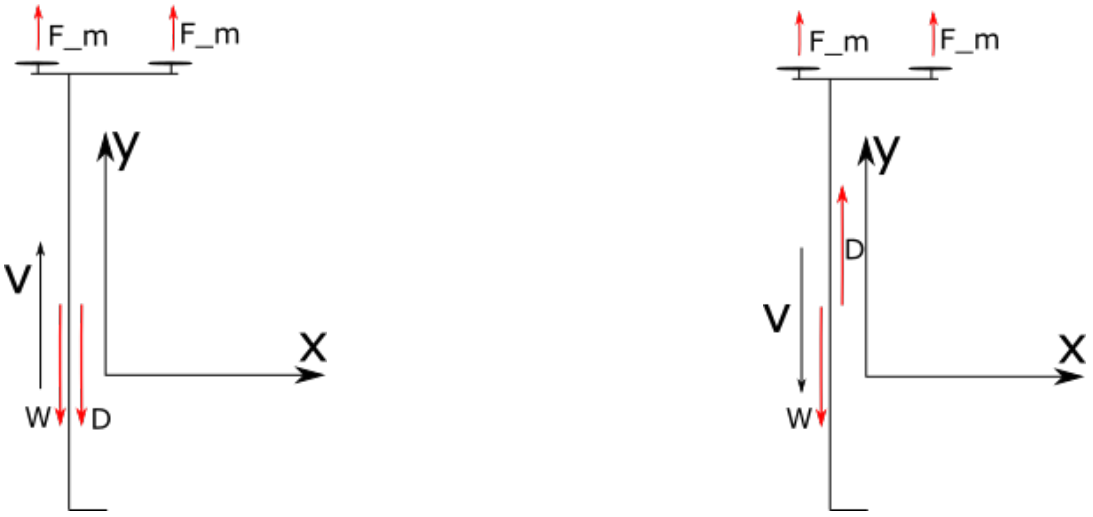

(a) Free body diagram during the vertical take-off (v > 0)

(b) Free body diagram during the vertical landing (v < 0)

Figure 10.7: Free body diagrams required for the sizing of the propulsion required for VTOL

Within figure 10.7 the free body diagram (FBD) case for take-off is included in figure 10.7a and for landing the FBD can be observed in figure 10.7b. In both diagrams the weight is constant, the thrust per engine can be altered and the drag is depended on the vertical velocity.

$$\begin{cases} \sum F_x : F_m n_{engine} - D - W & (figure\ 10.7a) \\ \sum F_x : F_m n_{engine} + D - W & (figure\ 10.7b) \end{cases} \tag{10.3}$$

$$\Rightarrow \begin{cases} \sum F_x : F_m n_{engine} - \frac{1}{2}\rho V^2 S C_D - mg \\ \sum F_x : F_m n_{engine} + \frac{1}{2}\rho V^2 S C_D - mg \end{cases} \tag{10.4}$$

The above equations are static equations (meaning the acceleration is zero). The equations can be rewritten to find the thrust force required for hover (during hover the velocity is zero). For both the take-off and landing procedure the same equation can be setup, as observed in equation (10.5)

$$F_m = \frac{mg}{n_{engine}} \tag{10.5}$$

The above equation provides the minimum thrust required per engine to ensure hover is possible. However to ensure operation altitude can be reached additional thrust is required to induce an acceleration. For this the upwards equation in equation (10.4) can be utilised and made dynamic (sum of forces can be written as acceleration times mass).

$$ma_y = F_m n_{engine} - \frac{1}{2}\rho V^2 S C_D - mg \tag{10.6}$$

$$\Rightarrow \frac{m(a_y + g) + \frac{1}{2}\rho V^2 S C_D}{n_{engine}} = F_m \tag{10.7}$$

In equation (10.7) the thrust per engine required to ensure a specific acceleration that can be achieved can be observed. The function depends on the set acceleration, the velocity, the number of engines and aircraft parameters.

10.8.2. Simulating the 2D flight path

Utilising the equations in section 10.8.1 a first estimate can be performed into simulating the vertical motions of the airborne element.

In order to simulate the motion backwards Euler will be utilised. The set of equations that will be utilised can be observed in equation (10.8) and section 10.8.1.

$$\begin{cases} v = v + adt \\ s = s + vdt \end{cases} \tag{10.8}$$

A first simulation was performed into the flight parameters during take-off. Here the initial acceleration is a set value and gets adapted based on the stage of flight. Furthermore, a maximum velocity is added to the system. To reach the operational altitude in a state of rest the acceleration is dynamically adapted once a specified altitude is reached using equation (10.9). equation (10.9) is dependent on the objects current velocity and the distance to the endpoint. The results of the simulation can be observed in figure 10.8

$$a = -\frac{v_{current}^2}{2d_{remaining}} \tag{10.9}$$

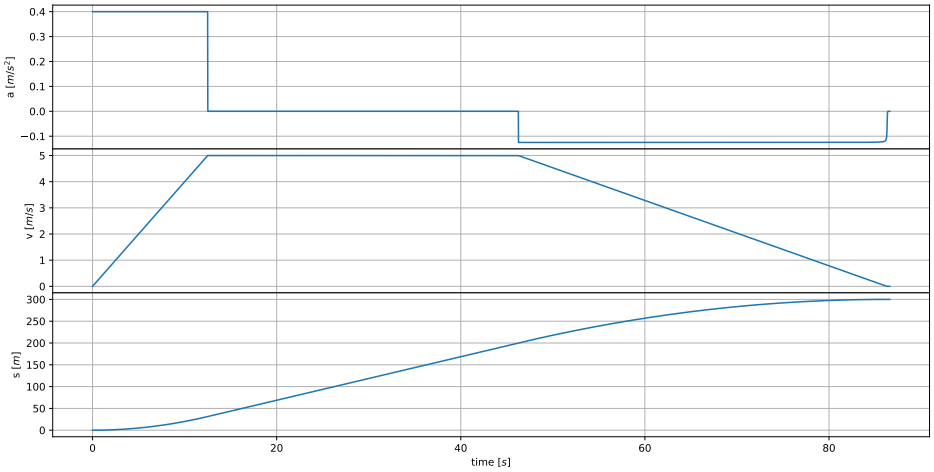

Figure 10.8: Simulated flight path during take-off

The flight analysis was performed utilising the following input parameters. The mass of the system is 2313 $[kg]$, the rotor diameter = 3.2 m, C_D = 0.18, frontal area = 118 $[m^2]$, the number of rotors is 8 and the total efficiency is 60%.

Key figures that can be derived from the simulation are: If the deceleration process starts at an altitude of 200 $[m]$ then the operational altitude of 300 m is reached after 86.59 s where the starting acceleration is 0.04 $[m/s^2]$ and the maximal velocity is 5 m/s. Furthermore, the maximal thrust per engine required during take-off is 2992.6 N and the total instantaneous average power required is 132475.3 W and the instantaneous peak power required is 199508.1 W.

11 Airborne Electronics layout

This chapter uses the design as specified before and elaborates on the electrical subsystem. The electrical lay-out is defined in section 11.1 which shows the main parts of the subsystem and their interactions. Section 11.2 estimates the power losses from different parts of the electrical system.

11.1. System Electrical Diagram

”To visualise the required electronics of the system, a diagram is used showing the electronics of one airborne wind energy system (AWES). This electronics diagram can be seen in figure 11.1. This layout draws inspiration from Makani’s M600 prototype [14]. The diagram shows the airborne element in blue and the floating base in red connected by the tether. The airborne element uses eight motor generators connected to their respective motor controller. Each motor generator also has cooling units. The generators are connected together with the medium voltage network. The generators are connected in pairs of two in parallel. These parallel duos are then connected in series. This layout leaves enough degrees of freedom in the current flow paths for controllability. It also means that the voltage sent through the tether is four times the voltage of a single motor, reducing tether losses. For this reason, this layout is preferred over an all-parallel layout. One problem with this is that when one engine fails during take-off, all current will flow through the other engine of the pair. This is not desirable. For this reason, each pair can be bypassed by a controllable switch. When a problem is detected, the switch can be closed. This does however mean that when one engine fails, two engines will be turned off. The control system should be able to handle this. Furthermore, the thrust-to-weight ratio of the craft should be at least 1.33 to keep flying in case of an engine-out scenario.

To provide power to the avionics, control system and communication systems, a low-voltage network is also required. This network draws power from the medium-voltage network via a converter. It also uses a storage system to have a consistent amount of power available. The floating base uses the same methodology to power its sensors, communication and winch [3].”

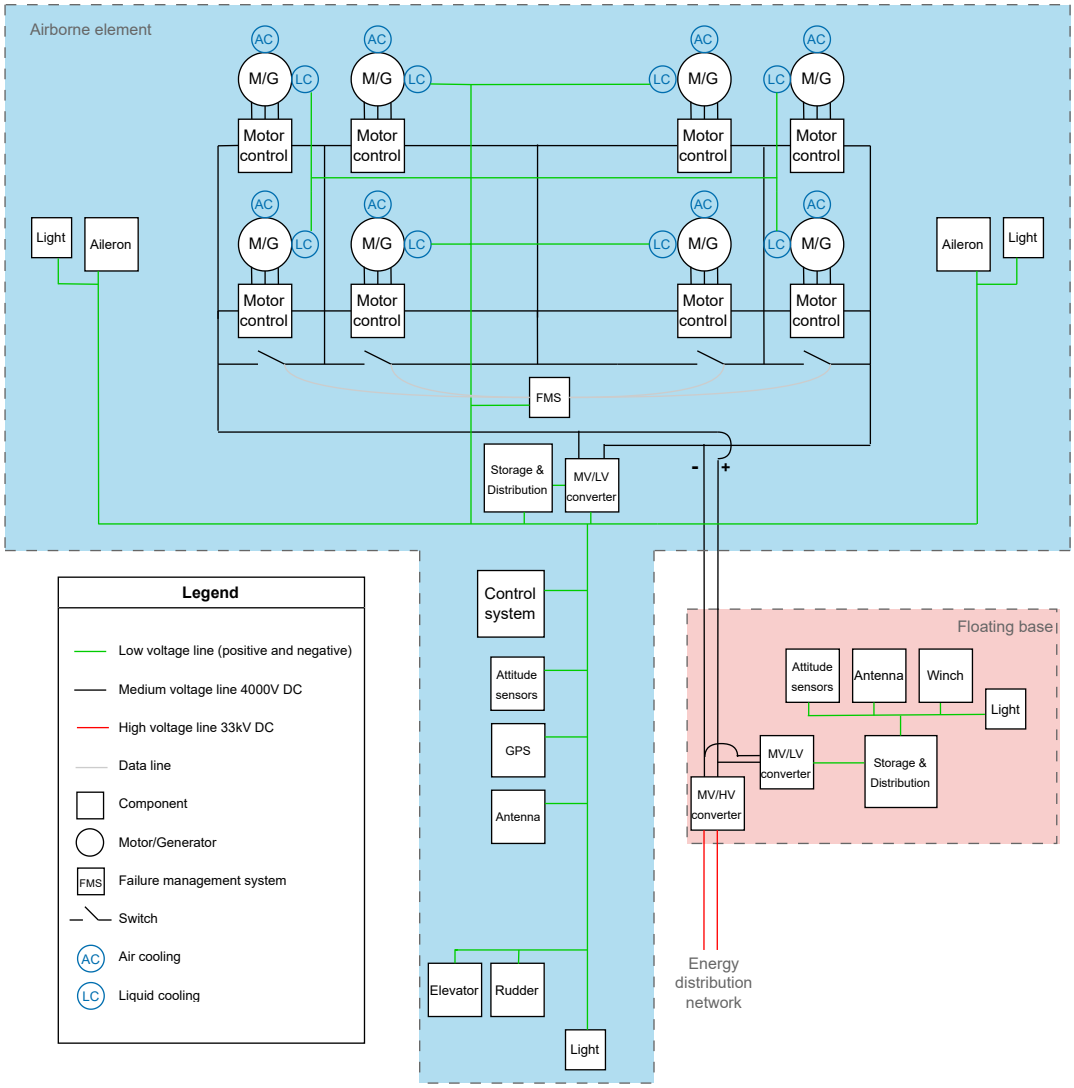

Figure 11.1: Electrical block diagram for a single AWES

”The electrical motor/generator forms the heart of the system. It will need to function both as a propulsion and generator unit. During the take-off and landing, the sub-system will need to switch to propulsion mode and should therefore be able to provide thrust to ensure the airborne element reaches the operational altitude and landing platform smoothly and safely. Secondly, when operational altitude is reached the sub-system shall be able to switch to generator mode. Here instead of using power to generate thrust, the element will convert the kinetic energy of the wind into electrical energy. In addition to these tasks, the electrical network must be able to power all system components that require electrical energy.

Electrical motor/generators are capable of both generating power and using power. Due to the change in magnetic flux induced by the rotation of the blades, a current can be created. Or, when a current is applied, a magnetic field can be induced which then is used to rotate the blades. There are multiple electrical motor types available, however, not all of the options are as suitable for this use case [3].” During the trade-off phase discussed in the midterm report, axial flux direct current motors were selected [3]. This motor type is chosen because it has a high power-to-weight ratio, small form factor and high controllability. This type of motor is controlled by a motor controller. The controller takes the direct current (DC) voltage and turns it into three-phase alternating current which then creates the alternating magnetic field

needed to rotate the motor. Because of this, there is no need for a brush connection in the motor, which makes this type of motor more reliable and less maintenance intensive. When generating power, the conversion is reversed, which means DC power is produced.

The voltage level of an electric motor is dependent on multiple design parameters. Most importantly, it is dependent on the number of poles and the number of windings per pole. This then also influences the relationship between rotational speed, torque and power produced at a specific rotation rate. The design of electric motors is a complex problem which depends on rotor design, which is not in the scope of a preliminary design. For this reason, existing axial flux motors were investigated and compared to find a relation between rated power and mass, which is discussed in chapter 8. Furthermore, to be able to size the tether conductor, the voltage in the tether must be determined. Because the motors are wired in four series-connected pairs, this voltage is equal to four times the motor voltage. To estimate the motor voltage, data from the Makani M600 was used since it is the only fly-gen system of comparable power scale to have operated using the same motor type. It was found that a motor voltage of 1000 V is a reasonable first estimate [14]. This means the voltage in the medium voltage network and tether is 4000 V.

At the base station, the voltage will be converted to a high voltage for transmission within the farm. This is done to reduce power losses. It was found that 33 kV is a common voltage level for turbine interconnection in conventional wind farms[1].

11.2. Power Loss Estimation

There are multiple electrical losses within an AWES. Figure 11.1 shows the main components between the power generation of the motors and the power delivery to the distribution network. These components will induce losses, which will be analysed in this section as well as the losses induced by transmission to shore. The main AWES components and their efficiencies are shown in table 11.1.

Table 11.1: AWES components and their losses

Component	Efficiency
Motor/Generators	95%[2]
Motor Controllers	98%[3]
Tether	98%[4]
Step-up converter at base	99%[5]

With these values, the total efficiency of an AWES can be estimated to be:

$$\eta_{AWES} = 0.95 \cdot 0.98 \cdot 0.98 \cdot 0.99 = 0.90 = 90\% \tag{11.1}$$

Next to the AWES components, there are further losses within the wind farm. Figure 13.5 shows the main power transmission components of the wind farm. It can be seen that the main loss-inducing components are: the transmission lines from the AWESs to the offshore substations, the offshore substations, the high voltage line to shore and the DC to AC transformer on shore.

[1] windandwaterworks.nl [Cited 8 June 2023]
[2] Average of data from motors selected in section 8.7
[3] powerelectronicsnews.com[Cited 9 June 2023]
[4] As discussed in section 8.4
[5] vietnamtransformer.com[Cited 9 June 2023]

The losses within the wind farm distribution network from an AWES to a collection station are difficult to determine at this stage. The losses depend on the type of submarine cables and the distance from an AWES to a collection station. This is thus highly dependent on the farm site. Next, the efficiency of the offshore substations must be found. These substations are intended to step up the voltage from farm voltage to interconnector voltage (38 kV to 525 kV). Furthermore, these stations will regulate the voltage level and stabilise the power fluctuations from the AWESs. This will introduce additional losses. From the offshore substations, the power is transmitted using high-voltage direct current interconnectors. Direct current interconnectors are preferred compared to alternating current because of the long distance from shore and the fact that the electricity is already direct current from the AWESs. Longer distances make direct current transmission more cost-effective because it induces less loss in the cables. It is found that on average, losses from high voltage direct current transmission are around 3.5% per 1000 km [34]. Lastly, since national energy grids are alternating current, the electricity needs to be transformed from direct current using a transformer. High voltage transformers can have an efficiency of up to 99%[6]. To conclude, the efficiency of transmission can only be accurately determined when a site is known for the farm, but due to the high voltages, the power losses are not expected to be above 10%.

[6]linquip.com [Cited 21 June 2023]

12
Seaborne Design

A seaborne element has to be designed to operate the airborne element offshore. The sizing of the floaters and the distance between the floaters is calculated in section 12.1. To keep the system in its place, a mooring system is designed in section 12.2. The final design is visualised in section 12.3 after which the specifications are shown in section 12.4.

Assumptions

- All external forces are assumed to act in the same direction.
- It is assumed that one mooring line and anchor should be able to withstand the full load of the floating system.
- It is assumed that all loads on the floating system are the highest expected at the same time.

12.1. Semi-Submersible Floater Sizing

From the trade-off, it was decided that a semi-submersible architecture would be utilised as floating structure to support the airborne energy-generating unit. Within this section, the first-order sizing procedure of the seaborne floater will be provided. The sizing of the floater will be made based on two considerations: buoyancy and stability. Analysis regarding buoyancy gives the submerged height of the floaters, the height of ballast water inside the floaters, and the above-sea water level height of the floaters in section 12.1.1. A stability analysis is performed to obtain the distance between the middle point of the structure to the centre of each of the three offset columns in section 12.1.2. This section ends with a frequency analysis in section 12.1.3.

12.1.1. Sizing for Buoyancy

The first consideration for the sizing of the floater is based on the buoyancy. The scaling with respect to buoyancy force is a static analysis to ensure that the floater has a sufficient amount of its structure above water, to allow smooth operation.

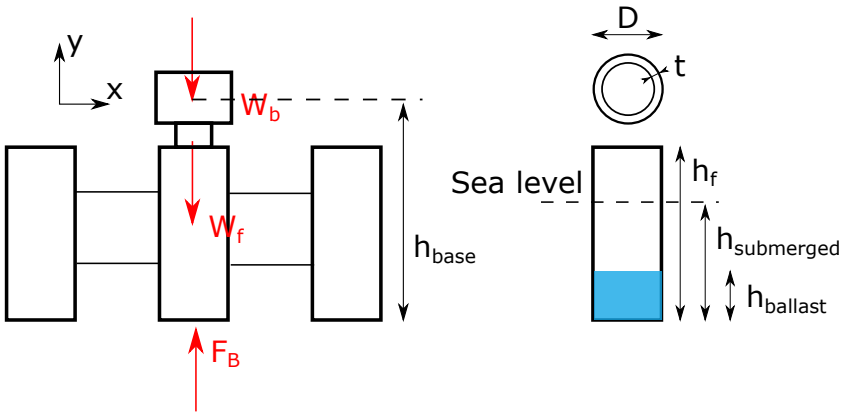

Figure 12.1: Floater illustration for the sizing based on buoyancy

Using the diagram in figure 12.1, the sum of forces in the y direction can be described.

$$\sum F_y : F_B - W_f - W_b = 0 \tag{12.1}$$

where F_B is the buoyancy force described by the density of seawater, displaced water volume and the gravitational acceleration. W_f is the weight of the floater and W_b is the weight of the base unit on top of the floater. Expanding equation (12.1), the following equation can be observed; noting that the floater structure is comprised of 3 cylinders.

$$\Rightarrow m_{base}g + 3m_{floater}g - 3\rho_{sea}V_{disp}g = 0 \tag{12.2}$$

$$\Rightarrow m_{base}g + 3h_f \left[2\pi \left(\frac{D}{2}\right) t\right] \rho_{floater}g + 3\left(\frac{D}{2}\right)^2 \pi h_{ballast}\rho_{water}g - 3\rho_{sea}h_{submerged}\left(\frac{D}{2}\right)^2 \pi g = 0$$

From literature, the following consideration was made: the mass of the added water ballast is twice the mass of the floater structure [35]. As a result, the equation can be written in terms of the mass (or weight) of the floater structure only. The relation written to solve for the submerged height in meters of the floater structure is written in equation (12.3).

$$h_{submerged} = \frac{m_{base}g + 3(h_f \left[2\pi \left(\frac{D}{2}\right) t\right] \rho_{floater})3g}{3\rho_{sea}g \left(\frac{D}{2}\right)^2 \pi} \tag{12.3}$$

For the wall thickness, a value of $t = 3\ cm$ was selected from literature [36]. Consequently, the submerged height of the offset column is 6.55 m from the lowest point of the structure, the above-SWL height is 3.45 m. The mass of each offset column can be estimated from all these dimensions: approximately 37 $tons$. The water ballast mass is then 74 $tons$, which results in the height of the ballast being 3.7 m with the equation:aa

$$m_{ballast} = 74tons = \rho_{sea}\pi \left(\frac{D}{2}\right)^2 h_{ballast} \tag{12.4}$$

This completes the analytical sizing for the semi-submersible's offset column. The only sizing left to do is the distance between the middle of the structure to offset the columns' centre.

12.1.2. Sizing for Stability

The floating structure is assumed to rotate around its centre of gravity during the oscillations. The vertical location of the centre of gravity is dependent on the structural layout of the floater and can be derived using equation (12.5).

$$\bar{y} = \frac{\sum \bar{y}_i m_i}{\sum m_i} \tag{12.5}$$

$$= \frac{1.5h_f m_{base} + 3\left(\frac{1}{2}h_f m_f\right) + 3\left(\frac{1}{2}h_{ballast}m_{ballast}\right)}{3m_f + 3m_{ballast} + m_{base}} = \frac{1.5h_f m_{base} + 3\left(m_{floater}(h_f + 2h_{ballast})\right)}{9m_{floater} + m_{base}}$$

The centre of gravity's location is about 4.75 m above the lowest point of the floating structure. Now, stability analysis can be performed. The following figures are provided to aid the visualisation.

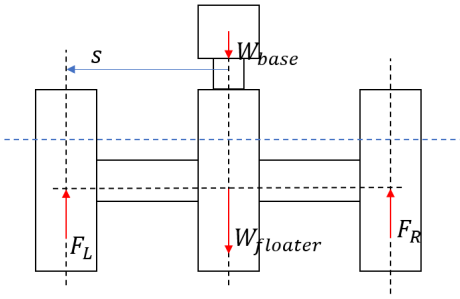

Figure 12.2: Static free body diagram of Semi-submersible structure

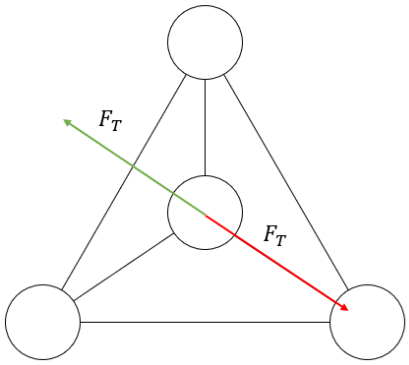

Figure 12.3: Tether force taken into consideration

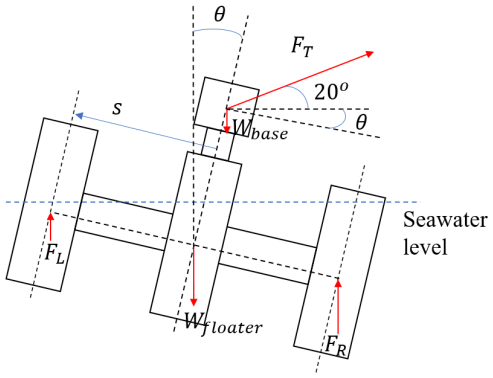

Figure 12.4: Quasi-static free body diagram of Semi-submersible structure with Tether tension

In figure 12.2, distance between the middle of the structure to the centre of the offset columns is defined as s. Figure 12.3 visualises the moment when tether force occurs. More specifically in this figure, the direction of red tether force is deemed to be more critical than its green counterpart because there is only one offset column countering this force; meanwhile, for the green tether force, two of the offset columns counter the force. Figure 12.4 is the visualisation of the moment the floating structure rotating around its centre of gravity by an angle of θ where the sum of moments around the centre of gravity is zero. This is possible when the counterclockwise moment due to buoyancy force on the right offset column F_R is great enough to offset all the clockwise moment caused by base weight W_{base}, tether force F_T, and buoyancy force of the left offset column F_L. After this happens, the structure might rotate in clockwise a bit more due to inertia. Nevertheless, F_R will get even bigger, resulting in net positive counterclockwise moment, which rotates the floating structure back to equilibrium.

This analysis is done intentionally to over-design the floating structure to be able withstand extreme events. The tether force only gets to 500 kN (including safety factor of 2, it will be 1 MN) when the wind speed is 25 ms^{-1}. In addition, the lowest angle, with respect to the horizontal line, that airborne flies in its flight path is 30 degrees, 10 degrees higher than the one used to analyse from figure 12.4.

Nevertheless, the sum of moment around centre of gravity with counter clockwise positive is:

$$F_R cos(\theta)s - F_T cos(\theta + 40^o)(2h_{base} - y_{cg}) - W_b sin(\theta)(\frac{3}{2}h_{base} - y_{cg}) - F_L cos(\theta)s = 0 \quad (12.6)$$

where

$$F_R = \rho_{sea} g \pi r^2 (h_{submerged} + sin(\theta)s)$$

$$F_L = \rho_{sea} g \pi r^2 (h_{submerged} - sin(\theta)s)$$

where θ indicates the angle of tilting thus $sin(\theta)s$ is the change of level of submerging of for the side columns. Substituting the elements results in the following derivation:

$$\rho_{sea} g \pi r^2 \left[2sin(\theta)s\right] cos(\theta)s = \rho_{sea} g \pi r^2 s^2 sin(2\theta) = F_T cos(\theta + 40^o)(2h_{base} - y_{cg}) + W_b sin(\theta)(\frac{3}{2}h_{base} - y_{cg})$$

Lastly, a relation between s and tilt angle θ can be formed:

$$s = \left(\frac{F_T cos(\theta + 40^o)(2h_{base} - y_{cg}) + W_b sin(\theta)(\frac{3}{2}h_{base} - y_{cg})}{\rho_{sea} g \pi r^2 sin(2\theta)} \right)^{1/2} \tag{12.7}$$

The tilt angle θ is looked up in literature of conventional floating offshore wind turbine. For conventional floating offshore wind turbine, θ needs to be as small as possible because a large tilt angle reduces the effectiveness of the wind turbine; and a θ value of 10 degrees is accepted as an operational limit [37]. Regarding the Deep WattAir project, power generated is almost always during airborne operation; thus, the tilt angle is less detrimental. The group decided to opt for a maximum θ of 15 degrees. Figure 12.5 shows the required minimum distance s from the structure's centre to the centre of offset columns as a function of the tilt angle θ.

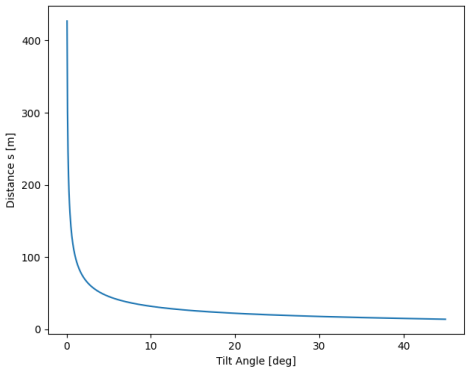

Figure 12.5: Tilt angle vs distance from the structure's centre to the centre of offset columns

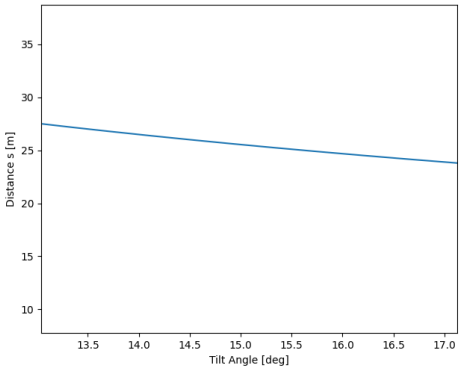

Figure 12.6: Detailed 15 degrees tilt angle vs distance from the structure's centre to the centre of offset columns

12.1.3. Natural Frequency

To estimate natural frequency of the floating platform, the platform can be modelled as a spring mass system, as shown in figure 12.7, where the "spring" force is the buoyancy force.

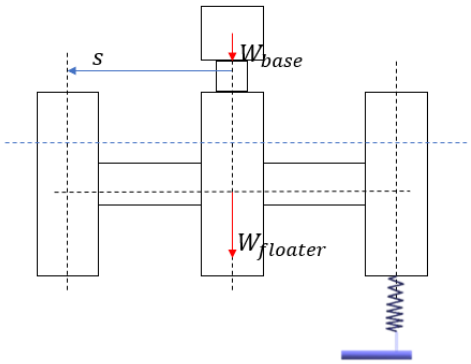

Figure 12.7: Floating platform as spring mass system

The spring is in neither tension nor compression when all offset columns submerge by the same amount. When there is one offset column submerging more than the others, the buoyancy of that column will be higher and will have the tendency to push the floater back to equilibrium. It is sensible then to model this as a spring mass system to find the spring stiffness in order to find the natural frequency.

The formula for buoyancy force is the weight of displaced seawater that is $\rho_{sea} V_{disp} g$ where $V_{disp} = \pi r^2 h_{submerged}$. When one column submerges by an extra amount Δh, the buoyancy force increases by $\rho_{sea} \pi r^2 \Delta h g$. As a result, the spring stiffness of the model can be estimated to be $k = \rho_{sea} \pi r^2 g = 1020 \cdot \pi \cdot 2.5^2 \cdot 9.81 = 196 \cdot 10^3 Nm^{-1}$. The natural frequency of the spring mass system can be found with the following equation:

$$f_n = \frac{\omega_n}{2\pi} = \sqrt{\frac{k}{m}} \frac{1}{2\pi} = \sqrt{\frac{196 \cdot 10^3}{393 \cdot 10^3}} \frac{1}{2\pi} = 0.112 Hz \tag{12.8}$$

It is worth noting that the natural frequency is of merely when one offset column submerges more than the others. If all three columns submerge at the same time due to sudden rise of water, the spring stiffness will increase by 3; hence, frequency increases by $\sqrt{3}$, which is 0.194 Hz. Ultimately, the time period ranges from 5.15 s to 8.93 s.

12.2. Mooring System Design

Mooring is essential for the positioning of the seaborne floater. The semi-submersible will be mounted to the seabed utilising three sets of drag anchors and catenary mooring chains [3]. In this section, the sizing relations for the mooring system will be discussed.

The main components which affect the sizing of the mooring include the design parameters of the floating element, the wind and wave conditions and the sea depth.

For the sizing procedure of the mooring, a N2 chart is constructed which is shown in figure 12.8. Within the chart, the main relational flow can be observed for the mooring system design. Also, external inputs and output to the system are provided.

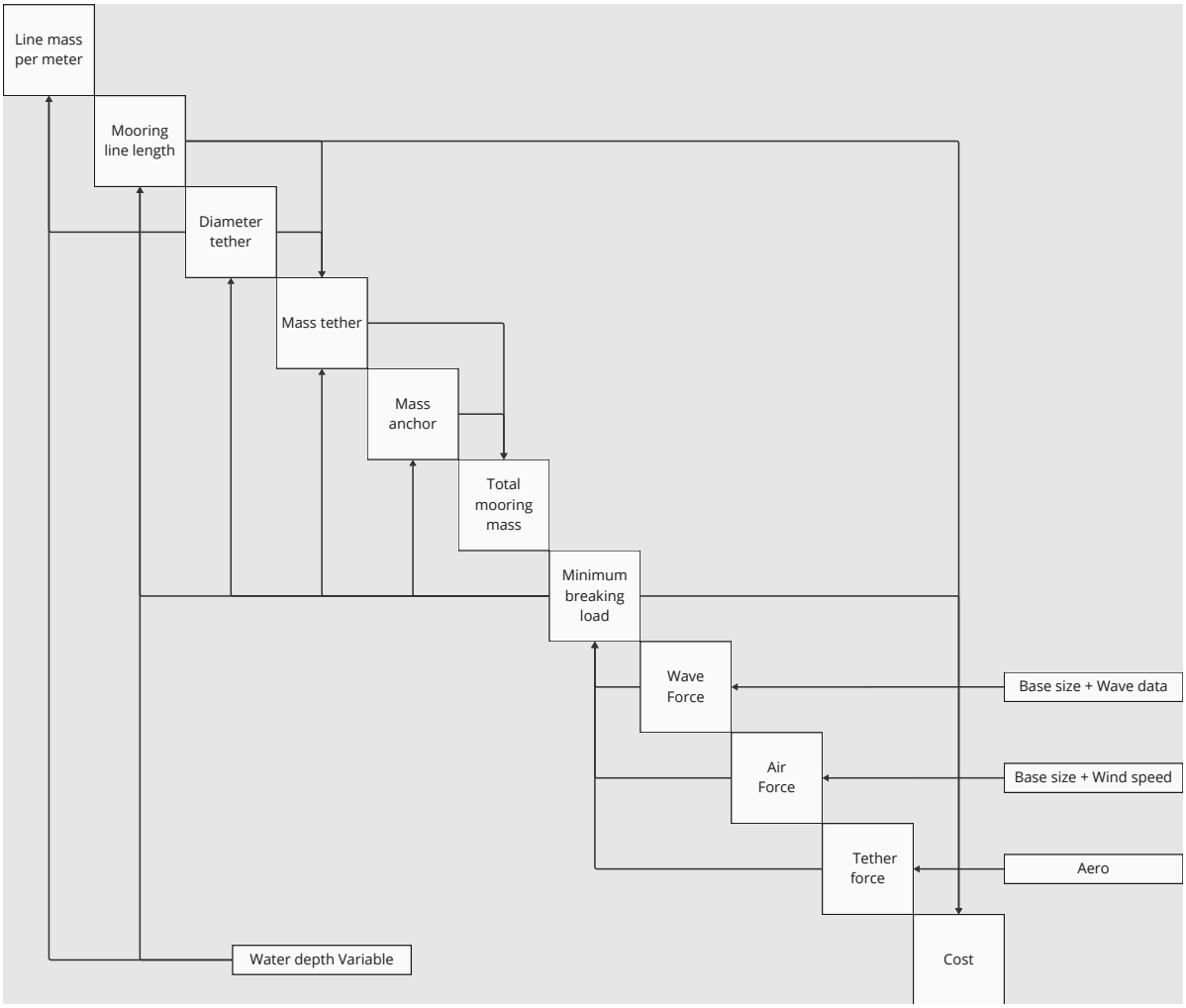

Figure 12.8: N2 chart for the seaborne mooring element

12.2.1. Sizing relations

First, the length of a catenary mooring line can be found using equation (12.9) [1] The length of the mooring line is dependent on the water depth, the force applied to the line and the weight of the mooring line (pulling the mooring line downwards). The water depth is dependent on the site which is selected for operation. For this reason, the depth will remain a variable in the calculations. Both the weight and the force are dependent on further relations.

$$L = \sqrt{d_w \left(\frac{2F}{W} - d_w \right)} \quad \text{[m]} \tag{12.9}$$

The minimum break load (MBL) is the maximum load that can be held by the mooring. For the sizing, the MBL is set equal to the maximum expected load that the floating substructure is expected to encounter. This way it is ensured that the mooring does not fail. The three mooring lines will be spaced 120°apart, which means it is possible for the force on the floater to align with only one of the lines perfectly. In this case, only one mooring line must carry all the load. For this reason, it is considered the worst-case scenario and is used as the design case.

[1] weebly.com [Cited 1 June 2023]

The MBL(in kN) is described by the sum of the wave, wind and tether force, acting on the floating system. In equation (12.10) the underlying equation can be observed.

$$MBL = F = \frac{(F_{wave} + F_{air} + F_{tether}\cos\theta)}{1000} \quad \text{[kN]} \tag{12.10}$$

The wave force is given by equation (12.11) derived from [38]. The tether force is determined from aerodynamic analysis in chapter 7. The tether force is decomposed into a horizontal and vertical component. It is assumed that the mooring only needs to resist the horizontal component. For this reason, the tether inclination angle θ is used to determine the horizontal component of the tether force. Again, a worst-case scenario is assumed where all forces are the highest expected in the lifetime of the farm. The forces are also assumed to align perfectly with each other. These assumptions are strong but they are conservative so they are safe to make.

$$F_{wave} = \left(\frac{\pi}{4}\rho_{water}\left[C_M D\dot{u}(t) + \frac{1}{2}\rho_{water}C_D|u(t)|u(t)\right]\right) \quad \text{[N]} \tag{12.11}$$

For equation (12.11), u and $\dot{u}$ are given by equation (12.12)

$$u(t) = u_a(z)\cos\omega t \qquad \dot{u}(t) = -\omega u_a(z)\sin\omega t \tag{12.12}$$

In the above equations equation (12.11) and equation (12.12), ρ_{water} is the density of water in . C_d is the drag coefficient, C_m the inertial force coefficient equal to 0.65 and 2.0 respectively [38]. D is the diameter of the seaborne element in meters. Lastly, u_a is the horizontal wave velocity, t is the time and omega is the wave frequency. Omega is 2π divided by the wavelength. For the calculations of the wave, the maximum is taken of the wave force over time to size the system.

Next, the force of the wind on the floating base is investigated. For this, the general equation for drag force is used (equation (12.13)).

$$F_{air} = C_D\frac{1}{2}\rho V^2 A \quad \text{[N]} \tag{12.13}$$

$$m_{te} = 21.9d^2L \quad \text{[MT]} \ [2] \tag{12.14}$$

Equation (12.15) shows the relation between the anchor mass and MBL for a drag-embedded anchor in medium clay seabed type. The relation is based on interpolation of rated MBLs of different anchor masses [39, p. 74], but the exact rating of an anchor will only be known exactly once an anchor is chosen. However, this is not possible at this stage of the design. The relation is deemed sufficiently accurate for the first-order estimation.

$$m_{arch} = 0.076F_{anchor} - 3.0612 \quad \text{[MT]} \tag{12.15}$$

$$m_{mooring} = 3(m_{te} + m_{arch}) \quad \text{[MT]} \tag{12.16}$$

[2] orcina.com [Cited 1 June 2023]

Lastly to obtain the force acting within the anchor the following expression is utilised. In equation (12.17) the force is dependent on the MBL, the horizontal displacement between the anchor and loading structure (x) and L is the mooring length.

$$F_{anchor} = MBL\frac{x}{\sqrt{L^2 + x^2}}[kN] \tag{12.17}$$

Here, x is the horizontal distance between the anchor and the floating structure as expressed in equation (12.18). Both equations were derived from Weebly.[3]

$$x = (\frac{1000MBL}{w} - d_w)ln(\frac{L + \frac{1000MBL}{w}}{\frac{1000MBL}{w} + d_w}) \tag{12.18}$$

12.3. Seaborne Element Configuration

The seaborne element consists of the floater, base, platform, landing arm and winch. The full configuration can be seen in figure 12.9.

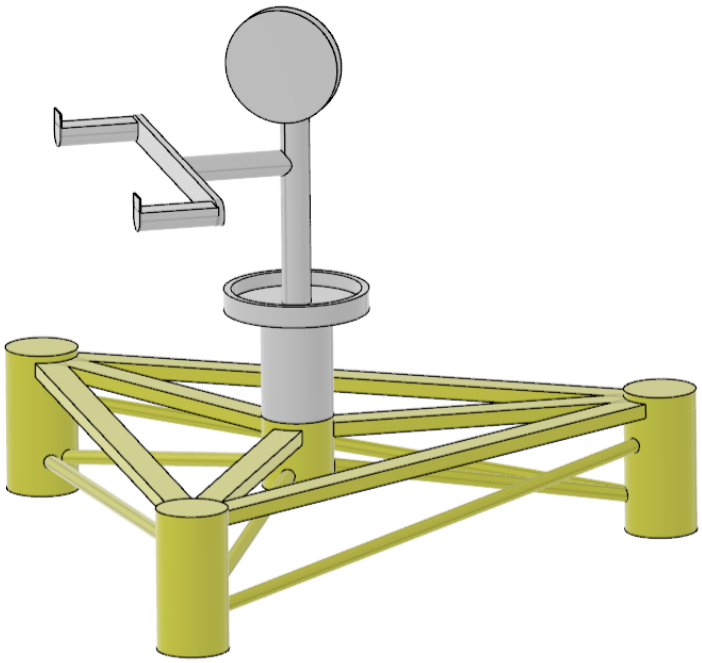

Figure 12.9: CATIA drawing of the seaborne element

In the seaborne element, electrical components are present. The hardware components consist of the motors, computer, transformer, wires as shown in the electrical diagram in chapter 11. The different hardware components have different places within the seaborne element, which are shown in Figure 12.10.

[3]weebly.com [Cited 1 June 2023]

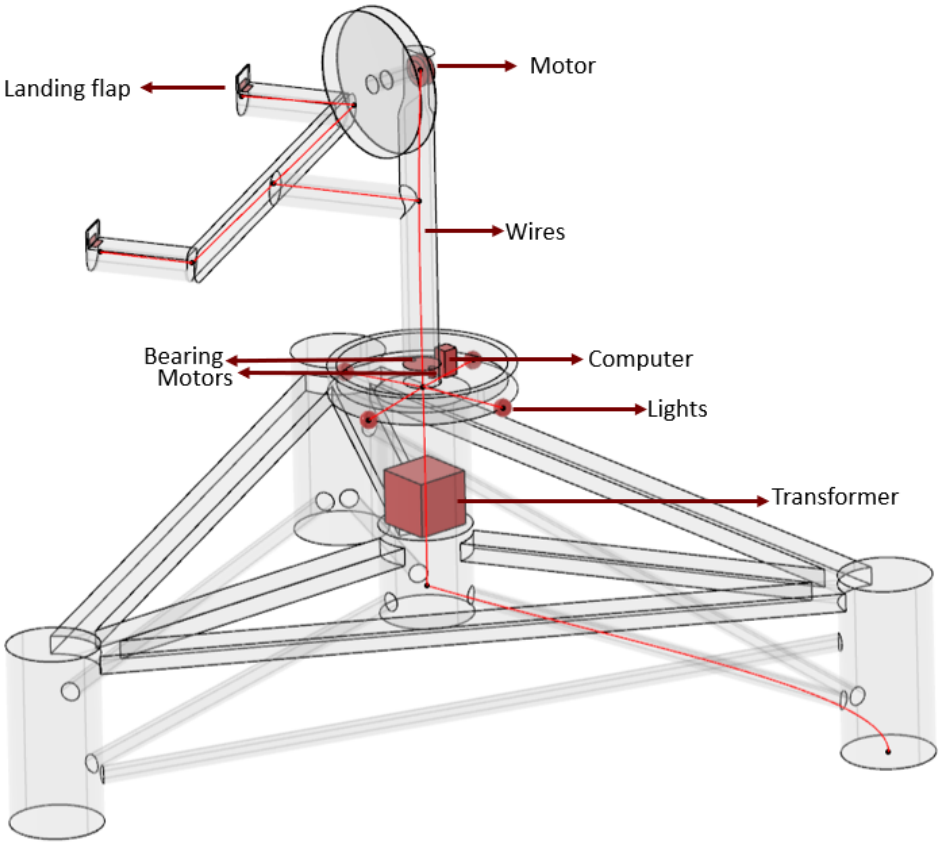

Figure 12.10: Hardware in the seaborne element (components not on scale)

12.4. Seaborne Element Specifications

The specification of the seaborne elements, in terms of the sizing and the total mass are shown below. Table 12.1 shows the size of the floaters, table 12.2 shows the sizing of the platforms used for maintenance, table 12.3 shows the size of the launch and landing attachment and table 12.4 gives the mass for both aspects of the seaborne element.

Table 12.1: Floaters parameters

Parameter	Value	Unit
Height floater	10	m
Diameter floater	5	m
Spacing	44	m

Table 12.2: Human Platform parameters

Parameter	Value	Unit
Diameter platform	10	m
Height platform	1.5	m
Height above waterline	11	m

Table 12.3: Arm and tether holder parameters

Parameter	Value	Unit
Span	25	m
Length waterline	20.5	m
Diameter tether holder	8	m

Table 12.4: Mass of the seaborne elements

Sub-parts	Value	
Seaborne element	112	$tons$
Mooring and anchors	237	$tons$

Part 3

Farm Layout & Management

In this part the layout and the management aspects of the farm are touched upon including the design of the farm, the operations & logistics, the finances of the project and the verification & validation of the user requirements. The design of the farm involves careful positioning of the systems, resource allocation and the bill of materials. The operations & logistics encompasses a description of the possible day-to-day tasks during production, operations, and decommissioning. The finances of the project involve a cost breakdown, the levelised cost of energy, and the return of investment breakdowns. Verification and validation ensures that the user requirements are met by using a compliance matrix, a sensitivity analysis, and a validation plan.

13
Farm Design

After the single system is designed, the farm layout is developed. Deep WattAir's 1 GW farm consists of 1000 systems. First, an appropriate site for a wind farm must be chosen prior. Subsequently, a detailed farm layout can be designed, regarding aspects such as the distance between systems, number of offshore power substations, and more. This chapter describes the selection of the farm site in section 13.1, and the layout of the farm in section 13.2. After that, section 13.3 explains how the farm will deliver the generated electricity to the electrical grid, section 13.4 will talk about the mass and power budgets of the system and farm, and lastly, table 13.5 will present the Bill of Materials (BoM) of the farm.

13.1. Exemplary Site Selection

The site selection process started with narrowing the choices to wind sites located in the North Sea, with a specific focus on the deep water region. These sites can be found in the comprehensive Energy Atlas provided by North Sea Energy[1]. Ultimately, after careful consideration, Hornsea IV [2] is selected as the optimal choice due to the following reasons:

- Hornsea IV is strategically situated in the deep water region of the North Sea with water depth of from 22 to 73 meters.
- The proximity of Hornsea IV to an offshore electricity grid presents great advantages such as reducing power loss.
- The size of Hornsea IV is able to accommodate all systems: The site has an area of 492 km^2 [2]. However for the project not the whole area will be utilised.

Hornsea IV is located in the North Sea near the shore of the United Kingdom. The precise location is shown in red within figure 13.1[2].

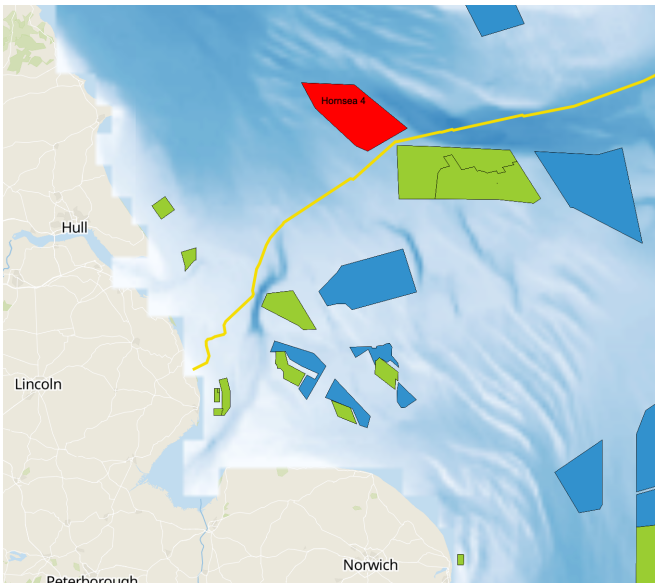

Figure 13.1: Location of Hornsea IV

[1] North Sea Energy [Cited 9 June 2023]
[2] Hornsea IV project [Cited 9 June 2023]

In the above figure, the yellow line is the offshore electricity grid. The red area is Hornsea IV. It is approximately 69 km from the Yorkshire coast of the United Kingdom.

13.2. AWES Spacing & Farm Layout

The wind farm shall be designed for the most probable wind direction in the North Sea, which is southwest. As a result, it is desirable to distribute systems as extensively as possible in the northwest-southeast direction. In the case of wind blowing in a different direction, the stability and control system of the airborne element will ensure that the system is still capable of generating power.

Within the designated area of Hornsea IV, only a part of it will be utilised for the Deep WattAir project. This allocated area is further divided into 10 sub-areas, referred to as sub-lots. Nine of these sub-lots will consist of the AWES and the remaining sub-lot is allocated for an operations station. For the maintenance of the farm, multi-purpose offshore vessels will be used with an approximate length of 150 m, [3]. The turning circle of the vessels should have a radius of 3-4 times its length [4], between the perpendicular sub-areas, resulting in a width of 600 m.

The spacing between the systems within a sub-lot has to also be determined.

There are two main types of spacing and one minor type:

- Wind direction
- Perpendicular to the wind direction
- The distance between the last unit to the boundary

All distances can be estimated with the length of the tether and different flight path angles, with the use of the following three equations are listed as follows:

$$d_1 = \frac{L_{\text{max}}}{sin(\beta - \Delta\beta)\left[\frac{1}{tan(\beta-\Delta\beta)} + \frac{1}{tan(\beta+\Delta\beta)}\right]} \tag{13.1}$$

$$d_2 = 2L_{\text{max}} sin(\phi) \tag{13.2}$$

$$d_3 = L_{\text{max}} cos(\beta - \Delta\beta) \tag{13.3}$$

where d_1 and d_2 are the distance in the direction parallel, and perpendicular to the direction of the wind, respectively; d_3 is the distance between the last unit to the boundary of the lot. Multiple systems in the d_1 direction are defined as a column: red, green, blue, and yellow as displayed in figure 13.2, and multiple systems in the d_2 direction are defined as a row. β is the average of the maximum and minimum elevation angle between the tether and the ground station; $\Delta\beta$ is the difference in the maximum elevation angle and β; the maximum azimuth angle is denoted by ϕ. Lastly, L_{max} is the maximum tether length. The following figures 13.2 and 13.3 provided by Roque, Paiva, Fernandes, *et al.* [40] help visualise the variables in three previous equations.

[3] Ship Technology[Cited 9 June 2023]
[4] Maritime Page[Cited 9 June 2023]

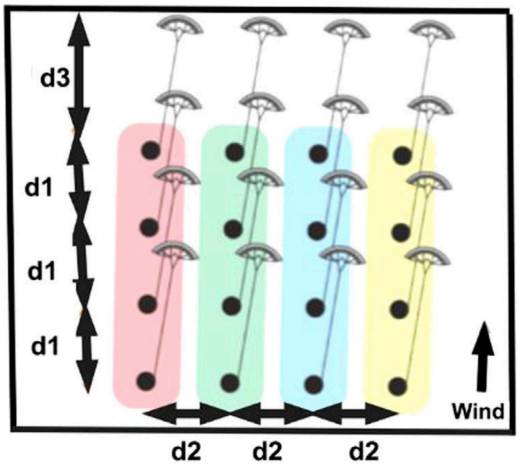

Figure 13.2: Defined distances between systems

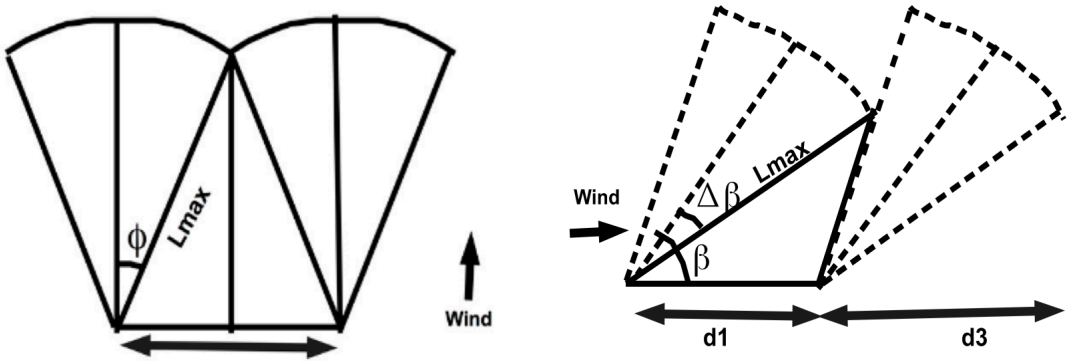

Figure 13.3: Defined angle for system spacing

Given the single system design; the tether length $L_{\text{max}} = 400\ m$, $\beta = 40^o$, $\Delta\beta = 20^o$, and $\phi = 45^o$. As a result, $d_1 = 352\ m$, $d_2 = 566\ m$, $d_3 = 376\ m$.

In total, the 1 GW farm will consist of 1000 systems. Therefore, for the nine sub-lots', the dimensions are determined. The eight smaller sub-lots' are designed to be 6 km x 5 km and each consists of 105 systems, and one bigger sub-lot of 10 km x 5 km and it consists of 160 systems. Figure 13.4 shows a proposed farm layout.

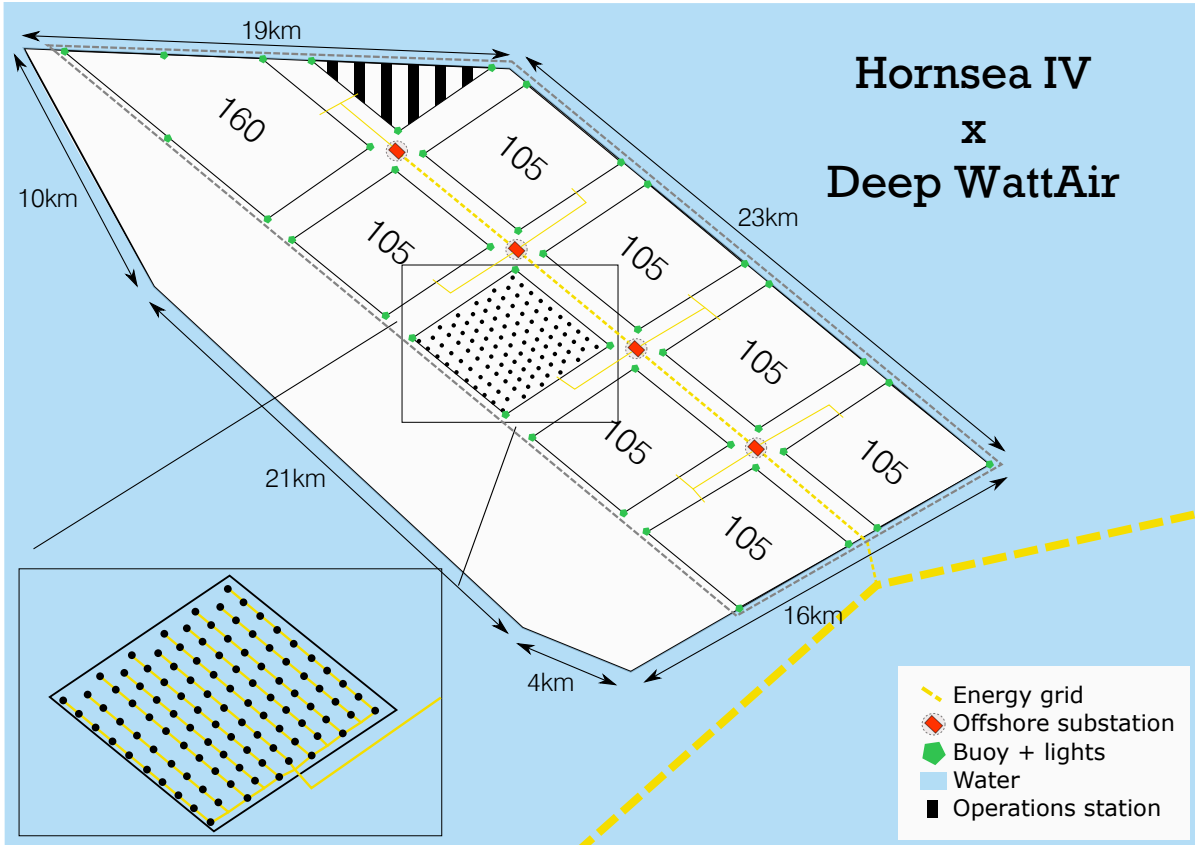

Figure 13.4: Wind farm layout (not to scale)

Included in this figure are additional elements of the farm, such as the grid, substations, buoys, and operations station. The 41 buoys with lighting to indicate locations where the vessel should start to turn and mark the boundary of each lot, four offshore substations: two 350 MW located as the two junctions closest to the grid to minimise power loss, one 250 MW and one 200 MW. The operations station where system replacements and the maintenance and operations team are stored is situated in the top left corner. In the bottom left corner, the detailed view of one lot consisting of 105 wind energy systems is shown. There are 11 rows in which the rows are staggered, meaning that the system of one row is located right in the middle of two systems of preceding and following rows. Having a staggered configuration minimises the wake effect or interference/disturbance of one system to another system in the wind direction.

13.3. Electrical Network Layout

In the previous section, a farm layout was proposed for the Hornsea IV location. Within this section, the electrical layout accompanied by an electrical diagram of the farm will be provided.

The purpose of the electrical grid is to transport electricity within the farm and create a connection to the national grid so that the energy can then be brought to the consumers. The electrical grid mainly consists of the electrical cabling linking systems together (either in series or parallel), transformers (changing the voltage level) and converters (alternating current to direct current or vice versa). In figure 13.5 a compact electrical diagram is provided detailing the main electrical components

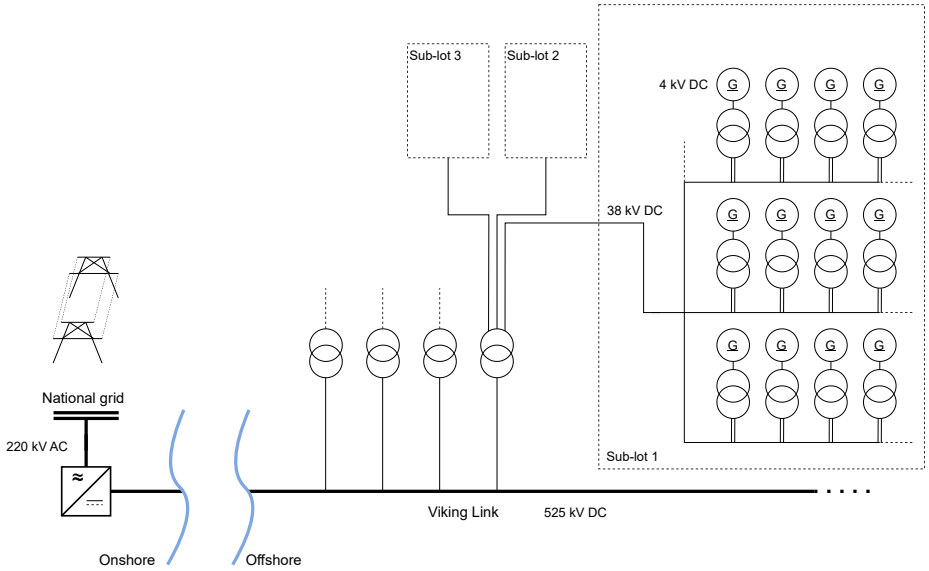

Figure 13.5: Electrical diagram for the proposed farm

Within each sub-lot, the main AWES units are located, which are displayed by circles with a G (for generator). These generators operate at 4 kV direct current and are connected in series and parallel. The voltage produced by the generator is then converted at the base to a 4 kV direct current. First, the individual AWES units are connected in strings (series connected units) of 9 or 10 units. As a result of this string connection, the individual strings will operate at a voltage of 36 or 40 kV. Within each sub-lot of the farm, the strings are afterwords connected in parallel to the main cable leading to the substation. The same procedure is utilised for the remaining sub-lots. It must be noted that the substation has a rated capacity of 250 MW, meaning that, as depicted in figure 13.4 each substation will be connected to a limited amount of sub-lots.

At the offshore substation, the 38 $kVDC$ gets transformed to 525 $kVDC$ which is then transported to shore through the national grid. For this transportation the proposed farm located at the Hornsea four plot would make use of the existing Viking Link: KB0093 [5][6]. Onshore the 525 $kVDC$ is then transformed to 220 $kVAC$ by a transformer, and afterwards transported to the consumer on the national grid.

13.3.1. Voltage, Current and Series vs Parallel

The electrical wiring of an offshore wind farm allows for many different unique design conditions to be taken. Such as should the farm make use of high voltage for transport, what type of current should be used and, lastly, how should the various elements be connected in series or parallel.

Firstly for a constant voltage, power losses scale with the current squared. Meaning that a lower current is preferred, this can be obtained by amplifying the voltage level ($P = UI$).

A second consideration which can be made is whether a system should opt for direct current or alternating current to transport electricity. Firstly the generator, in this case a brushless

[5]north-sea-energy.eu [cited 12 June 2023]
[6]Viking Link team completes the onshore cable installation [Cited 26 June 2023]

direct current motor produces power in DC. At the base, this is then converted to a stable 4 kV. However, here a first choice can be made. Should the farm use AC for further transport or should DC be used? Typically in offshore wind farms the energy is generated at AC power and is then transported at HVAC to shore. This is done since these farms are located close to shore and the cost benefits outweigh the efficiency benefits. However, when the distances become larger the cost and complexity become less of a problem due to the higher transportation efficiencies (HVDC transmission have less energy losses then HVAC) [41].

For the farm, the individual elements can be connected in series or parallel. Within the farm, a combination between series and parallel connections will be utilised. Series connections are more efficient with respect to resources. Since not every element is connected in a loop. However, it offers less redundancy in the event that an element within the string fails. To increase the redundancy of the groups connected in series, a bypass will be implemented at the base of an AWES where if a failure at an AWES occurs it will be bypassed.

In parallel, the voltage remains constant; however, the current increases. The main benefit of connecting elements in parallel is to provide redundancy. Contrary to the series of stringed elements, the failure of one element will not lead to the failure of the entire string. One downside of parallel connections is that this method is material inefficient since all units will have to be connected individually. Furthermore, cable limitations need to be taken into account, as the current increases in a series.

13.3.2. Farm-Level Power Losses

Next to the AWES components, there are further losses within the wind farm. Figure 13.5 shows the main components of the wind farm power transmission. It can be seen that the main loss-inducing components are: the transmission lines from the AWESs to the offshore substations, the offshore substations, the high voltage line to shore and the DC to AC transformer on shore.

The losses within the wind farm distribution network from an AWES to a collection station are difficult to determine at this stage. The losses depend on the type of submarine cables and the distance from an AWES to the collection station. Next, the efficiency of the offshore substations must be found. These substations are intended to step up the voltage from farm voltage to interconnector voltage (38 kV to 220 kV). Furthermore, these stations will regulate the voltage level and stabilise the power fluctuations from the AWESs. This will induce some losses. For airborne wind, the power will fluctuate more compared to conventional wind turbines, so a slightly lower efficiency is expected. From the offshore substations, the power is transmitted using high-voltage direct current interconnectors. Direct current interconnectors are preferred compared to alternating current because of the long distance from shore and the fact that the electricity is already direct current from the AWESs. Longer distances make direct current transmission more cost-effective because it induces less loss in the cables. It is found that on average, losses from high voltage direct current transmission are around 3.5% per 1000 km[34]. Lastly, since national energy grids are alternating current, the electricity needs to be transformed from direct current using a transformer. High voltage transformers can have an efficiency of up to 99% [7]. Concluding, the efficiency of transmission can only be accurately determined when a site is known for the farm, but due to the high voltages, the power losses are not expected to be above 10%.

13.4. Mass & Power Budgets

This section includes mass budget and power budget of the airborne element.

[7] linquip.com[Cited 20 June 2023]

13.4.1. Mass budget

A mass requirement given is that all components in the farm should weigh less than 50% of a floating HAWT-basted (Horizontal Axis Wind Turbine) wind farm. Therefore, a comparison is made in table 13.1. For the HAWT-based wind farm, Hywind[8] wind turbines are used, each generating 6 MW, thus 167 turbines would be needed. The airborne-based wind farm uses 1000 of 1 MW systems.

Table 13.1: Mass comparison of a 1 GW farm of conventional floating offshore wind turbine and Deep WattAir

Component	HAWT-based [t]	Airborne-based [t]	Airborne-based [t] 20Y
Turbine	167 · 1,095	x	x
Airborne element	x	1,000 · 2.313	1,500 · 2.313
Seaborne element	167 ·2,300	1,000 · 112	1,000 · 112
Tether	x	1,000 · 0.375	10,000 · 0.375
Mooring & anchors	167 · 2,100	1,000 · 237	1,000 · 237
Substation	12,500	12,500	12,500
Total	930,165	364,188	368,720
Relative percentage	100 %	39.15 %	39.64 %

From table 13.1, it can be seen that in the first year of operations, Deep WattAir 1 GW consists of around 364 thousands tonnes of material. Throughout 20 years of operations, only tethers have to be replaced once every 5 years: for 1,000 AWES, it would require 4,000 tethers in total. To be more conservative, the assumption is that tethers must be replaced once every 2 years; thus, in total, at the end of 20 operation years, 10,000 tethers are used. Nevertheless, this does not drive the material mass of the project significantly. While conventional floating offshore wind farm does not require replacements of parts, total material mass still amounts to more than 900 thousand tonnes of material. To conclude, the Deep WattAir 1 GW airborne offshore wind farm- meets the mass requirement.

For the mass budget of airborne and seaborne elements, table 13.2 and table 13.3 respectively display more details for both.

Table 13.2: Mass budget of components from airborne element

Components	**Mass** [kg]
Motor/ Generator	333
Propellers	365
Nacelle	70
Wings	1371
Tails	420
Struts	36
Fuselage	118
Tether	375

Table 13.3: Mass budget of components of seaborne elements

Components	**Mass** [kg]
Base station	30,000 [a]
Floating platform	82,000
Moorings	87,000
Anchors	150,000

[a] Makani [Cited 20 June 2023]

13.4.2. Power Budget

The power consumption of the system must be minimised to maximise the power generated by the system. Therefore, a power budget is set up in table 13.4a, where the capacity factor

[8] Hywind-Scotland, [Cited 16 June 2023]

and availability effects are subtracted from the rated power.

The power used in a single system during VTOL and crosswind flight has to be subtracted from the generated power. The power used during VTOL as seen in equation (13.4) is dependent on the time spent in VTOL, the amount of take-offs and landings and the power usage of the generators. The amount of take-offs is dependent on how often the windspeed moves in and out of the operational window, which is still to be analysed. Furthermore, the system will make use of lights, actuators, sensors, communications, and controllers. The choice between hydraulics and electric controllers has not been decided and is therefore not included in the power budget. In table 13.4b the power usage of the airborne element is presented during VTOL and crosswind flight. The power usage makes use of specific components and the power usage in UAV's[9] and small aircraft. A number of different generators have been selected as a possibility for the design which lead to the selected range in power. During crosswind flight, the power usage of the system is minimal, only the motor/generator is not used.

$$P_{VTOL} = P_G \cdot t_{VTOL} \cdot N_{VTOL} \tag{13.4}$$

Table 13.4: Power budget estimations

(a) First order estimation for Power Budget of Deep WattAir wind farm

Energy	[GJ/y]
Rated power	$31.5 \cdot 10^6$
Capacity factor effect	$-11.7 \cdot 10^6$
Availability effect	$-1.58 \cdot 10^6$
Total energy	$18.2 \cdot 10^6$

(b) Power usage of single system AWES

Mode	**Power usage** $[W]$
VTOL	125,530 - 125,660
Crosswind flight	530 - 660

13.5. Bill Of Materials

A bill of materials (BOM) for the wind farm is a comprehensive list of all the components and materials required for the construction and operation of the wind farm. It serves several important purposes such as helping in accurately estimating the costs, streamlining the procurement process, and spare parts management, among others. For that reason, a list of components is included and if possible, their material.

[9] LSA-02 Power Budget [Cited 20 June 2023]

Table 13.5: Bill of Components/Materials for the full farm

Part ID	Name	Description	Quantity	Material
SYS	**AWES**	The complete Airborne Wind Energy System	1000	-
SYS-AB	**Airborne Element**	Flying, power generating subsystem	1	-
SYS-AB.1	Power System	Wing-mounted propellor unit		
SYS-AB.1.1	Motor/Generator	Device for converting kinetic energy to electrical energy and vice versa	8	-
SYS-AB.1.2	Rotor	Rotating aerdodynamic component	8	Al7075-T6
SYS-AB.1.3	Nacelle	Streamlined casing around the power system unit	8	Carbon-Fibre Epoxy
SYS-AB.2	Wing configuration	Aerodynamic component needed to generate lift		
SYS-AB.2.1	Airfoil	Cross-sectional shape of the wing structure	1	-
SYS-AB.2.2	Wingbox	Load carrying component inside the wing	2	Al7075-T6
SYS-AB.2.3	Skin	Outer surface which covers the wing	2	Al7075-T6
SYS-AB.2.4	Strut	Structural component between wings	10	PPS
SYS-AB.3	Empennage	Tail structure needed for stability and controllability		
SYS-AB.3.1	Tail boom	Spar that connects the wing structure to the tail	2	Al7075-T6
SYS-AB.3.2	Horizontal tail plane	Horizontal stabiliser acting as a small lifting surface	1	Al7075-T6
SYS-AB.3.3	Vertical tail plane	Tail fin used to stabilise in yaw	2	Al7075-T6
SYS-AB.4	Control System	Manages, commands and directs the behaviour of the airborne element		
SYS-AB.4.1	Flaperon	Flight control surface in the wing that combines aspects of flaps and ailerons used for roll	4	Al7075-T6
SYS-AB.4.2	Elevator	Flight control surface in the horizontal tail plane which controls the pitch	2	Al7075-T6
SYS-AB.4.3	Rudder	Flight control surface in the vertical tail plane which controls the yaw	2	Al7075-T6
SYS-AB.4.4	Flight controller	Processing unit that gets inputs from sensors and controls the airborne element autonomously	1	-
SYS-AB.5	Measurement System	Sensors and positioning systems for data collection and operations		
SYS-AB.5.1	GPS sensor	Sensors used to accurately measure position, orientation, velocity, and acceleration	1	-
SYS-AB.5.2	IMU/RTK sensor	Sensor with same functions as GPS used as a redunant system	1	-
SYS-AB.5.3	Altimeter	Instrument used to measure the altitude of the aiborne element	1	-
SYS-AB.5.4	Electrical sensor	Sensor used to monitor the electrical consumption/generation	-	-
SYS-AB.5.5	Pitot tube	Instrument used to measure the velocity of the airborne element	1	-
SYS-AB.6	Data transmitter and receiver	Ensures communication between the airborne element and the ground station	1	-
SYS-AB.7	Electrical wiring	Connection between electrical components	1	Aluminium
SYS-AB.8	Lights	Lights to make the airborne element visible in the air	2	LED
SYS-TE	**Tether**	Connection between the airborne and seaborne element		
SYS-TE.1	Conductive cable	Wires (and insulation) needed to transport electricity from the generators to the seaborne element	1	Aluminium
SYS-TE.2	Strength member	Structural component of the tether that is in tension during operations and offers high fatigue tolerance	1	Dyneema
SYS-SB	**Seaborne Element**	Floating base of the AWES	1	
SYS-SB.1	Station	Structure that controls the tether and provides launching and landing capabilities	1	-
SYS-SB.1.1	Winch and Drum	Anchors and stores the tether	1	-
SYS-SB.1.2	Drivetrain and Brake	Controls reel in/out and orientation (azimuth and inclination) of the tether	1	-
SYS-SB.1.3	Perch	Acts as the system for launching and landing	1	-
SYS-SB.1.4	Human platform	Provides access for maintenance	1	-
SYS-SB.1.5	Transformer	Eletrical component that transforms the electricity to higher voltage	1	-
SYS-SB.2	Mooring Cable	Cables that attach the floating seaborne element to the anchors	3	Steel
SYS-SB.3	Anchor	Heavy object used to moor the seaborne element to the sea bottom	3	Steel
SYS-SB.4	Electrical Cable	Connection between the AWES and the substation	1	Aluminium
SUB	**Substation**	Unit that converts the electricity to that suitable for further transport and monitors the environment	4	
SUB.1	Transformer	Eletrical component that transforms the electricity to higher voltage	1	-
SUB.2	Weather Measurement System	Collection of measurement tools that monitor the weather	1	-
SUB.2.1	LIDAR	Light detection and ranging used to measure windspeed	1	-
SUB2.3	Barometer	Instrument measuring atmospheric pressure	1	-
SUB2.4	Thermometer	Instrument measuring temperature	1	-
SUB2.5	Wave measurement device	Instrument measuring wave amplitude and frequency	1	-
SUB2.6	Hygrometer	Instrument measuring the humidity of the air	1	-
SUB2.7	Rain radar	Radar used to locate precipitation	1	-
SUB.3	Communication System	Collection of radars capable of interconnection and interoperation to form an integrated whole	1	-
SUB.3.1	Base station	Acts as a reference for positioning and communicates with the AWESs	1	-
SUB.3.2	Maritime radar	Detects objects within the perimeter of the farm	1	-
SUB.3.3	Communication Tower	Ensures proper data transfers between offshore and onshore elements	1	-
BUOY	**Buoy**	Floating objects used to indicate the outline of the farm and the ship routes inside the farm	+/- 50	-
OPS	**Operations Station**	Hub where personnel can be accommodated and maintenance ships/helicopters can dock/land	1	-

14
Operations & Logistics

As discussed in the midterm report [3], operational and maritime expenses are a significant component of an offshore wind farm. This is mainly due to the large cost of construction and transport vessels and the large distances from shore. In this chapter, a detailed investigation of operational and logistical requirements and strategies is carried out. This investigation will focus on operational aspects of the floating airborne wind energy farm that differ from conventional floating wind farms since similar operations can simply be adopted from existing wind farm operations.

First, section 14.1 presents the general overview of the operational and logistical requirements, building on previous work in the midterm report. Then, section 14.2 discusses the in-port assembly of the farm subsystems. Next, section 14.3 shows the logistical challenges for the transportation of components and systems. Then, section 14.4 discusses logistics during on-site assembly. Section 14.5 will discuss maintenance and repair logistics. In section 14.6 the end-of-life (EoL) logistics are discussed, including the possibilities for the system after the end of life. Lastly, section 14.8 discusses the autonomous operations of the wind farm.

14.1. Operations & Logistics Description

Operational expenses contribute around 30% to the total lifetime cost of a conventional offshore wind farm [42]. Considering that the project's goal is to deploy airborne wind energy systems (AWESs) to deep-sea areas further offshore, this fraction is expected to be larger for the intended system. The analysis in chapter 15 shows that the fraction of operational expenses are expected to be between 30 and 39% of the total project cost.

The main goal of operations and logistics planning is to optimise for the lowest levelised cost of energy (LCoE) while retaining energy security. This means finding an optimum case for low cost and high availability. When comparing floating airborne wind to conventional offshore wind, the following can be noted. ”Significant cost savings can already be achieved compared to conventional offshore wind farms. Due to the smaller size of floating wind systems, they can be fully installed in port and then towed to shore. This means large expensive floating cranes are not needed. Furthermore, floating systems do not require a foundation, again removing large and expensive pile-driving ships from the logistics. On the other hand, the airborne wind energy farm is expected to have an increased maintenance load. This is mainly due to a higher expected number of generating units, the lower maturity of the system, and the higher system complexity [3].” Furthermore, a comparison with the offshore oil and gas (O&G) industry can be made. The offshore O&G industry has a lot of experience in offshore construction, maintenance, logistics, and operations, and therefore has a lot of accumulated knowledge. It would be beneficial for this industry to transition to floating offshore wind projects, where their expertise can be utilised fully. Furthermore, knowledge transfer could aid the development of offshore floating wind.

To investigate the operations and logistics in more detail, a diagram [3] is made showing the operations, logistics and tools required at each stage of the project. The diagram can be seen at the end of the section. As can be seen, a distinction can be made between manufacturing, in-port assembly, transportation, on-site assembly, farm control, maintenance & repair and end-of-life. Manufacturing is expected to be very similar to conventional wind turbines, and is even expected to be less complex since there is no large tower that needs to be produced for

airborne wind energy systems. ”The operations and logistics diagram also shows the need for storage warehouses for replacement parts. The number of replacement parts stored needs to be considered carefully. On the one hand, warehouse volume is expensive. However, not having a part available in time can cause delays in repair procedures. A balance must be found to minimise the total cost. The same can be said about the strategies involving the manufacturing and transportation of equipment. Here a balance should be made between ensuring the availability of tools and cost (lease or buy) [3].” The other mission stages are significantly different compared to conventional offshore wind farms so they will be discussed in more detail.

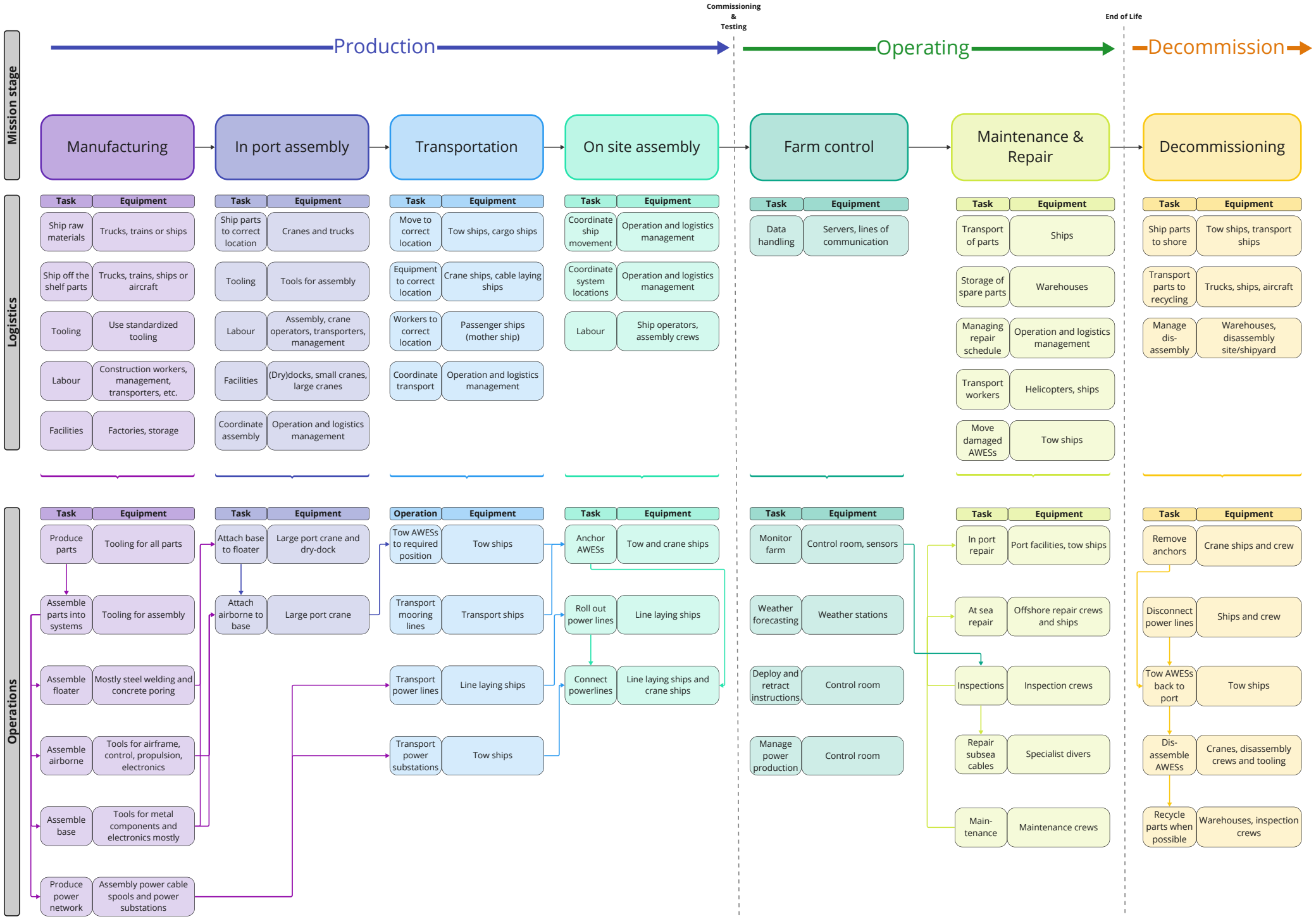
Mission stage
Production
Commissioning & Testing
Operating
End of Life
Decommission
Manufacturing
In port assembly
Transportation
On site assembly
Farm control
Maintenance & Repair
Decommissioning
Logistics
Task
Equipment
Ship raw materials
Trucks, trains or ships
Ship off the shelf parts
Trucks, trains, ships or aircraft
Tooling
Use standardized tooling
Labour
Construction workers, management, transporters, etc.
Facilities
Factories, storage
Ship parts to correct location
Cranes and trucks
Tooling
Tools for assembly
Labour
Assembly, crane operators, transporters, management
Facilities
(Dry)docks, small cranes, large cranes
Coordinate assembly
Operation and logistics management
Move to correct location
Tow ships, cargo ships
Equipment to correct location
Crane ships, cable laying ships
Workers to correct location
Passenger ships (mother ship)
Coordinate transport
Operation and logistics management
Coordinate ship movement
Operation and logistics management
Coordinate system locations
Operation and logistics management
Labour
Ship operators, assembly crews
Data handling
Servers, lines of communication
Transport of parts
Ships
Storage of spare parts
Warehouses
Managing repair schedule
Operation and logistics management
Transport workers
Helicopters, ships
Move damaged AWESs
Tow ships
Ship parts to shore
Tow ships, transport ships
Transport parts to recycling
Trucks, ships, aircraft
Manage dis-assembly
Warehouses, disassembly site/shipyard
Operations
Produce parts
Tooling for all parts
Assemble parts into systems
Tooling for assembly
Assemble floater
Mostly steel welding and concrete poring
Assemble airborne
Tools for airframe, control, propulsion, electronics
Assemble base
Tools for metal components and electronics mostly
Produce power network
Assembly power cable spools and power substations
Attach base to floater
Large port crane and dry-dock
Attach airborne to base
Large port crane
Operation
Tow AWESs to required position
Tow ships
Transport mooring lines
Transport ships
Transport power lines
Line laying ships
Transport power substations
Tow ships
Anchor AWESs
Tow and crane ships
Roll out power lines
Line laying ships
Connect powerlines
Line laying ships and crane ships
Monitor farm
Control room, sensors
Weather forecasting
Weather stations
Deploy and retract instructions
Control room
Manage power production
Control room
In port repair
Port facilities, tow ships
At sea repair
Offshore repair crews and ships
Inspections
Inspection crews
Repair subsea cables
Specialist divers
Main-tenance
Maintenance crews
Remove anchors
Crane ships and crew
Disconnect power lines
Ships and crew
Tow AWESs back to port
Tow ships
Dis-assemble AWESs
Cranes, disassembly crews and tooling
Recycle parts when possible
Warehouses, inspection crews

14.2. In-Port Assembly

An advantage of floating airborne wind energy systems is their compact size compared to conventional floating wind turbines. The low height of these systems makes in-port assembly much easier since it can be performed with relatively small cranes that are available in almost all ports. Furthermore, the selected semi-submersible floating structure has a shallow draft, making in-port installation of the AWES onto the floating structure achievable in a lot of ports (depending on the port depth). This will result in significant cost savings since no floating cranes will be needed for the assembly of the systems. These cranes are expensive and would need to make long trips to reach the farm site. Furthermore, the airborne element could already be connected to its base in port. It can then be placed on its landing structure and strapped down for transportation. This means no separate trips are needed for the airborne elements. Additional considerations for assembly that influence cost are the time in port for assembly and transportation of components and subsystems. By coordinating the delivery of subsystems and components efficiently, less warehouse space is needed at the port. Furthermore, with efficient assembly, the assembly time of one system can be minimised. This reduces the time in port, which reduces cost.

14.3. Transportation

The transportation stage consists of all steps required to move the manufactured subsystems from the port to the farm location. The main systems to be transported are the airborne wind energy systems, the mooring components, the energy network components and the maintenance facilities. The maintenance facilities will be discussed in section 14.5.

As stated previously, the AWESs can be towed fully assembled. This is commonly done with tugs or Anchor Handling Tug and Supply vessels (AHTSs) [43]. Only one AHTS is needed for towing a system because of its large towing capacity, while multiple tugs would be needed. Furthermore, AHTSs can tow at a higher speed. However, tugs are roughly ten times cheaper to operate[43]. Towing speed becomes a more important criterion when constructing a farm further offshore. The further the distance, the more effect transit speed will have on the total duration of the trip which also impacts the shipping cost. Furthermore, longer transit times will increase the chance of transport delays due to weather conditions. There will be limiting wave and wind conditions for the transportation of the floating elements. Increased shipping time will thus increase the chance of these conditions exceeding their limits within the transportation window. One possible solution to this is to set up a ”safe haven” halfway between the port and the site. Here, the floaters can be anchored if harsh sea conditions are predicted. For floating conventional wind turbines, transporting three turbines took three days for a 20 kilometre trip. Because an AWES is designed to have less mass, the transit time might be lower. An optimum must then be found between the number of ships used and the duration of the transportation phase. Optimally, the AHTS towing the floater is also transporting the anchoring materials. Then it can anchor the AWES as soon as it reaches its location, eliminating a trip per system.

Mooring components and electrical cables can be transported on the same ship that will install them. This means no separate trips are needed to transport these components. The offshore substations can be transported on a barge or with multiple towing vessels depending on their design. These systems will probably be the most costly to transport due to their size.

14.4. On-Site Assembly

On-site assembly will consist of multiple phases. Firstly, the electrical cables must be placed on the seabed. This will be done by cable-laying vessels. These are large ships which carry a spool of sub-sea cable. This spool gets unwound and the cable gets lowered to the seabed

in a desired path. The ends of the cables that need to be attached to the AWESs are attached to floaters in the planned locations. The other ends of the cables are attached to the offshore substations that will connect the farm network to the connection to shore.

Next, the AWESs will be placed in the planned locations and they will be anchored to the seabed. This will be done by the AHTSs. Three chains will be attached to each AWES. Then the anchors are placed at the correct angle and distance from the AWES. The anchors can be installed by lowering them to the seabed, where they will embed themselves when they are dragged by the AWES. This process is much cheaper than installing foundations for conventional wind turbines. It will also have less ecological impact.

Then, the floating end of the power line will be attached to the AWES and the straps used for the airborne element during shipping will be removed. This completes the assembly of the farm. The next step will be to thoroughly test all aspects of the farm. This will include checking the electrical network, checking sensors, checking for any damage during transportation and test flights for the airborne elements. After the testing regime, the farm can start to operate.

14.5. Maintenance & Repair

Maintenance and repair are expected to be more extensive compared to conventional wind turbines. This is because airborne wind energy systems are more complex and have more moving components. For this reason, maintenance should be planned efficiently. Firstly, the maintenance frequency is investigated, which then is taken into account in the maintenance method and logistics.

14.5.1. Maintenance and Repair Logistics

The most important maintenance task of the wind farm will be on the mechanical components. This includes the control surfaces of the airborne element, the tether drum, the rotation mechanism of the base, the bearings in the generators and the generator cooling systems. These mechanical systems will wear over time and will need replacement or refurbishment. The saline environment will also impact these systems. Furthermore, the tether wear will need to be checked regularly and worn tethers must be replaced.

The unexpected repairs will likely occur mostly due to electronic malfunctions, malfunctions of the control system, or malfunctions due to wind gusts. The effects can range from minor electronics replacements to the loss of a full airborne element after a crash. Repair crews should be properly equipped to deal with even this worst-case scenario.

14.5.2. Maintenance Strategy

”Maintenance can be scheduled, condition-based, or corrective. Scheduled maintenance follows a pre-determined schedule. Sometimes, it can be more efficient to perform maintenance outside of a schedule when a certain condition is met, also known as condition-based maintenance. Conditions include component age initiated, failure initiated, anomalies detected, opportunity initiated, or weather initiated. Under weather initiated, the following can be understood. It is more efficient to perform maintenance when the wind is low since the system is not active then. Opportunity initiation can be that the system is down due to another issue. Then it is efficient to perform maintenance on other parts at the same time.

In addition, maintenance can be performed correctively. This is the case when maintenance only occurs when the system fails. This is not preferred since a failure can damage other parts of the system, making replacement more expensive. However, in some cases, it can be used when maintenance costs are higher than replacing the entire system.

For maintenance, two methods can be employed. Either the maintenance is done on-site or

alternatively, although not preferred, it is done by towing an entire AWES to port and performing maintenance there. It could even be replaced with a new system while the old one is being repaired. This way no energy production is lost. Repair in port can also be cheaper or the only option if there is extensive damage and cranes are required. In addition, repair work in the port is not interrupted by bad sea conditions.

Due to the increased size of turbines and the data available on their failure methods, the trend is to move towards preventive (condition-based) maintenance. This condition-based maintenance strategy uses sensors to continuously monitor the state of components to estimate their remaining lifetime, this is used as an input for deciding the maintenance strategy to optimise the availability. This condition-based maintenance is the maintenance strategy that will be used for the airborne wind energy system.

A key element of the maintenance strategy that should not be neglected is the accessibility of the site and the mobilisation of the crew. Even when all components and tools are ready to perform maintenance, it must be realised that the site may not always be accessible with a certain transportation mode due to the local weather forecasts. Second, it also requires a certain amount of time to mobilise the crew. Both of the aforementioned topics can and will have an effect on time strategy and should therefore not be carefully planned for [3].”

14.5.3. Accessibility and Availability

The accessibility of floating platforms is an important factor in maintainability. It is difficult to transfer crew from a floating ship to a floating AWES. A solution to this is a so-called ”walk-to-work” (W2W) vessel. It uses a motion-compensated gangway to provide the crew with a stable bridge from the boat to the AWES. Another possibility is to include a helicopter landing platform onto each floater. This way, trips can be taken by helicopter, which is much quicker. However, there will be a restriction on weather conditions. Most importantly, the helicopter will not be able to fly through the farm when the system is running. For this reason, W2W vessels are preferred. Furthermore, the maintenance crew should be able to access the airborne element when it is parked on the base. Since it will be parked on an arm, away from the tower, this will be challenging. To simplify the maintenance of the airborne element, an areal work platform should be integrated onto the base. With this, workers can position themselves close to the airborne element with ease.

In addition to accessibility, the availability of personnel and parts is critical. Since the farm is expected to operate far offshore, parts and personnel will need to make long trips to reach the farm. For this reason, the farm will have an on-site maintenance facility. This facility will store spare parts, replacement tethers, replacement airborne systems and even a few full systems. These systems can be used to replace a heavily damaged AWES. This damaged AWES can then be towed to a dock for repairs. This will reduce downtime and thus increase availability. The maintenance facility could even house a small crew if needed. This could be done for the first few operating years to account for any teething problems.

14.6. End of Life

”Decommissioning again requires a lot of ships to remove all components. Maritime cost during decommission can account for 80% of the decommission cost [43]. Shipping activities must be coordinated efficiently to keep costs as low as possible. All components are planned to be removed except for the electricity network. This network is expected to be reused for a new wind farm.

Decommissioned systems must be disassembled in port. The aim should be to recycle as many components as possible and sustainably discard the materials that remain. The floating

platform can be refurbished and put back to use for either a new farm or a different application. Metal components can be recycled into new raw metal stock. Electronic components should be sent to specialised electronic recycling firms to recover rare earth metals.

It must be noted that at end-of-life there are two other options instead of immediate decommissioning. The farm can either be re-powered or it can simply just keep on running (life extension) [3]."

Re-powering means replacing the old turbines with newer and more efficient technology. For the floating airborne wind farm, this would mean re-using the electricity network and floaters and maybe even the bases. The airborne element could for example be replaced by a lighter, more refined design with 20 years of extra development time. This would lead to higher power production and better energy yields. To make this option attractive in the future, the electricity network and floating base should be slightly overdesigned to be able to handle the additional power and loads generated by an airborne wind energy system with a higher power rating.

Life extension can also be considered. As long as the proceeds of the energy production remain higher than the operational expenses, life extension increases the revenue of the farm. This is because the capital expenses of the farm will be paid off at the end of the planned life of the farm. This means the only consideration is the increasing maintenance cost of an ageing wind farm. Once it is determined that the farm is no longer profitable, it can then be decommissioned.

14.7. Availability Optimisation

An important consideration is the effect of maintenance and repair on the availability of the wind farm. A user requirement states that the availability of the farm should be at least 95%. This means that a system can not be offline more than 5% of its life. It has been found from wind data that, in the north sea, it can be expected that the wind speed will be below the cut-in speed of the farm (4 m/s) approximately 10% of the time [3]. This time should be fully used for maintenance since the maintenance will not affect the capacity factor if the farm is already down due to lack of wind. At this stage, it is assumed that downtime due to unexpected failures will be in the order of 1%. Considering this, 4% of the farm can be down for maintenance at a time to ensure a 95% availability. To achieve this, the farm will be split into maintenance zones. Each zone will be shut down entirely to ensure safe passage for transport vessels. Assuming that it will take one day for a maintenance crew to maintain and repair a single system, multiple maintenance crews will be needed to fit within the maintenance schedule. Then, after all systems have been maintained and repaired, the section is deployed again and the next section will be put offline. This is determined to be a feasible way to reach a 95% availability of the farm. If during this time another system unexpectedly fails, it will be bypassed for the current maintenance time. If many systems fail in one sector, the decision can be made to change the maintenance schedule and visit that sector first.

14.8. Autonomous System Applications

Due to the remoteness of the location, being offshore and in deep waters, it would be preferred if many operations conduct themselves autonomously. For the identification of the elements required for autonomy, the method described in [44] will be used. Here, the functional flow and functional breakdown structure are utilised to identify the different stages during operation. After identification, a plan and system can then be created to automate the various stages. The main operation stages include:

Phase 0: Pre-Launching checks

Phase 1: Takeoff procedure

Phase 2: Energy generation phase

Phase 3: Landing procedure

Phase 4: Post-Landing checks

Other phases include autonomy when risks fire, autonomy during parking state, and autonomous monitoring of component health and status for maintenance. The *pre-launching and post landing checks* includes weather data processing to ensure that wind speeds measured fall within the operational window, it includes systems checks of component once the weather conditions are within the operational window for launch and the subsequent course of action after the checks. The *launching and landing phase* encompasses reaching the operational altitude and then performing the manoeuvre to commence the energy generation phase and going back to the stored state. It also encompasses the reeling of the tether through the winch, the control signals sent to the motor/generator, to switch them to propulsive mode, and to control surfaces on the airborne element. *The energy generation phase* consists of the interface between the motor / generator, the actuation of the control surfaces and the airborne control unit, but also consists of a more complex trajectory planning system. Within this phase, the main focus is put on the energy generation. Lastly, *catastrophic risks* like the breaking of the tether, tether entanglement of neighbouring AWESs, trajectory overlaps, and unexpected changes in the environment, and component failures are mitigated through the proposed autonomous system.

14.8.1. Autonomous System Architecture

When looking at the autonomous system architecture, a hardware and software diagram of the complete control system can be constructed in a way that the unit works autonomously.

The different control units, their connections to the hardware components, and the type of signals they receive and send per individual AWES are all depicted in figure 14.1. As seen there will be two main control units, one on the airborne and one on the seaborne element. The diagram also showcases a decision tree that the control unit shall perform to navigate between and choose the appropriate phase of the AWES. There are five phases spanning from phase 0 to phase 4 as described in the diagram.

Another area of interest is the type of software developed in different nodes within the airborne control unit; the sensor data processing node, the state estimation node, trajectory planning and control, and the communication node. The software options for the *sensor data processing node* would be to work in conjunction with the software of each sensor, weighing options among a host computer, a control area network (CAN) bus, FlexRay, a local interconnect network (LIN) bus, or other options not included or under development. Each option has a different communication and interaction method and based on this system's use case, the best one should be chosen or developed upon. The *state estimation node* tackles the state system calculations, however should also look into algorithms like Kalman Filtering with its different types (extended, unscented, cascaded) for the airborne element localisation. Other algorithms that could be used consist of particle filters, ensemble random forest filter (ERFF) or simply using a reliable GPS system. For *trajectory planning and control*, controllers like Stanley-PID (proportional–integral–derivative) controller, Programmable Logic Controller (PLC), Model Predictive Controller (MPC), or other trajectory controllers that could also include machine learning or neural networks if applicable and feasible for this case. In terms of *communications* software, interfaces like Dedicated short-range communication (DSRC), an interface similar to that found in autonomous vehicles like Vehicles to everything (V2X) that includes V2V and V2I.

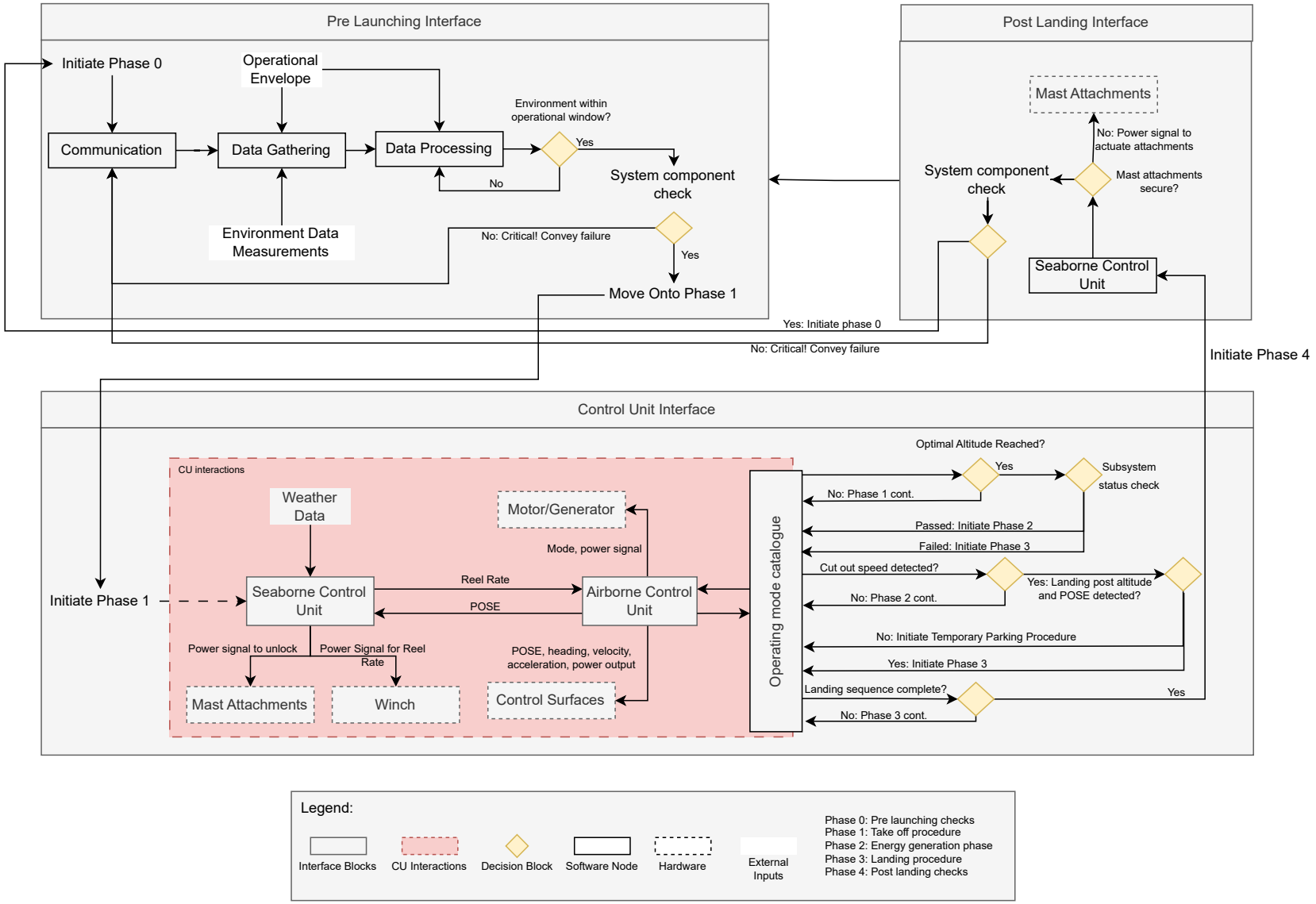

Figure 14.1: Software diagram of the wind farm

To enable the autonomy described in figure 14.1 the hardware needs to be constructed to allow for this autonomy. Within the hardware groups four critical to be designed groups were identified for the successful autonomous operation of the farm. The following groups were identified the airborne and seaborne element, offshore substation, and the onshore segment. In figure 14.2 the hardware components for the various elements can be observed.

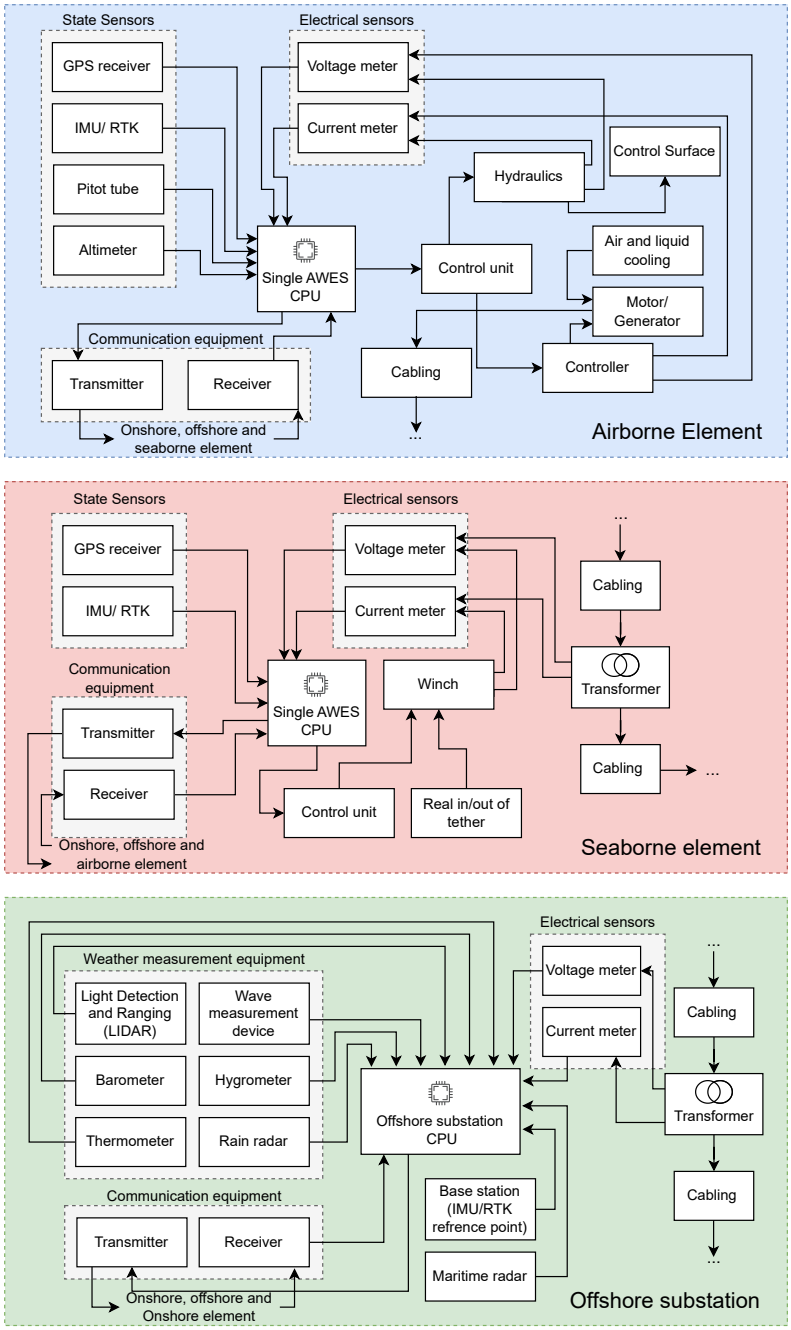

Figure 14.2: Hardware diagram of the wind farm

Two elements which were not directly described in figure 14.2, include the onshore headquarters and the GPS satellites. The onshore headquarters will have a passive connection with all

the elements within the farm. It will mainly behave as a data processing centre and will organise the logistics of the whole system. Lastly during extreme conditions the onshore element will have a emergency line of communication with the elements within the farm to adequately react when required. Secondly the GPS satellites will connect with the various positioning elements within the farm for position determination (GPS receiver and IMU/ RTK (Inertial measurement unit/ Real time kinematic)). The data communication trough the receivers and transmitters will also be enabled trough the GPS link. A last note which should be made is that the maritime radar is a component which will be utilised to sense objects within the farms perimeter such as the airborne unit and birds.

14.8.2. Communications Diagram

To enable autonomy, strong systems should be set in place for transferring data between various components. A communications diagram is an effective way of visualising these communication lines within a system. It can be utilised to give an overview of the various elements included within a project and how they communicate with each other to guarantee and ensure smooth operation. In figure 14.3 the communications diagram for the offshore floating airborne wind energy farm can be observed.

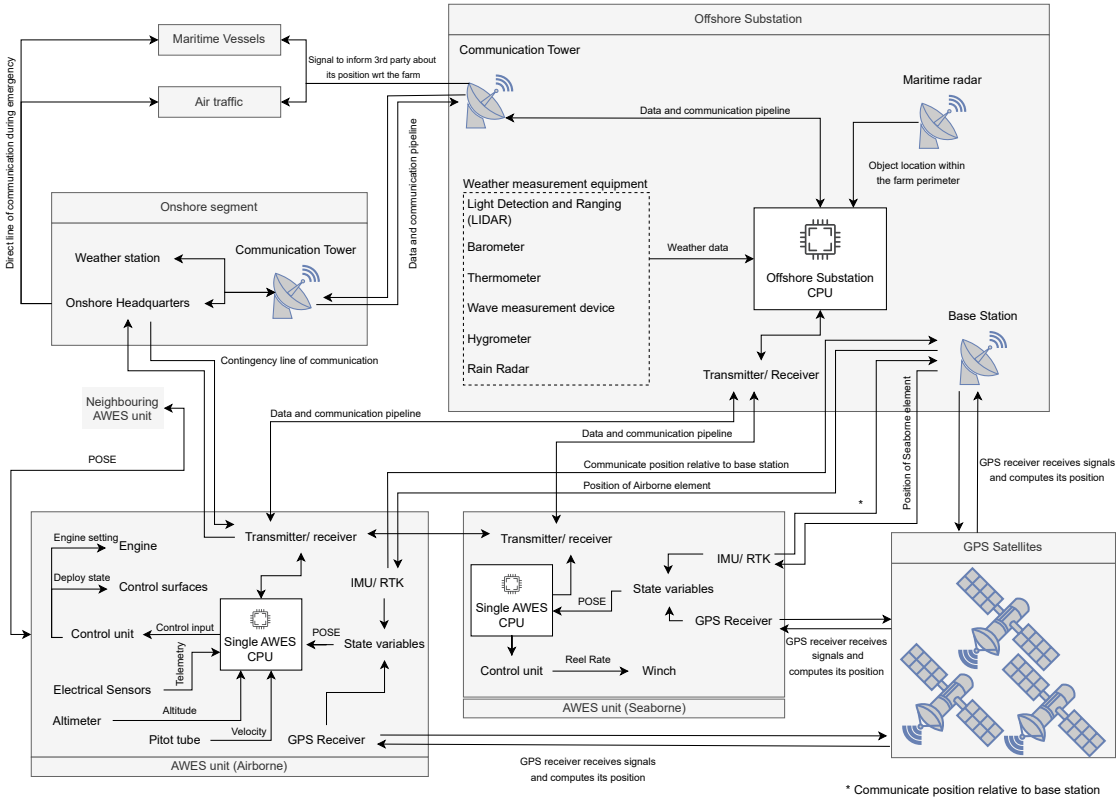

Figure 14.3: Communications diagram for the offshore floating airborne wind energy farm

Within the the communications diagram, all relevant data pipelines can be observed. At the bottom, the diagram elements involved in the communication process of the an AWES unit are shown. Here elements can be found such as inertial measurement devices, altimeters, sensors for collecting system telemetry, controllers, and communication devices.

The AWES unit is part of a whole system, to enable autonomous operation of the farm, data transmission lines are setup. First there is line of communication between an AWES unit and its

neighbours, through this line of continuous communication, the elements will be provided with information on where the neighbouring elements are (enable using GPS) and their heading. This systems was implemented to enable autonomy and ensure the systems don't collide. Secondly, a line of communication is set in place between the AWES unit and the offshore substations. Through this line, various items such as weather data, system performance and telemetry, and automatic emergency call outs will be communicated. This offshore element is in contact with the onshore segment for data transmission. Besides that, a radar system will ensure the outside and inside environment is fully defined to ensure maritime vessels and aircraft are made aware of the farms existence, also to ensure birds and the AWES units are all positioned in 3d space for to allow for a central control system to act when necessary (mainly during emergencies). Lastly there will exist a contingency line of communication from the AWES to the Onshore headquarters for emergency situations.

14.8.3. Considerations for the Present and the Future

Currently, there have been no large-scale airborne wind energy systems. And in general, individual airborne wind energy systems are still in the early stages of development. Many companies and research groups are currently researching the topic and/or creating small-scale systems of singular airborne wind energy units. As a result, the method of implementing an airborne wind energy wind farm will be strongly dependent on the maturity of the AWES system. If the AWES would be implemented into a farm today a more conservative approach will have to be taken, to reduce operational risk. During the first implementation, many different elements would still need to be investigated and new operational elements would be found. Whereas when the system is mature, a more lean approach could be taken employing more modern operational techniques. This would be possible since many of the flaws of the systems will have been solved and a greater general understanding will exist.

If a system would be implemented this would assume the individual systems have been sufficiently developed to allow for operation within a farm. Meaning that the operation and control of a singular unit will have been fully understood. To minimise the risk in a first farm, the elements would be spaced in such a way as to limit the chance of critical interaction between an element and its neighbour. For the spacing the stacking system described in chapter 13 would be utilised; however, safety factors would be taken on flight path to allow for anomalies during flight. Another element which will also be implemented is a stronger communication link with the onshore element, this would offer quicker reaction times and would allow for mistakes to be corrected from a remote location. Here, the system will autonomously be able to monitor and detect problems and communicate this to shore, together with an applicable solution to the problem.

More aggressive operational approaches could be used. Now, smaller safety margins would be utilised, enhancing spatial efficiency of the farm. The systems would be stacked more aggressively and more complex control systems would be used. Depending on local conditions and the positions of the neighbouring elements, the systems would dynamically adapt their flight path and altitude for maximal efficiency. This enhanced communication between the AWES elements would allow for enhanced autonomy and reduces the chance of critical flight conditions since flight paths will be dynamically adapted. Furthermore due to this dynamic approach the flight path will be tailored to local conditions meaning the operational window would increase. The increased autonomy would also further reduce the need for a complex onshore element, reducing costs.

15
Project Finances

In this chapter, a cost analysis of the project will be performed. First, in section 15.1, the cost breakdown will be set up by taking floating wind turbines as a reference point. Then, in section 15.2, the levelised cost of energy (LCoE) of the system for different scenarios will be determined. Finally, in section 15.3, the return on investment will be calculated.

Assumptions

- The cost breakdown per MW of AWES can be based on the cost breakdown of floating wind turbines and aircraft
- The cost of maintenance per MW of the AWES farm is similar to that of floating wind turbines.
- The discount rate has been assumed to be 5%

15.1. Cost Breakdown

The cost can be broken down into the capital expenditure (CapEx), the operational expenditure (OpEx), and the decommissioning expenditure (DecEx). In this section, all will be discussed and highlighted. The cost breakdown of a floating HAWT wind farm has been taken as a template for the cost breakdown of the AWES farm[1].

The CapEx of the AWES farm depends on the cost of the development and project management, the power generation, the balance of the plant, the installation and commissioning, contingency and insurance and decommissioning.

The cost estimation of the airborne element has been calculated using two separate methods a top-down approach and a bottom-up approach.

The top-down approach makes use of statistical relations established by general aviation planes [45]. It estimates the engineering, tooling, and manufacturing man-hours using the weight of the aircraft, the apparent speed, and the production volume. By multiplying the cost per hour by the amount of man-hours the cost for each can be calculated. Then the cost of the development support, the flight test operations, the quality control, the materials, and the fixed-pitch propellers are also taken into account.

The bottom-up approach makes use of the weight of the component and the production volume [46]. The production volume leads to a learning curve component being included in the price calculation, where an increase in production volume leads to a decrease in price per system. The cost of the structural elements has been set up using relations proposed relating the mass of the wings, boom, nacelle, and avionics to the cost. The cost of the tether and engines are calculated separately and summed up to both approaches separately. The top-down and bottom-up approaches lead to a CapEx of the airborne element of approximately 225,000 and 960,000 Euros, respectively.

The balance of the plant consists of the seaborne element, the cabling, offshore substations, and the onshore substation. The seaborne element of a floating wind turbine has been scaled down to accommodate the design of the AWES, which can be found in section 13.4.1. Similarly, the costs have also been scaled down. The cabling will depend on the spacing between each system and the number of systems connected to each subsystem. The percentage

[1] Guide to Floating Offshore Wind [Cited 14 June 2023]

change between the floating wind turbine farm and the AWES farm has also been applied to the cost. To validate the cost of the balance of the plant the Ampyx sea air farm project can be used [47]. In this project, a semi-submersible floater including mooring and anchoring has been estimated to be between 2 and 3 million euros. Ampyx would have landed the airborne element horizontally, thus needing a larger landing area. Therefore, the presented estimate is reasonable.

Installation and commissioning consist of the installation of the farm and logistics. Due to the smaller size of the power generation and the seaborne element, the cost of installation will come down drastically. However, the electrical cable and the offshore logistics cost will increase due to the increase in cable length and complexity of multiple systems.

The OpEx of the system is based on the maintenance and operating cost of a floating wind turbine farm. The airborne element has more actuators than a wind turbine leading to more maintenance trips being necessary, however the size of the maintenance ships needed for the airborne element can be significantly smaller. Thus, the increase in the amount of maintenance trips might be compensated by the decrease in the cost of the trips. The failure rates of AWES must yet be studied more closely to be able to perform preventative maintenance. Furthermore, the OpEx are estimated to be 30-39 % of the total cost.

The cost of decommissioning has been found as a percentage of the installation cost for the seaborne element, the mooring lines, the cables and the substation in an article by Myhr, Bjerkseter, Ågotnes, *et al.* [48]. There is a possibility where the seaborne elements can be re-powered for conventional wind turbines, then the seaborne elements can be sold for the capital recovery factor [49]. For the optimistic case, the cost of decommissioning has been set to zero, in this case, the cost of decommissioning will be paid for by selling parts.

The simplified version of the cost breakdown per MW can be seen in table 15.1, where conventional floating horizontal axis wind turbines (HAWT) with and without economies of scale are compared to two cases of the proposed concept. The full cost breakdown can be found in Appendix A. The CapEx and OpEx of rigid wing fly-gen are in line with the estimations made by Vos [50], where the CapEx, the cost of deep floating rigid wing ground-gen has been estimated to get to 4 million €/MW in 2030 and to 2 million €/MW in 2050. The OpEx have been estimated to be around 100 thousand €/MW in 2030 and around 55 thousand €/MW in 2050.

Table 15.1: Simplified Cost Breakdown per MW

Expense	HAWT	HAWT ES	RW FG pessimistic	RW FG optimistic
CapEx	€ 4,380,000	€ 3,750,000	€ 3,590,000	€ 2,390,000
Yearly OpEx	*€ 80,480*	*€ 70,600*	*€ 71,100*	*€ 67,660*
DecEx	€ 162,450	€ 138,000	€ 83,780	€ 0

15.2. Levelised Cost of Energy

The levelised cost of energy (LCoE) is an economic measure used to showcase the lifetime cost of an energy-generating system expressed in money per MWh. The LCoE can be calculated using the net present value of the costs and the power over the lifetime of the project. The equation can be found in equation (15.1), where the costs are subdivided into CapEx, OpEx and DecEx. The r is the discount rate which has been set to 5 % for this project. The availability has been required to be 95 %.

The net power is the rated power multiplied by the capacity factor and the availability factor. The capacity factor has been calculated by overlapping the power curve with the frequency of

wind velocity. The frequency at an altitude of 200 m can be seen in figure 15.1. This concluded in a capacity factor of 63 %. The capacity factor of on-ground power airborne power generation is found to be between 40-60 %, with the fly-gen being a little lower [50].

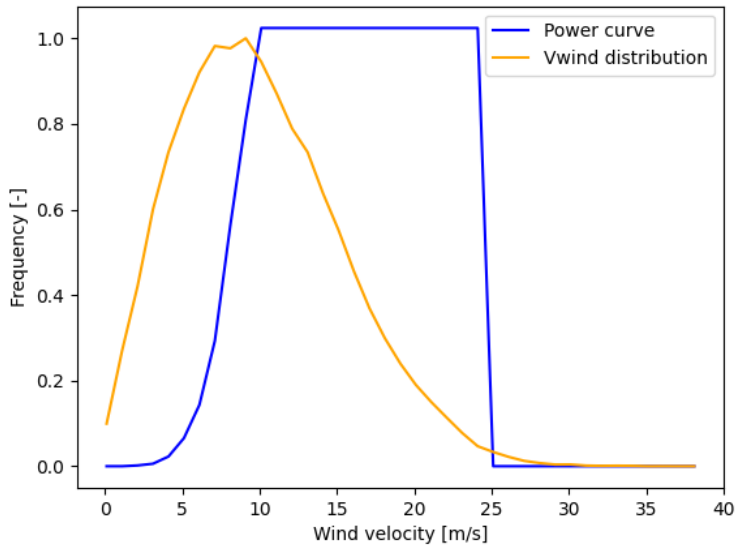

Figure 15.1: Frequency of wind velocity and power generation over wind velocity

$$LCoE = \sum \frac{\frac{CapEx+OpEx+DecEx}{(1+r)^t}}{\frac{P_{net}}{(1+r)^t}} \tag{15.1}$$

All the inputs to the LCoE calculation are represented by different cases: the optimistic case, the base case and the pessimistic case. In the cost breakdown, the optimistic and pessimistic options for CapEx, Opex and DecEx can be found. The base case takes the average of the values for CapEx, OpEx and DecEx. The DecEx has been set to zero for the base case, where all expenses of decommissioning can be paid for by selling parts of the system. The three different cases are presented in table 15.2. The LCoE calculation assumes an economy of scale and makes use of the learning curve of aircraft and floating wind substructures. Figure 15.2 shows that by increasing the lifetime of the project the LCoE can be decreased, increasing the lifetime to 31 years would lead to a 49.9 €/MWh for the base case. The bottom range is the optimistic case and the top-range is the pessimistic case. The requirement imposed on the LCoE was 50 €/MWh which is the green line that can be seen in figure 15.2. For comparison at this moment, the LCoE of floating wind sits above 100 €/MWh and is expected to drop below 40 €/MWh in 2050[2].

Table 15.2: LCoE and cost variables at a discount rate of 5%

Input	Pessimistic	Base	Optimistic
CapEx[B€]	3.6	3.0	2.4
OpEx [M€]	71	69	67
DecEx [M€]	84	42	-
t [years]	20	20	20
LCoE[€/MWh]	69	59	49.5

[2]Offshore Wind [Cited 14 June 2023]

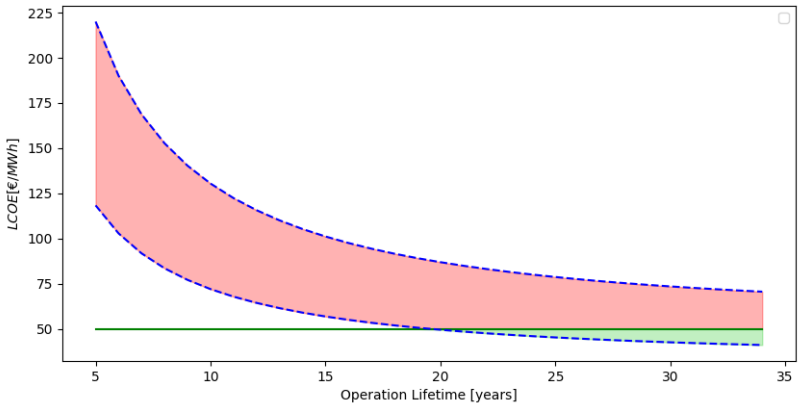

Figure 15.2: The LCoE compared to operating life at a discount rate of 5 %

15.3. Return on Investment

The return on investment of the project can be calculated by dividing the total return of the project by the total amount of investments. The total revenue (TR) is the amount of power produced multiplied by the price of the electricity. Summing the CapEx, the OpEx for twenty years and the DecEx leads to the total amount of investments (TC) necessary. For our base case, the price per MWh should stay above 42 euros in the pessimistic scenario and above 31 in the optimistic scenario to have a positive return on investment. Before December 2020, the electricity price for households in the Netherlands stayed below 42 €/MWh, afterwards the cost of electricity remained elevated to levels above 42 euros[3]. This does not account for potential government subsidies that could be made available for the AWES farm or if a customer would be willing to pay a premium for the electricity.

The pessimistic case for ROI would be selling to households in times of energy abundance while having the pessimistic LCoE scenario, i.e., before 2021. The base case would be to sell to a mix of households and industries before 2021, as industry pays more for electricity than households. The optimistic case is to sell to industry players, while also taking the price of electricity after 2021 into account.

$$ROI = \frac{TR - TC}{TC} = \frac{20 \cdot P_{net} \cdot P_{MWh} - (CapEx + 20 \cdot OpEx + DecEx)}{CapEx + 20 \cdot OpEx + DecEx} \tag{15.2}$$

Table 15.3: Return on investments at a discount rate of 5 %

Input	Pessimistic	Base	Optimistic
Electricity Price [€/MWh]	38.3	60.5	83.5
Price Period	2019-2020	2019-2023	2019-2023
LCoE[€/MWh]	69	59	49.5
ROI	-13%	+98%	+265%

[3]Statista [Cited 14 June 2023]

16
Sustainable Development Strategy

This chapter addresses various sustainability problems related to airborne wind energy, some aspects of the previous report [3] are included. Within this chapter various types of sustainability are analysed including environmental, social, and economic sustainability accompanied by an applicable mitigation plan/ strategy.

The chapter also includes a Life Cycle Analysis (LCA) that assesses the environmental impact of the project across its five main phases: material extraction, manufacturing, transportation, operations, and end of life. LCA focuses on CO_2 emissions and embodied energy, considering conservative values for material and part inventories. The results of the LCA estimate the emissions associated with each phase and provide a thorough understanding of the project's environmental footprint.

16.1. Sustainability Aspects

In the previous report [3], various problems regarding sustainability have been addressed, namely environmental, social, and economic sustainability. This section will provide mitigation plans for the corresponding sustainability problems.

16.1.1. Environmental

Material recyclability: More than 99% of the wind farm mass can be recycled and reused. For materials such as Dyneema, they might pollute the surrounding environment with microplastics. One of the solutions for the problem would be to further investigate the wear and tear of such materials, and replace them before they start to wear. Another solution is to provide a casing or housing for components with non-recyclable materials to limit the material release.

Marine wildlife: In conventional offshore wind farms, many logistics processes such as pile-driving process, transportation with huge sea vessel and offshore cranes disrupt the marine ecosystem due to upsetting level of noise made. Specifically, the noise can disturb the social interaction and migration of species. Deep WattAir can lessen these effects significantly. Because all systems no longer require the drilling of bottom-fixed foundation, the impact of the wind farm on the seabed is minimal. In addition, much smaller sea vessel and offshore crane and can be utilised. Another potential serious threats to marine life of Deep WattAir happens when high power transmission cables are exposed. Hence, in the process of designing the transmission cables, cables housing must be carefully designed.

Avian wildlife: Compared to a conventional wind farm, the airborne system can cover a wider range of altitudes. This also means that the impact of Deep WattAir on avian wildlife is, unfortunately, more serious like collision with birds. To mitigate the bird collision, airborne element can be painted in a certain colour or lighting can be installed onboard for birds to be able to avoid it visually. Another solution is to integrate avian radar detection system so that the flight altitude can be adjusted to actively prevent collision. Habitual displacement or alteration should also be looked into. There have been cases where kittiwakes, a bird species, were spotted nesting on structures of floating offshore oil rigs, according to Science Norway [1]. This is rather great for an ecological cause, especially when seabird population is declining rapidly, because also

[1] Science Norway [cited 15th June 2023]

according to Science Norway, seabird populations which reside on offshore platforms have higher chick productivity than ones residing on man-made coastal structures.

16.1.2. Social

Support the climate neutrality goals of EU: EU aims to be climate neutral by 2050 [2]. Deep WattAir greatly aids this aim as a 1 GW wind farm project.

Local energy security: A huge problem for Europe is that it depends heavily on Russia for energy. More specifically, only 42% of the energy was produced domestically, the other 58% was imported in which 29% of imported oil, more than 40% of imported natural gas [3] [4], and 54% of imported coal was directly from Russia. To be more energy independent, Europe needs to build more energy facilities. Deep WattAir is one of the said facilities.

Reduce noise, water, air pollution: In traditional energy plants, burning fuels for energy releases a noticeable amount of air, water, noise pollutants. Air and water pollution are no longer a problem for Deep WattAir. With respect to noise pollution, because it is an offshore project, it is located almost 90km offshore, noise pollution is also not a significant problem.

Offer job opportunities: Socially, Deep WattAir offers numerous jobs opportunities for society, especially high-skilled and specialised jobs, for example, construction, installation jobs, R&D jobs, project management and consulting jobs, etc.

16.1.3. Economic

Longevity and Repairability: The longer a system operates and the more repairable it is, the more cost-effective the model becomes as expenses are spent on repairing the parts that fail specifically instead of the whole system. In this case, a requirement of 20 years of longevity has been set where parts can be replaced at intervals that are also predefined.

Market Potential: The market potential is large as floating offshore wind is estimated to make up around 15% of the complete wind energy sector [6], while in the future, it has the potential to be part of the global market to further displace polluting energy sources such as oil an gas.

Resource depletion level: Wind is a great renewable resource. The undisturbed wind and unused surface area over deep waters are untapped potential and plentiful, and maintain a reasonable resource level with no worry of depletion. Space within the farm may be limited due to the large area needed for the wing but also in the air to operate in the chosen energy generation flight path. Also, materials used may not be plentiful and this should be carefully considered.

Apply for renewable energy grant and subsidise: Governments and some private organisations, funding offer subsidise and grants towards projects and research that promote green, renewable energy. Apply for such grants and subsidises offset the costs of R&D and innovation, and the cost of the farm.

Optimise cost through technology advancements: Investing in Research and Developments can boost the efficiency of the farm. Increased efficiency can be achieved from designing a more efficient airfoil or rotor, or designing a transmitting cable with less power loss. Another option is to implement new proven technology from literature which offers higher efficiency, lower loss.

Design an onsite maintenance lot: Having a maintenance hub located near or within the

[2] Climate Europe Commission [Cited 20 June 2023]
[3] Consilium Europa [Cited 20 June 2023]
[4] CNBC [Cited 20 June 2023]

wind farm could reduce the cost of operations significantly, which translates to higher yearly profit. Specifically, instead of having to depart from nearest shore to the site, a crew of staffs can depart from the onsite maintenance hub. The maintenance hub also acts as a storage for components and offers quicker inspection, repair, replacements.

16.2. Life Cycle Analysis

This section showcases an LCA with the scope of it being the 5 main phases of a product: material extraction, manufacturing, transportation, operations, and end of life (EoL). An inventory, impact and improvement assessment is carried out for every stage. The metric used will be CO2 emissions and the embodied energy at every stage. However, whenever possible, the Global Warming Potential metric shall be used in addition [51]. Material and part inventories are made based on previously carried out similar projects. It is important to keep in mind that these values are deliberately chosen to be more of the conservative side.

16.2.1. CO_2 emission per phase

This section shows the CO_2 emission per phase, for the raw material extraction, the manufacturing, operations and the end-of-life.

Raw material extraction

All systems consist of sub-components, which are made of different materials. Next, CO_2 emission of each sub-component can be estimated by multiplying its mass with the CO_2 emission per kg of the material. Finally, the sum of all the CO_2 emission mass is the total of the first stage.

The four most-used materials are: Aluminium, steel, Dyneema, Fibre glass. Within aluminium alone, there are different types of alloy: Al7075-T6, 5083-Al, etc. However, the specific CO_2 emission of each alloy is hard to estimate and is not available; therefore, only one value for aluminium is used: 17 metric tonnes of CO_2 per 1 metric tonnes of Aluminium extracted and processed. Additionally, there is no data on certain materials like PPS, which the struts are made out of. To be conservative, a value of 17 is also used for materials with unavailable data. The following table shows the CO_2 emission per kg of material extracted and processed:

Table 16.1: CO_2 emission of extracting and processing materials

Material	**CO2 emission** $[kg/kg_{material}]$
Aluminium	17
Steel	3.2
Dyneema	6
Fibre glass	2.2
Other minor materials	17

Using table 16.1, extracting and processing materials for each 1 MW system emit around 1,265 tonnes of CO_2, which translates to 1,265 thousand tonnes of CO_2 emitted for 1,000 1 MW systems.

Manufacturing

Estimating the carbon dioxide emissions of a manufacturing process is less straightforward than the previous process because there are few companies that are working with offshore floating airborne wind energy systems and no companies provide the CO_2 emission of the

manufacturing process. Nevertheless, for the first-order estimation, the group decided that data for CO_2 emission for Scope 1 & 2 of aircraft manufacturing can be utilised for the airborne element. The total CO_2 from Scope 1 & 2 of Airbus is 762 thousand tonnes [5] for the year 2022. This is the result of producing a total fleet of 661 aircraft [6]: 53 A220 units, 252 A319 and A320 units, 264 A321 units, 32 A330 units, and 60 A350 units. The total empty weight of all these 661 aircraft is approximately 36 thousand tonnes. Producing one ton of aircraft emits 21.14 tonnes of CO_2 ($\frac{762}{36} \approx 21.14$). It can be concluded that the production process emits about 24% more than the extraction process, as a simplification for later use for different subsystems, specifically for seaborne elements.

Regarding the seaborne element, data on CO_2 emissions from manufacturing semi-submersible floaters are also unavailable. The aforementioned simplification can be applied to the floating platform. Since steel accounts for most of its mass, namely almost 92 %, an assumption that seaborne element is made out of only steel is sensible.

Ultimately, manufacturing one system emits around 1,605 metric tonnes of CO_2; hence, producing systems for a farm of 1,000 systems accounts for 1,605 thousand tonnes of CO_2 emitted.

Operations

The operations phase includes the transport needed to maintain the farm. This includes different maritime vessels for the maintenance crew and also special bigger vessels to transport parts or complete airborne elements, whatever is needed, to carry out the maintenance required. In order to estimate the total CO_2 emissions, the total distance travelled during the operation lifetime is considered. Assuming one trip per month by the maintenance crew- as a conservative estimate under the pretence that maintenance other than part replacement will be needed more frequently- for systemic checks and repairs, and 50 trips with special vessels to carry substitute components, the total distance covered per type of transport is 100 km from the nearest port to the chosen wind farm zone of the Hornsea IV measured from the port in the city Grimsby. Inferring that both types of vessels use marine oil as a fuel, the total fuel used per vessel is 12.53 and 23,520 tonnes, respectively. This thus makes the CO_2 emission 74,128 tonnes for maintenance, which is a result of one ton of marine oil emitting 3.15 tonnes of CO_2 [7].

It is important to note that the emissions of the replacement parts that will be used during the operations phase is included in the raw material and production phase. Additionally, all logistical and fuel consumption values that were taken are conservative estimates.

End-of-Life

The end of life also consists of the transportation from the wind farm zone to the port during the dismantling phase. It is important to note the limitation of the estimation of this phase is that since the end-of-life (EoL) processing is outsourced, the estimations of the emissions are not considered and should be done for a more in-depth LCA. However, this phase may not play a significant role when compared to others and the addition of the EoL processing may not affect the conclusions that can be drawn. Again, the distance from the farm to the port in Grimsby is 100 km. It is assumed that there will be 100 large vessels for each type of decommissioning-sending removable parts to recycling facilities or sending removable parts to other disposal facilities. Again, this is considering the worst-case scenario where no part or component can extend its lifetime or can be reused for another project with potential upgrades. Using the

[5] Airbus [Cited 19 June 2023]
[6] Airbus [Cited 19 June 2023]
[7] Offshore Energy [Cited 19 June 2023]

same logic as the previous phase, the total fuel consumption and thus CO_2 emissions due to transportation is 9,800 tonnes and 30,870 tonnes, respectively.

16.2.2. LCA Results

In this subsection, the result of carbon dioxide emission for the four different phases in metric tonnes, figure 16.1, and their relative percentage to the total emission as a result of the sum of the four phases, figure 16.2, are shown.

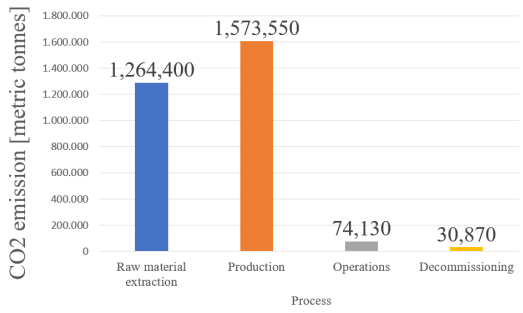

Figure 16.1: Total CO_2 emission of each phase

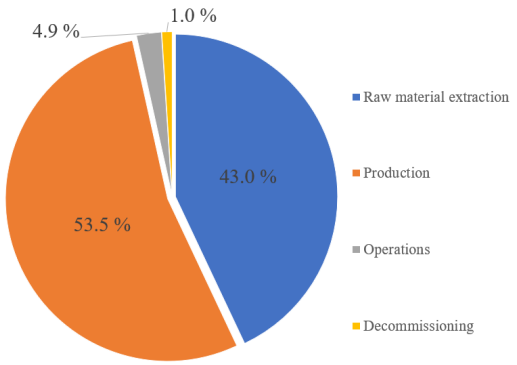

Figure 16.2: Relative emission percentage to total emission of each phase

In total, the Deep WattAir project gives off almost 3 million metric tonnes of CO_2 throughout its 20 years of operation. The two figures also show that manufacturing or production phase and raw material extraction contribute the most with 1.57 million metric tonnes and 1.26 million tonnes respectively, which amount to 53.5% and 43.0% respectively to the total amount. However, the estimation process is rather greatly conservative. Nevertheless, some mitigation plans needed to be enforced to even lower the amount.

16.2.3. LCA mitigation plan

In this subsection, mitigation actions are proposed as an attempt to reduce CO_2 emission of the project. All phases shall be done in a sustainable manner to minimise the carbon footprint or CO_2 emission of the whole project. Some of the following actions are proposed:

- Local sourcing: Sourcing of local raw materials shall be preferred to minimise the environmental impact. The shorter the transportation distance, the lower the energy consumption and carbon footprint. It is also a means to support local suppliers, which promotes social sustainability.
- Transparency in supply chain: Enhance transparency in the supply chain by mapping and understanding the origin of raw materials. Engage with suppliers to ensure compliance with social and environmental standards, and promote responsible practices throughout the supply chain.
- Sustainable procurement: Raw materials shall be ensured that they are sourced from responsibly managed and sustainable suppliers, preferable ones with a certification such as DNV's ResponsibleSteel certification [8] for steel extracting practices.
- Resource efficiency: Promote resource efficiency by reducing the overall amount of raw materials required. This can be achieved through product design optimisation, including lightweight, modular design, or the use of alternative materials with lower environmental footprints.

[8] DNV [Cited 19 June 2023]

- The 3R principles: embrace and promote 3R principles, namely Reduce, Reuse, Recycle. Systems and the farm shall be designed in such a way that enables easier decommissioning, material recovery, and material re-usage, which ultimately reduces the need for virgin raw materials and minimises waste generation.
- Cleaner Production Technologies: Invest in cleaner and more energy-efficient manufacturing technologies and processes to minimise environmental impacts, including the reduction of greenhouse gas emissions, water consumption, and air pollution.
- Waste Management with 3R: Develop strategies to minimise waste generation during manufacturing processes. Implement waste reduction measures, promote recycling and reuse of materials, and explore opportunities for converting waste into valuable resources through innovative waste-to-energy or waste-to-product technologies.
- Implementation of kite sails for sea vessels: The high CO_2 emission is due to the marine oil that vessels burn. This can be prevented by installing kite sails to make use of the abundant wind energy in the open sea. The fuel will then only be a backup source when there is not enough wind or the wind speed is too slow.
- Transfer of seaborne element for a conventional wind farm: At the end of the project, the seaborne element can be repurposed to be a floating platform for offshore wind turbines.

17 Verification & Validation

Verification and validation of the product are discussed in the chapter. The product is verified by fulfilling the requirements, assessed in the compliance matrix. A validation plan is then formulated. This plan will discuss the steps needed to validate the design. Section 17.1 shows the compliance matrix for the user requirements. Then, section 17.2 shows the sensitivity analysis performed on the design parameters. Lastly, section 17.3 discusses the validation plan.

17.1. Compliance Matrix User Requirements

In this section, the design will be evaluated to see if it complies with the user requirements. This is done using a compliance matrix, shown in table 17.1. In the matrix, 'compliant' means that the design fulfils the requirement, 'intend to comply' means that the design is intended to fulfil the requirement but not enough is known yet, and 'not compliant' means that the design does not meet the requirement. For both the 'intent to comply' and 'not compliant' statuses, actions are given that should allow the design to reach the requirement.

Table 17.1: User Requirements Compliance Matrix

User Requirement	Requirement Statement	Compliance status	Justification/value	Action(s) needed to comply
FA-04	The farm shall have a rated output of 1 GW	Compliant	The farm and systems are designed for this value	
FA_OP-01	The system shall have 95% availability to generate power	Intend to Comply	Current reliability and maintainability figures of the system are unknown, but expected to reach these numbers	Investigate reliability and maintainability figures in later stages of the design phase
FA_OP-02/03	The farm shall operate safely without risk to either shipping or air traffic	Compliant	Regulations for warning systems are followed in the design, and the farm is located outside of shipping routes	
FA_SU-01	The farm shall have components that are mass-wise 90% recyclable.	Compliant	Most materials selected for the system are either metal or thermoplastic	
FA_SU-02	The farm shall have components that are mass-wise 95% removable at the end of life.	Compliant	System is designed to be replaceable	
FA-06	The farm shall have a total mass of all the components less than 50% of an equivalent fixed bottom-mounted or floating HAWT-based wind farm.	Intend to Comply	Current calculations place the total mass at $\approx$ 39% of a floating HAWT-based farm, but the mass calculations are not validated yet	The mass and rotors sizing more accurately analysed by comparison with aircraft or drone sub-parts

Table 17.1: User Requirements Compliance Matrix

User Requirement	Requirement Statement	Compliance status	Justification/value	Action(s) needed to comply
FA_BU-02	The projected LCoE assuming technological maturity shall be less than 50 €/MWh	Not Compliant	The expected LCoE is 59 $\pm$ 10 €/MWh	LCoE could reach the requirement if the lifespan is increased and/or the decommissioning costs can be recouped
FA_OP-04	The lifetime of the AWES-based wind farm shall be 20 years	Compliant	The farm is designed to comply with this requirement	

As the compliance matrix shows, there are two requirements that are verified yet, the availability and mass, and one fails, the LCoE. To ensure that the failed requirements can be met by the design, a few actions need to be taken. The availability, reliability and maintainability of the system should be investigated when the design is reaching its final stages. The LCoE requirement can be met if the lifetime of the farm is extended to 25 years. However, the current total mass can not be validated as of yet, because there is no data available that compares to the chosen configuration in this report.

17.2. Sensitivity Analysis

To ensure that the design is robust, a sensitivity analysis is performed. This is done by changing certain parameters, and checking whether the design still meets the requirements. For a few of the requirements, a sensitivity analysis can not really be performed. These are the rated power of the farm, the safe operation, and the lifetime of the farm, as those are requirements around which the system is designed.

The sensitivity of the availability is very high at the moment because there is no data for the reliability and maintainability of such systems yet. There is also no plan for maintenance runs yet for AWES-based farms, due to how new the concept still is.

For sustainability, most of the sensitivity of the system lies in the floater, as that is currently by far the heaviest element. Should the seaborne mass be reduced significantly by using a lighter material, a better look needs to be taken at the materials used in the airborne element.

If only the airborne element is taken into account, the sensitivity is higher. Currently, the materials selected for the system are either metal or thermoplastic. The only components currently not recyclable are the tether and nacelles, which make up about 3.5% of the total mass of the airborne element.

Another part of sustainability is the removal of the systems at the End of Life. Currently, the system is designed to be 100% removable, but this can change if the anchorage is changed to fixed anchoring. This however only reduces the mass percentage that is removable by 0.65%. This means that the removability requirement has a very low sensitivity.

Two requirements that can be investigated slightly more quantitatively are the total mass requirement and the LCoE. For the total mass, the system is scaled up for a higher-rated power, meaning that there are fewer systems required. It is also assumed that the mass of the seaborne system does not change significantly. The system is analysed for 2 and 3 MW. The results of this analysis are shown in table 17.2.

Table 17.2: Sensitivity analysis for total mass.

P_{rated} [MW]	N_{units} [-]	Total mass w.r.t. HAWT [%]	Mass reduction [%]
1.0	1000	39.64	-
2.0	500	20.45	47.7
3.0	334	14.31	63.4

This table shows that an increase in the rated power of the system reduces the total mass of the farm by around the same factor. This indicates a high sensitivity to the total number of systems in the farm, which is a direct consequence of the rated power of the system.

The last analysis is performed on the LCoE requirement. At the moment, the LCoE requirement is not met, but analysis can show what could be done to ensure it will be. For the LCoE analysis, a few factors are investigated, those being a change in the discount rate, a change in mass, a change in the rated power, a change in the capacity factor and an increase in lifetime. This is done for both the pessimistic and optimistic LCoE estimation. The results of this analysis are shown in

Table 17.3: Sensitivity analysis for the LCoE

Factor investigated [unit]	**Value**	**Pessimistic LCoE [€/MWh]**	**Change in LCoE [%]**	**Optimistic LCoE [€/MWh]**	**Change in LCoE [%]**
Discount Rate [-]	1.02	56	-18.84	41	-16.33
	1.05	69	-	49	-
	1.08	84	21.74	59	20.41
Mass of Airborne Element [kg]			No impact on LCoE		
Rated power of system [MW]	1	69	-	49	-
	2	64	-7.25	43	-12.24
	5	62	-10.14	40	-18.37
Capacity factor [-]	0.45	92	33.33	66	34.69
	0.6	69	base	49	base
	0.75	55	-20.29	40	-18.37
Lifetime [yrs]	20	69	-	49	-
	25	62	-10.14	45	-8.16
	30	58	-15.94	42	-14.29

This analysis shows that, for the initial LCoE estimations, the capacity factor and discount rate have the most impact, for both the pessimistic and optimistic case. It also shows that the scaling of the system for more power quickly drops off in terms of LCoE gain, while the lifetime shows the same trend, but slower. Overall, the LCoE requirement is highly sensitive to changes in the design.

17.3. System Validation Plan

After the verification steps, the design needs to be validated. Different aspects of the design require different methods of validation. It is important that the project stakeholders will be involved in every step of the validation process. This section will discuss the validation plan for all elements of the system. And finally, for the full system.

Airborne element

The airborne element is a complex system on its own, so validation procedures for this element should be taken for this system to ensure it meets the requirements before implementing it into a full AWES. Multiple validation steps will be required. The aerodynamic calculations will be validated using a computational fluid dynamics (CFD) model, which will validate the lift and drag calculations. Because the system's power yield is highly dependent on the aerodynamic properties, there will be an additional validation step using wind tunnel testing. In these tests, a scale model of the entire airborne element with the tether will be tested to increase the confidence level in the design and the CFD models.

After these steps, the structural design will be validated using different kinds of tests. Individual components will be analysed using Finite Element Methods (FEM) to ensure that the design can carry the loads that it was designed to do. The design has to also be validated using physical tests, which start off small and lead to a structural load test of the complete airborne element. First, the material properties have to be validated using coupon tests. Afterwards, the main load-carrying components are tested in strength, fatigue, crack strength and joint strength. Lastly, two full-scale assemblies of the wing structures will be made and will be tested in both a static ultimate load test and a fatigue test. When these tests are completed successfully, the structural design is validated.

Once the structural integrity of the airborne element is validated, the other components can be integrated. After this, hover testing can be performed to validate the flight capabilities of the airborne element. This will include stability tests and tests for the autonomous launch and landing system.

Tether
To validate the tether compliance, short test sections will be produced. These sections will first be stress tested until failure. This will validate the tensile strength of the tether, while also giving insight into the strain characteristics. Next to this, a resistivity test will be performed to determine if the tether losses are as expected. Lastly, the lifetime of the tether will be tested. This will consist of both cyclic load testing and wear testing. The cyclic load tests will repeatedly impose tension on the tether for many cycles. This will determine the number of cycles the tether can reliably withstand and the amount of creep that will develop. Wear testing will be performed by running tether samples by a surface comparable to the tether drum's material many times. This test will give insight into the tether wear due to reel-in and reel-out cycles. Increasing the humidity and adding salt particles into the air around the tether can mimic the saline conditions of the operating conditions of the system.

Seaborne element
The seaborne element will need to be validated in terms of its stability and its lifetime. The stability will be validated using a scale model of the seaborne element which will be tested in a wave tank where different wave conditions will be simulated. The tests will be conducted using standard wave conditions, but there will also be tests with the largest waves that are possible during the lifetime. It is critical to validate the dynamics of the seaborne element due to the importance of stability in the landing phase.

Full-scale power generation testing
When the individual components are validated, a complete prototype of the airborne element and the tether-winch assembly will be tested onshore. This test will start by doing launch and landing tests, which leads to doing hover tests. These tests are focused on validating the control system. After doing hover tests, the airborne element will attempt to get to the target altitude where the transition into the figure eight flight path will be tested. If the control system is validated and is able to control the airborne element in all flight phases, the power yield will be validated by performing long-duration flight tests.

Full-scale offshore testing

A part of the validation process is to apply for certifications from regulatory authorities. These certifications are required before starting the offshore testing campaign and are required to ensure that the system is allowed to be used in a wind farm. The offshore tests are focused on the interaction between the airborne element and the seaborne element with the wind and wave interactions. The main focus will be on the autonomous launch and landing capabilities on a moving landing platform. These tests will be performed in increasingly more difficult wave conditions, starting from very small wave heights. The goal is to validate the autonomy of the complete system and to get confidence in the control system.

Part 4

The Next Steps

This part outlines the next steps to get from the current state of the design to a fully operational farm. Therefore a project design & development plan is set up, points of discussion are raised and recommendations are made.

18
Project Design & Development

To reach the end goal of an operational wind farm, it is important to establish the steps that will still be needed. The logical flow of operations starts after the end of the DSE until a production-ready system is shown in section 18.1. A production plan is written in section 18.2 where the production is discussed in terms of part production, then subsystem production, then a complete AWES assembly and finally the farm integration.

18.1. Project Design & Development Plan

The project design and development logic diagram as well as respective Gantt chart can be seen at the end of this chapter. These diagrams show the order of tasks that are required to end up with a finalised detailed design that is ready for production. The design and development logic diagram is ordered in nine phases, going from the project mobilisation to the finalisation and documentation. It shows the further required design steps, the analysis of this design both in aerodynamic and structural aspects, the system integration and the development and testing of a full-scale prototype. Once this prototype has been tested, a verification and validation phase is executed after which an optimisation is performed for the farm layout. The final design is then refined and documented such that production can start.

18.2. Production Plan

The manufacturing, assembly and integration plan must be set up to guide the production of the airborne wind farm. It will detail how the parts of the system will be manufactured, how the parts will be assembled into components, how the different components will be assembled into subsystems and how the subsystems will be integrated to make up the farm.

18.2.1. Part Production

The wind farm will consist of a large amount of individual parts. At this stage, these parts will be generalised into categories to create a general production plan.

Firstly, there are sheet metal parts. Within this category fall the wing box components, wing and tail skin and mounting brackets for the electronic components. These components can be stamped from metal sheets and bent or stretch formed into shape. This will need large and expensive pressing machines, but these machines can produce a lot of parts quickly. Also, the machines can be used to make a wide variety of parts. Each part will need its own mould, Making common parts in the final assembly will reduce the number of different moulds needed and thus the manufacturing cost.

A different part category consists of bigger metal parts that need to be stiffer than sheet metal parts. This includes mounting points for heavier components like motors or rotors. The attachment points for the tether also fall into this category. These parts will be made by machining down metal stock material into the preferred shape. For complex parts, this can be done with CNC mills. The machines can be programmed once for every part and then produce batches of these components. This will reduce the need for manual labour. Again, these machines are expensive, but very flexible in their use.

Next, there will be composite panels. These panels will be used mostly for the motor nacelles and cowling panels. They can either be made using layup or resin transfer moulding (RTM). For layup, a layer of fibre sheets will be placed in a mould and coated with resin. This gets

repeated until the part is complete. It will then be cured in an autoclave. RTM uses a closed mould and infuses the fibre with resin using pressure.

Long structural elements like the tail booms and wing struts can be made from aluminium or composite. If aluminium is chosen, these parts can be produced using extrusion. This is the process of forcing metal through a dye to create the required shape. If composite material is chosen, filament winding can be used. This process uses a machine to run fibre filament through a resin bath and wrap it around a mould to reach the desired shape.

For the tether, the structural core and the conductors will most likely be bought from suppliers. They will only need to be assembled into the final tether. Next to the tether parts, most electrical components will als

The floating base will consist of large metal components. These components will be bulk formed with methods like forging, rolling and extrusion. These components will rely a lot on the manufacturing experience of the offshore industry.

The parts can be produced in batches and shipped to the assembly line. Another option would be to produce the parts right when they are needed. This will reduce storage costs, but will increase the risk of delays in case a part is delayed or a machine is broken.

18.2.2. Subsystem Assembly

With the production of parts known, the assembly procedures can be discussed. All produced parts need to be assembled into components. These components can then be joined to form subsystems. There are four main subsystems: the airborne element, the tether, the base and the floater. The airborne element will have a drastically different tooling requirement compared to the base and floater. For this reason, these assembly processes will take place at different facilities.

The base and floater consist of large steel parts which need to be welded together. After this, electrical and mechanical components can be integrated. This will mostly be done with bolts, to make replacement of components easy.

The airborne element consists of a lot of components: the wings, electronics and mounting, rotors, flap assemblies, tailplanes and tail booms and a pod containing electrical and communications components together with the flight computer. These components must first be assembled. Then the components are joined to form the airborne subsystem. The wing will be joined together mostly with rivets since this is a very common joining method for aircraft. It is a reliable and efficient way of assembling the wing. The same method will be used to assemble the tail. The actuators for the control surfaces will be bolted, to make the control surfaces easily repairable. Also, the wiring in the wings should be easy to access and replace. An interesting option for the repairability of the airborne element would be to make the electronics pod fully removable including the electrical components within. This would make it possible to quickly replace the complex electrical components by simply removing bolts and unplugging the electrical connectors. This would be beneficial since electronic malfunctions are expected to be the most common and finding the cause of the fault can take time.

The assembly process will then continue by building the subassemblies: wings, motor assembly, tail assembly and control pod. The wing assembly will include mounting points to join the other assemblies to the wing, wiring harness, lights in wing tips, and (for the bottom wing) the tether attachment. The motor assembly will consist of the motor mount, motor electronics, cooling components and cowling panels. The tail will include the tailplanes attached to the tail booms and the wiring through the booms to the rudders and elevator. The control pod will include the flight computer, voltage regulator and transformer, sensors and communication

equipment. These subassemblies will then be joined together. The wings will be stacked with the struts, the tail will be connected to the wings, the motor assemblies will be connected to the electronics in the wings and be bolted in place and the control pod will be installed.

The tether will be assembled by a cable-winding machine that can wind the conductors around the structural tether. This tether can be attached to the drum and wound onto the drum during this process. Then the free end will get a connector attached, with which the tether can be connected to the airborne element. With all subsystems assembled, the single AWESs can be constructed.

18.2.3. AWES Construction

As discussed in chapter 14, the AWESs can be fully assembled in a port. The steps needed for this process are the following. First, the floater will be finished and placed in a dry dock. Next, the base can be installed onto the floater using a crane. This base consists of the tower structure, the tether drum, the airborne landing arm, the mechanical and electrical components and the sensors. The base should be designed such that it can be lifted as one piece and bolted to the floater. Next, the crane will lift the airborne element and place it onto the landing arm of the base. Then, workers will attach the tether (which is already rolled onto the tether drum before the base installation) to the airborne element. They will also secure the airborne element for transport. The dry dock can then be flooded, after which the AWES can be towed out and the process can be repeated.

18.2.4. Farm Integration

The component integration to construct the farm primarily consists of maritime processes. These have been discussed in detail in chapter 14. In summary, the AWESs, sub-sea cables, offshore substations and maintenance facility will be transported to the farm location. The AWESs will be anchored to the seabed and the sub-sea cables will be placed by specialised ships. The AWESs will then be connected to these sub-sea cables. Crews will then remove the transport restraints from the airborne element. At this point, the offshore substations should be in place and connected to both the wind farm electrical network and the connection line to shore. Then, the farm is fully assembled and a thorough testing regime can be started. During this testing, the electrical network and the AWES software will be checked for faults. Next, the AWESs will be checked for transportation damage. If no defects are found and the AWESs are deemed flight ready, they will perform a test flight. If these test flights are performed nominally, the farm can be put into operation.

18.2.5. Effect of Layout on Manufacturing

During the design of a system, it is critical to consider the implications of the design choices on the manufacturing process. Not everything that looks optimal theoretically can be manufactured or can be manufactured within the budget. Firstly, the choice to combine metal components and composite components must be discussed. Interfacing composite and metal components requires more detailed analysis, because of the corrosive effects on the metal components. This problem can be overcome since the aviation industry already uses combinations of composites and aluminium components extensively. Secondly, the choice of a bi-wing design has implications for manufacturing. It means that two wings must be manufactured per system instead of one. The fact that the two wings are slightly smaller does not outweigh the extra parts and assembly steps needed to make two wings. Furthermore, the bottom wing will need to have reinforcement because it will have a tether attachment. This means the two wings are not the same, thus two separate assembly procedures are required. This will also increase costs. An in-depth analysis will be required to properly compare the cost of a single-wing or bi-wing design.

0 - Project Mobilisation

0.1: Finance the Project
- **0.1.1** Apply for grants
- **0.1.2** Find investors

0.2: Hire Personnel
- **0.2.1** Recruit engineers
- **0.2.2** Hire technicians

0.3: Permitting
- **0.3.1** Select specific site location
- **0.3.2** Apply for permits and licenses

1 - Detailed Design

1.1: Survey Site Conditions
- **1.1.1** Measure wind speed and direction
- **1.1.2** Measure wave intensity

1.2: Refine Requirements
- **1.2.1** Refine airborne requirements
- **1.2.2** Refine seaborne requirements

1.3: Detailed Airborne Design
- **1.3.1** Calculate the wing area
- **1.3.2** Calculate the tail size
- **1.3.3** Select the airfoil shape

1.4: Airborne Structural Design
- **1.4.1** Define the structural lay-out
- **1.4.2** Choose the material per member
- **1.4.3** Consider manufacturing in the design

1 - Detailed Design

1.5: Seaborne Design
- **1.5.1** Define final structural dimensions
- **1.5.2** Design the launching and landing attachment
- **1.5.3** Analyse the platform stability

1.6: Technical Drawings
- **1.6.1** Airborne CAD drawing
- **1.6.2** Seaborne CAD drawing

2 - Aerodynamic Analysis

2.1: Flight Path Optimisation
- **2.1.1** Analyse optimal launch and landing velocity
- **2.1.2** Define optimal flight path
- **2.1.3** Define maximal bank, yaw, pitch characteristics

2.2: CFD simulation
- **2.2.1** Analyse the Lift and Drag
- **2.2.2** Analyse stability characteristics
- **2.2.3** Design control surfaces
- **2.2.4** Evaluate rotor performance
- **2.2.5** Analyse tether tension and drag
- **2.2.6** Model wake effects

2 - Aerodynamic Analysis

2.3: Optimise Design
- **2.3.1** Optimise wing shape
- **2.3.2** Select optimal airfoil
- **2.3.3** Perform optimal rotor sizing
- **2.3.4** Optimise energy generation
- **2.3.5** Minimise tether drag

3 - Structural Analysis

3.1: Airborne Structural Analysis
- **3.1.1** Analyse airborne loads
- **3.1.2** Analyse airborne stresses
- **3.1.3** Analyse airborne fatigue
- **3.1.4** Perform airborne finite element analysis

3.2: Seaborne Structural Analysis
- **3.2.1** Analyse Seaborne loads
- **3.2.2** Analyse airborne stresses

3.3: Tether Structural Analysis
- **3.3.1** Analyse tether loads
- **3.3.2** Analyse tether stresses
- **3.3.3** Analyse tether fatigue

4 - System Integration

4.1: Tether Attachment
- **4.1.1** Design Airborne tether attachement
- **4.1.2** Design Seaborne tether attachment
- **4.1.3** Ensure efficient conduction

4 - System Integration

4.2: Generator Integration
- **4.2.1** Position the generators
- **4.2.2** Optimise energy conversion
- **4.2.3** Maximise power transmission

4.3: Ensure Compatibility and Accessability
- **4.3.1** Ensure structural alignment of components
- **4.3.2** Provide access for regular maintenance
- **4.3.3** Provide adequate launch and landing platform

4.4: Optimise Connectivity and Data Communication
- **4.4.1** Optimise electrical cable layout
- **4.4.2** Establish connections between subsystems
- **4.4.3** Integrate data acquisition systems for autonomy

5 - Prototype Development and Testing

5.1: Aerodynamic Prototype Testing
- **5.1.1** Decide on the required wind tunnel tests
- **5.1.2** Build aerodynamic scale model
- **5.1.3** Perform wind tunnel tests
- **5.1.4** Analyse the wind tunnel test results
- **5.1.5** Validate the CFD model

5 - Prototype Development and Testing

5.2: Full-Scale Prototype Construction
- **5.2.1** Fabricate the wing structure
- **5.2.2** Attach the electrical components
- **5.2.3** Integrate all additional components

5.3: Full-Scale Prototype Testing
- **5.3.1** Integrate the tether with the airborne element
- **5.3.2** Test launch and landing sequence
- **5.3.3** Perform complete flight test
- **5.3.4** Perform tests with failure mechanisms

5.4: Prototype Tests Data Analysis
- **5.4.1** Determine the aerodynamic characteristics
- **5.4.2** Identify potential possibilities for improvement
- **5.4.3** Calculate the expected energy yield

6 - Verification and Validation

6.1: Verification
- **6.1.1** Verify the airborne element structural rigidity
- **6.1.2** Verify the tether strength
- **6.1.3** Verify the energy output

6.2: Validation
- **6.2.1** Perform full autonomous tests
- **6.2.2** Perform long duration offshore tests
- **6.2.3** Test the system at maximum wind speed

7 - Farm Layout

7.1: Design Optimal AWES Spacing
- **7.1.1** Decide on minimal stacking distance
- **7.1.2** Design grids of AWES on the farm location
- **7.1.3** Design the grid location to minimise wake losses

7.2: Design Ship Routes
- **7.2.1** Decide on the required ship routes
- **7.1.2** Graphically visualise the complete farm

8 - Refinement and Iteration

8.1: Design Refinement
- **8.1.1** Refine the airborne element with test data
- **8.1.2** Continue iterative testing on refined designs

8.2: Stakeholder Feedback
- **8.2.1** Discuss the design specifications with the stakeholder
- **8.2.2** Ensure the design aligns with stakeholder requirements

9 - Finalisation and Documentation

9.1: Design Documentation
- **9.1.1** Compile all design methods in a single document
- **9.1.2** Compile all final design parameters in a single document

9.2: Manufacturing Documentation
- **9.2.1** Write the manufacturing instructions
- **9.2.2** Document the manufacturing tolerances

ID	Task Name	Duration	Start	Finish
0	**Project Gantt post-DSE**	**1871 wks**	**3-7-2023**	**9-5-2059**
1	**1: Project Design and Development**	**416 wks**	**3-7-2023**	**20-6-2031**
2	**0 - Project Mobilisation**	**20 wks**	**3-7-2023**	**17-11-2023**
3	**0.1: Finance the Project**	**10 wks**	**3-7-2023**	**8-9-2023**
4	0.1.1: Apply for grants	3 wks	3-7-2023	21-7-2023
5	0.1.2: Find investors	10 wks	3-7-2023	8-9-2023
6	**0.2: Hire Personnel**	**7 wks**	**11-9-2023**	**27-10-2023**
7	0.2.1: Recruit engineers	4 wks	11-9-2023	6-10-2023
8	0.2.2: Hire technicians	4 wks	2-10-2023	27-10-2023
9	**0.3: Permitting**	**3 wks**	**30-10-2023**	**17-11-2023**
10	0.3.1: Select specific site location	3 wks	30-10-2023	17-11-2023
11	0.3.2: Apply for permits and licenses	3 wks	30-10-2023	17-11-2023
12	**1 - Detailed Design**	**57 wks**	**20-11-2023**	**20-12-2024**
13	**1.1: Measure Site Conditions**	**5 wks**	**20-11-2023**	**22-12-2023**
14	1.1.1: Measure wind speed and direction	5 wks	20-11-2023	22-12-2023
15	1.1.2: Measure wave intensity	5 wks	20-11-2023	22-12-2023
16	**1.2: Refine Requirements**	**5 wks**	**25-12-2023**	**26-1-2024**
17	1.2.1: Refine airborne requirements	5 wks	25-12-2023	26-1-2024
18	1.2.2: Refine seaborne requirements	5 wks	25-12-2023	26-1-2024
19	**1.3: Detailed Airborne Design**	**18 wks**	**29-1-2024**	**31-5-2024**
20	1.3.1: Design wing and airfoil	10 wks	29-1-2024	5-4-2024
21	1.3.2: Calculate the tail size	10 wks	29-1-2024	5-4-2024
22	1.3.3: Perform rotor sizing	8 wks	8-4-2024	31-5-2024
23	**1.4: Airborne Structural Design**	**35 wks**	**8-4-2024**	**6-12-2024**
24	1.4.1: Define the structural lay-out	15 wks	8-4-2024	19-7-2024
25	1.4.2: Choose the material per member	15 wks	22-7-2024	1-11-2024
26	1.4.3: Consider manufacturing in the design	5 wks	4-11-2024	6-12-2024
27	**1.5: Seaborne Design**	**40 wks**	**29-1-2024**	**1-11-2024**
28	1.5.1: Define final structural dimensions	10 wks	29-1-2024	5-4-2024
29	1.5.2: Design the launching and landing attachment	10 wks	22-7-2024	27-9-2024
30	1.5.3: Analyse the platform stability	5 wks	30-9-2024	1-11-2024
31	**1.6: Technical Drawings**	**7 wks**	**4-11-2024**	**20-12-2024**
32	1.6.1: Airborne CAD drawing	2 wks	9-12-2024	20-12-2024
33	1.6.2: Seaborne CAD drawing	2 wks	4-11-2024	15-11-2024
34	**2 - Aerodynamic Analysis**	**30 wks**	**9-12-2024**	**4-7-2025**
35	**2.1: Flight Path Optimisation**	**10 wks**	**9-12-2024**	**14-2-2025**
36	2.1.1: Analyse optimal launch and landing velocity	5 wks	9-12-2024	10-1-2025
37	2.1.2: Define optimal flight path	5 wks	9-12-2024	10-1-2025
38	2.1.3: Define maximal bank, yaw, pitch characteristics	5 wks	13-1-2025	14-2-2025
39	**2.2: CFD simulation**	**15 wks**	**17-2-2025**	**30-5-2025**
40	2.2.1: Analyse the Lift and Drag	5 wks	17-2-2025	21-3-2025
41	2.2.2: Analyse stability characteristics	5 wks	17-2-2025	21-3-2025
42	2.2.3: Design control surfaces	10 wks	24-3-2025	30-5-2025
43	2.2.4: Evaluate rotor performance	5 wks	17-2-2025	21-3-2025
44	2.2.5: Analyse tether tension and drag	5 wks	17-2-2025	21-3-2025
45	2.2.6: Model wake effects	5 wks	24-3-2025	25-4-2025
46	**2.3: Optimise Design**	**15 wks**	**24-3-2025**	**4-7-2025**
47	2.3.1: Optimise wing shape	5 wks	2-6-2025	4-7-2025
48	2.3.2: Select optimal airfoil	5 wks	2-6-2025	4-7-2025
49	2.3.3: Perform optimal rotor sizing	5 wks	24-3-2025	25-4-2025
50	2.3.4: Optimise energy generation	10 wks	28-4-2025	4-7-2025
51	2.3.5: Minimise tether drag	5 wks	24-3-2025	25-4-2025
52	**3 - Structural Analysis**	**47 wks**	**4-11-2024**	**26-9-2025**
53	**3.1: Airborne Structural Analysis**	**10 wks**	**7-7-2025**	**12-9-2025**
54	3.1.1: Analyse airborne loads	5 wks	7-7-2025	8-8-2025
55	3.1.2: Analyse airborne stresses	5 wks	7-7-2025	8-8-2025
56	3.1.3: Analyse airborne fatigue	5 wks	7-7-2025	8-8-2025
57	3.1.4: Perform airborne finite element analysis	10 wks	7-7-2025	12-9-2025
58	**3.2: Seaborne Structural Analysis**	**5 wks**	**4-11-2024**	**6-12-2024**
59	3.2.1: Analyse seaborne loads	5 wks	4-11-2024	6-12-2024
60	3.2.2: Analyse airborne stresses	5 wks	4-11-2024	6-12-2024
61	**3.3: Tether Structural Analysis**	**2 wks**	**15-9-2025**	**26-9-2025**
62	3.3.1: Analyse tether loads	2 wks	15-9-2025	26-9-2025
63	3.3.2: Analyse tether stresses	2 wks	15-9-2025	26-9-2025
64	3.3.3: Analyse tether fatigue	2 wks	15-9-2025	26-9-2025
65	**4 - System Integration**	**40 wks**	**7-7-2025**	**10-4-2026**
66	**4.1: Tether Attachment**	**5 wks**	**29-9-2025**	**31-10-2025**
67	4.1.1: Design airborne tether attachement	5 wks	29-9-2025	31-10-2025
68	4.1.2: Design seaborne tether attachment	5 wks	29-9-2025	31-10-2025
69	4.1.3: Ensure efficient conduction	5 wks	29-9-2025	31-10-2025
70	**4.2: Generator Integration**	**15 wks**	**7-7-2025**	**17-10-2025**
71	4.2.1: Position the generators	5 wks	7-7-2025	8-8-2025
72	4.2.2: Optimise energy conversion	10 wks	11-8-2025	17-10-2025
73	4.2.3: Maximise power transmission	10 wks	11-8-2025	17-10-2025
74	**4.3: Ensure Compatibility and Accessability**	**8 wks**	**29-9-2025**	**21-11-2025**
75	4.3.1: Ensure structural alignment of components	5 wks	29-9-2025	31-10-2025
76	4.3.2: Provide access for regular maintenance	2 wks	29-9-2025	10-10-2025
77	4.3.3: Plan for removability at End-of-Life	3 wks	3-11-2025	21-11-2025
78	**4.4: Optimise Connectivity and Data Communication**	**20 wks**	**24-11-2025**	**10-4-2026**
79	4.4.1: Optimise electrical cable layout	10 wks	24-11-2025	30-1-2026
80	4.4.2: Establish connections between subsystems	5 wks	2-2-2026	6-3-2026
81	4.4.3: Integrate data acquisition systems for autonomy	10 wks	2-2-2026	10-4-2026
82	**5 - Prototype Development and Testing**	**170 wks**	**13-4-2026**	**13-7-2029**
83	**5.1: Aerodynamic Prototype Testing**	**22 wks**	**13-4-2026**	**11-9-2026**
84	5.1.1: Decide on the required wind tunnel tests	5 wks	13-4-2026	15-5-2026
85	5.1.2: Build aerodynamic scale model	10 wks	13-4-2026	19-6-2026
86	5.1.3: Perform wind tunnel tests	2 wks	22-6-2026	3-7-2026
87	5.1.4: Analyse the wind tunnel test results	10 wks	6-7-2026	11-9-2026
88	5.1.5: Validate the CFD model	3 wks	13-4-2026	1-5-2026
89	**5.2: Full-Scale Prototype Construction**	**72 wks**	**14-9-2026**	**28-1-2028**
90	5.2.1: Fabricate full AWES	52 wks	14-9-2026	10-9-2027
91	5.2.2: Attach the electrical components	10 wks	13-9-2027	19-11-2027
92	5.2.3: Integrate all additional components	10 wks	22-11-2027	28-1-2028
93	**5.3: Full-Scale Prototype Testing**	**52 wks**	**31-1-2028**	**26-1-2029**
94	5.3.1: Test communication of control unit	6 wks	31-1-2028	10-3-2028
95	5.3.2: Test launch and landing sequence	26 wks	13-3-2028	8-9-2028
96	5.3.3: Perform complete flight test	10 wks	11-9-2028	17-11-2028
97	5.3.4: Perform tests with failure mechanisms	10 wks	20-11-2028	26-1-2029
98	**5.4: Prototype Tests Data Analysis**	**24 wks**	**29-1-2029**	**13-7-2029**
99	5.4.1: Determine the aerodynamic characteristics	8 wks	29-1-2029	23-3-2029
100	5.4.2: Identify potential possibilities for improvement	8 wks	26-3-2029	18-5-2029
101	5.4.3: Calculate the expected energy yield	8 wks	21-5-2029	13-7-2029
102	**6 - Verification and Validation**	**32 wks**	**16-7-2029**	**22-2-2030**
103	**6.1: Verification**	**10 wks**	**16-7-2029**	**21-9-2029**
104	6.1.1: Verify the airborne element structural rigidity	5 wks	16-7-2029	17-8-2029
105	6.1.2: Verify the tether strength	5 wks	16-7-2029	17-8-2029
106	6.1.3: Verify the energy output	10 wks	16-7-2029	21-9-2029
107	**6.2: Validation**	**22 wks**	**24-9-2029**	**22-2-2030**
108	6.2.1: Perform full autonomous tests	8 wks	24-9-2029	16-11-2029
109	6.2.2: Perform long duration offshore tests	10 wks	19-11-2029	25-1-2030
110	6.2.3: Test the system at maximum wind speed	4 wks	28-1-2030	22-2-2030
111	**7 - Farm Layout**	**25 wks**	**25-2-2030**	**16-8-2030**
112	**7.1: Design Optimal AWES Spacing**	**20 wks**	**25-2-2030**	**12-7-2030**
113	7.1.1: Decide on stacking distance	10 wks	25-2-2030	3-5-2030
114	7.1.2: Design plots of AWESs on the farm location	5 wks	6-5-2030	7-6-2030
115	7.1.3: Locate the substations to minimise energy losses	5 wks	10-6-2030	12-7-2030
116	**7.2: Optimise Ship Routes**	**5 wks**	**15-7-2030**	**16-8-2030**
117	7.2.1: Make ship routes and add buoys	5 wks	15-7-2030	16-8-2030
118	7.2.2: Locate operations station	5 wks	15-7-2030	16-8-2030
119	**8 - Refinement and Iteration**	**28 wks**	**19-8-2030**	**28-2-2031**
120	**8.1: Design Refinement**	**26 wks**	**19-8-2030**	**14-2-2031**
121	8.1.1: Refine the AWES design with test data	26 wks	19-8-2030	14-2-2031
122	8.1.2: Continue iterative testing on refined designs	26 wks	19-8-2030	14-2-2031
123	**8.2: Stakeholder Feedback**	**2 wks**	**17-2-2031**	**28-2-2031**
124	8.2.1: Discuss the design specifications with the stakeholder	2 wks	17-2-2031	28-2-2031
125	8.2.2: Ensure the design aligns with stakeholder requirements	2 wks	17-2-2031	28-2-2031
126	**9 - Finalisation and Documentation**	**16 wks**	**3-3-2031**	**20-6-2031**
127	**9.1: Design Documentation**	**8 wks**	**3-3-2031**	**25-4-2031**
128	9.1.1: Compile all design methods in a single document	8 wks	3-3-2031	25-4-2031
129	9.1.2: Compile all final design parameters in a single document	8 wks	3-3-2031	25-4-2031
130	**9.2: Manufacturing Documentation**	**8 wks**	**28-4-2031**	**20-6-2031**
131	9.2.1: Write the manufacturing instructions	8 wks	28-4-2031	20-6-2031
132	9.2.2: Document the manufacturing tolerances	8 wks	28-4-2031	20-6-2031
133	**2: Production Phase**	**234 wks**	**23-6-2031**	**14-12-2035**
134	2.1 Prepare for the Production	13 wks	23-6-2031	19-9-2031
135	2.2 Decide Production Process	13 wks	22-9-2031	19-12-2031
136	2.3 Source Material	26 wks	22-12-2031	18-6-2032
137	2.4 Provide Adequate Infrastructure	52 wks	22-12-2031	17-12-2032
138	2.5 Produce Parts	104 wks	20-12-2032	15-12-2034
139	2.6 Assemble Systems	130 wks	20-12-2032	15-6-2035
140	2.7 Test System on Land	26 wks	18-6-2035	14-12-2035
141	**3: Deployment**	**104 wks**	**17-12-2035**	**11-12-2037**
142	3.1 Check Weather for Transport	4 wks	17-12-2035	11-1-2036
143	3.2 Ship Elements to Base	25 wks	14-1-2036	4-7-2036
144	3.3 Place Seaborne Elements	25 wks	7-7-2036	26-12-2036
145	3.4 Attach Airborne Elements	26 wks	7-7-2036	2-1-2037
146	3.5 Test the System	12 wks	5-1-2037	27-3-2037
147	3.6 Install Additional Operation related Structures	25 wks	30-3-2037	18-9-2037
148	3.6 Initiate Operations	12 wks	21-9-2037	11-12-2037
149	**4: Operate and Maintain the Farm**	**1040 wks**	**14-12-2037**	**16-11-2057**
150	**5: End of Life (EoL)**	**77 wks**	**19-11-2057**	**9-5-2059**
151	5.1 Asses EoL Possibilities	10 wks	19-11-2057	25-1-2058
152	5.2 Life Extension of System	15 wks	28-1-2058	10-5-2058
153	5.3 Repower System	15 wks	28-1-2058	10-5-2058
154	5.4: Decommission System	52 wks	13-5-2058	9-5-2059

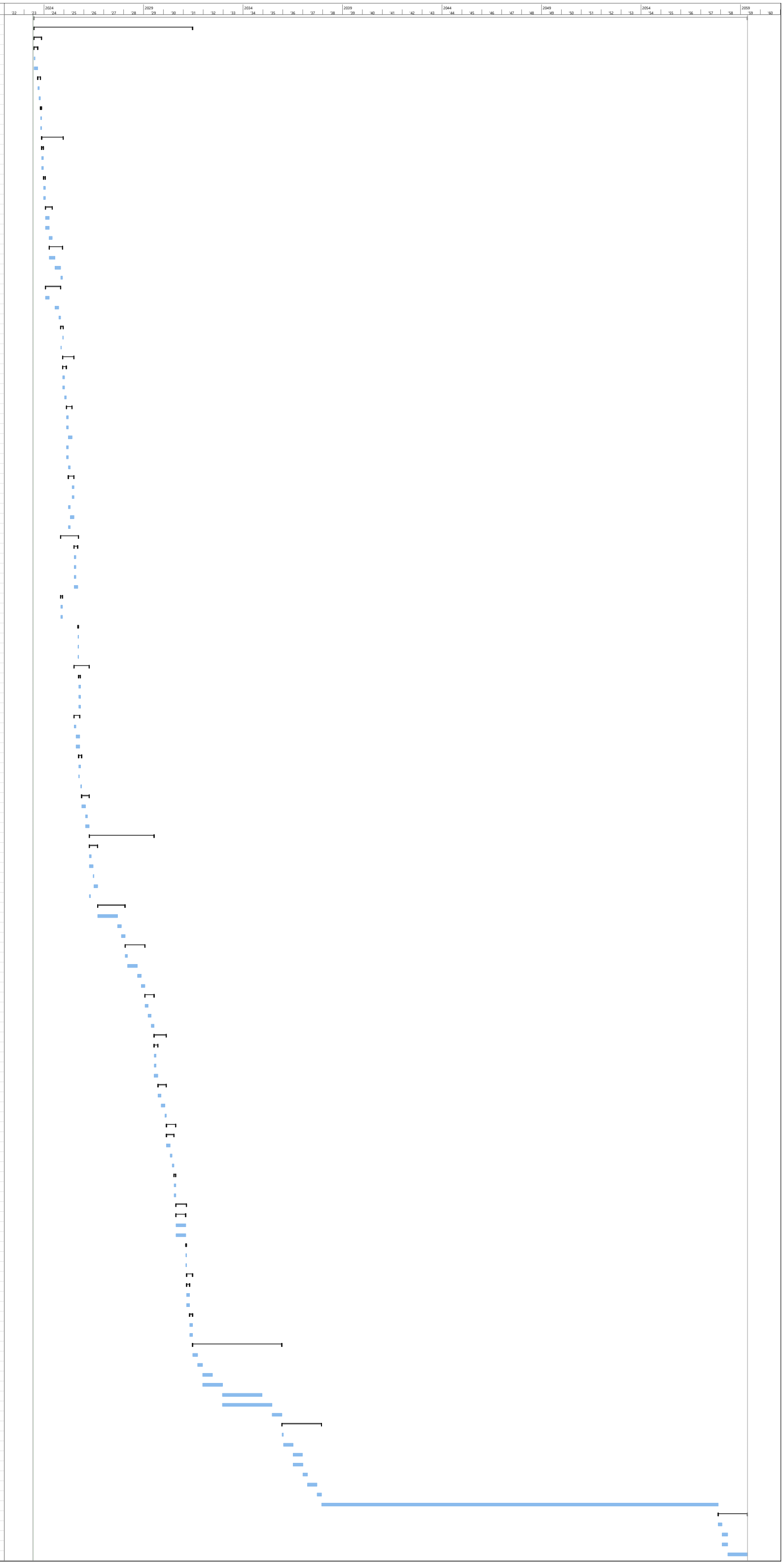

19
Discussion and Recommendations

This chapter will present a final discussion on the design methodology and results of this project. Furthermore, the team will share their opinion on the concept of airborne wind and its use offshore. First, the relevance of the research done is discussed in section 19.1. Then, a discussion of the limitations of the analysis will follow in section 19.2. Finally, recommendations for further research will be presented in section 19.3.

19.1. Findings

In this section, research topics, which the team feels provide the most relevant addition to the field of airborne wind energy, are discussed in this report.

19.1.1. Overview of Challenges

The challenges of designing a large-scale farm based on AWESs can be broken down to two main considerations. The AWESs have to be scaled up tenfold and yet the farm needs to manage one thousand systems. Scaling up an airborne system is far more challenging than a conventional turbine as the additional weight has to be carried by the craft itself. Limits are predicted due to the required increase in altitude detailed in section 19.1.4. In addition to that, having a thousand large-scale, heavy AWESs flying at high speeds poses a threat to the operators. To mitigate the threat a large amount of resources have to be assigned to the management and operations. Balancing the scale of one AWES is therefore the biggest challenge as it requires deep understanding of both of the aforementioned aspects. In this project we approached the problem by expanding the established theory by conducting secondary design and analysis on both the farm and the AWESs.

19.1.2. Concept Trade-Off

The trade-off has been performed for a 1 MW system between three AWES concepts: soft wing ground-gen, rigid wing ground-gen and rigid wing fly-gen. The soft wing solution was deemed highly unreliable due to the folding of the sides at lower wind speeds, and sensitivity to gusts. In addition to that launching and landing alongside sensitivity to changes in wind direction remains an unsolved issue. Furthermore ground generation concepts introduce microplastics into the environment by reeling in and out. Avoiding it requires the use of expensive materials, putting stress on the financial feasibility. On the other hand fly generation offers easier operations due to its controllability and VTOL capability. Making operations autonomous and reliable is the priority, therefore the rigid wing fly generation concept was deemed the most promising.

19.1.3. Farm Design

Optimally packing the systems so that the least amount of area is used is made more complicated by the need for an efficient and safe wind farm. When creating a farm many different items should be considered such as the operational environment, the location of the site, the placing of systems and grid interconnection, the flight envelope, and the accessibility for maintenance. Ideally before implementation of the system into a farm, the maturity of the technology should be high. More specifically the maturity of the autonomy will significantly affect the methods utilised for spacing individual elements within the farm. If the maturity of the autonomous systems is high more aggressive approaches could be utilised in which stronger interactions are implemented between the airborne units and their flight envelope. This stack-

ing can be done through adjustment of the flight altitude, path and spacing between elements. The site selection showed the wide range of elements had to be considered when choosing a location. These elements included shipping routes, fishing activity, water depth, size of the site, and soil type and many more. The addition of substations, an operations station and buoys are important for the smooth operation and maintenance of the farm. To further optimise this farm design, the amount, and capacity of these substations can be further analysed. The connection between systems can also be studied more in-depth to be confident that the power losses are minimised. Finally, systems should be installed in such a way that vessels can reach each system to perform adequate maintenance on a regular basis.

19.1.4. Effect of System Scaling and its Limits

Another interesting result comes from the tool discussed in the previous section. Using the tool developed showed that scaling AWESs is one of the most complex problems. The snowball effect is clearly present, therefore an upper limit will exist alongside an optimal size. As the system gets bigger it becomes heavier, which results in several issues. It increases the required velocity which further contributes to increasing the wing loading at the turns. Assuming the tether length is only a few hundred meters and the apparent velocity is 20 - 80 m/s the period is really low. The turns are sharp and in order to maintain them the wings are loaded by the square of the velocity multiplied by the before-mentioned increased mass. The additional loading makes the wing even heavier, hence the strong snowball effect. The only way to reduce the loading is to make the turns less sharp, meaning making the flight path larger. The flight path can be increased by either increasing the inclination angle or increasing the tether length. increasing the inclination angle is limited, on the other hand increasing the tether length is effective and has high potential bounds. One of which is the increased drag and weight due to increasing the tether length, which further contributes to the snowball effect. In conclusion, scaling up the airborne element has to be coupled with an increase in altitude and careful flight path design.

19.1.5. Feasibility of AWES Based Offshore Wind Farm

Finally, the team would like to elaborate on the feasibility of the project as a whole. After extensive research and design work, the team has developed an opinion on the feasibility of floating wind farms using airborne wind energy systems. On one hand, floating airborne wind energy does promise feasible advantages in material use and reduction in wake losses, while costs could be comparable to conventional wind turbines in the future. On the other hand, airborne wind introduces a lot of complexity and risk. Systems are much more dynamic and have more moving parts. Component failures can more easily escalate into a total system failure which can destroy the airborne element. Significant development will be needed to reduce these risks. Introducing these systems into an offshore farm introduces even more complexity. For one, maintenance costs will increase significantly. Furthermore, launching and landing on a moving base increases the complexity of autonomous systems. Lastly, saline conditions will introduce more wear to the system. For these reasons, the team recommends first implementing an airborne wind energy farm onshore. This farm will generate a lot of data that can be used to assess the feasibility of an offshore farm more clearly.

19.2. Limitations on Analysis

All analyses have limitations. It is impossible to model complex systems perfectly, especially in a preliminary design phase. To get a first estimate of the parameters of the system, assumptions must be made and some aspects must be neglected to reduce the complexity of the problem. It is critical to understand the effects of the assumptions made to determine the quality of the analysis. This section will discuss the effect and reasoning behind the most

important assumptions made.

19.2.1. Inaccuracy of Mass Estimation due to Assumptions

The mass estimations are one of the most significant parts of the design. It is assessed by adding up the mass of the main components such as the wing, tail, tail boom, struts and rotors. The biggest contributor is the wing. Our validation effort shows that we overestimate the mass by quite a significant margin. As a statistical model was used to design the wing, based on smaller scale prototypes, presumably it is not accurate enough to our scale or application.

19.2.2. Variation over Flight Path

The variation of the generated power is studied but it is still inaccurate. C_L varies as the flight dynamics require different lift coefficients at different points in the flight path. C_D changes due to a change in C_L and due to a change in the velocity, therefore the power generation also changes. Furthermore, arguably the most significant loss in power is due to the banking angle over the turns. Solving the dynamic problem is required to solve analyse this loss.

19.2.3. Validation Limitations

As the technology is still in its early phase, not much data has been made available to the public. Only a handful of companies develop AWESs, of which a few failed to succeed. Validation of the subsystem properties is viable by looking at similar elements of other applications with similar loads. However, concluding the validity of the design or the design code, especially concerning the power, is limited due to the lack of data.

19.3. Recommendations for Future Research

Airborne wind energy is still at an early stage of development. Because of this, there are still a lot of topics to be researched before a full farm can be realised. In this section, recommendations for further research are provided which can help the development of airborne wind technology.

19.3.1. Improve on Sizing Tool

First of all, the limitations in section 19.2 can be investigated and improved upon. This will make the preliminary estimation tool developed for this project more accurate. For each subsystem calculation, the relations have to be more thorough and they have to be verified and validated before being implemented in the larger code. With improved accuracy, the tool can be used reliably to determine the optimum layout and scale for a fly-gen AWES.

19.3.2. Tether Wear

Another recommendation is to investigate the tether wear in operating conditions. Tether replacement is a time-consuming and costly operation. Reducing tether wear can thus reduce the operating costs of the system. Valuable information would be to quantify the effect of the winding and unwinding of the tether, compared to the cyclic tensile loading. This would provide better information for the trade-off between ground- and fly-gen concepts. Furthermore, the amount of microplastics released should be monitored during this research.

19.3.3. Power Fluctuation Reduction

Additionally, an investigation can be conducted into the optimum way of combining the fluctuating power levels of all AWESs in the farm and smoothing out the fluctuations. This will require storage and regulation substations. By combining multiple AWESs, it is expected that the sum of fluctuations becomes smoother. This would mean less storage is needed at the substations. It should be investigated to what extent the storage required can be reduced.

19.3.4. Bird Strikes and Migration Disruption

Something that comes up often in public debate about wind energy is bird strikes. This can have a big effect on public opinion. Currently, no large-scale systems have been tested long enough to get a clear understanding of the effect of airborne wind energy systems on birds. For this reason, it is recommended to research the effect of AWESs on bird migration and bird strikes and to compare this to conventional wind turbines.

19.3.5. Floater Stability

Floater stability is important, especially during launch and landing. There will be a maximum amount of movement after which the airborne element cannot land. This could pose a serious risk to the airborne element during a storm for instance. Additional research should be performed into the autonomous landing capabilities onto a floating base to find the landing limit of the airborne element. Next to this, tests and simulations should be performed to investigate the wave-induced motion of a semi-submersible. With the results, improvements to the semi-submersible design could be found that would reduce these motions.

19.3.6. Reliability and Safety During Maintenance

A testing campaign should be set up for a fly-gen system, where the reliability of such systems is investigated over a long period of time. With this, the goal is to determine the probability of failure of the system and the most probable failure mode. With this data, a clearer maintenance plan can be created and the operational costs of a farm can be more accurately determined. Furthermore, the probability of a catastrophic failure should be investigated. Based on this information, it can then be determined if it is safe to move maintenance boats through an operating airborne wind farm. Should this be proven, it would remove the need to shut down entire sections for maintenance, increasing the availability of the wind farm.

19.3.7. Multi-Element Wing Lift and Drag Coefficient Estimation

The multi-element wings influence the aerodynamic characteristics of the airborne element. The flow disruption between the wings reduces the lift coefficient. This reduction is approximated to be 20%. This however should be proven for our design. The reduction in lift coefficient reduced the lift-induced drag coefficient, which is beneficial. The parasite drag, however, increases with approximately 50%. This also has not been proven for our design. In the drag coefficient calculations, the wings, tether and rotors are taken into account while the structures imposed drag is neglected. A more detailed analysis should be done on the entire drag of the airborne element.

19.3.8. Analysing Stability and Control

By making a dynamic model and simulation of the flight the stability can be analysed and the control surfaces can be determined. At the moment the tail sizing of the airborne element is done by using statistical data. Since the concept is highly unconventional the tail sizing is most certainly inaccurate. In addition to that, the stability of the system largely contributes to its reliability, therefore it is important to analyse this in detail.

19.3.9. Project Finance

The finances of the project have been based on the finances of aeroplane and floating wind turbines making use of the learning curves of both technologies. As more data on the finances of AWES becomes available, a more AWES specific model can be created. For instance, by looking into the failure rates of AWES components the amount and cost of maintenance trips can be estimated. Furthermore, a more complete study must be done on the discount rate of the project.

20 Conclusion

This report documented the final steps that the team has taken to meet the mission need statement: *"Provide a cost-competitive way to harvest wind energy in deep water with a more sustainable alternative to conventional wind turbines." [1]* The mission need statement shows that there is a need for a more sustainable alternative for a floating offshore wind farm, with a requirement of being cost-competitive.

The cost-competitive and more sustainable requirements are defined by doing a market analysis, where some clear advantages of airborne wind energy were highlighted to conventional wind energy. In addition, we highlight some threats and weaknesses. The main advantage of airborne wind is the ability to vary operating altitude to harvest the best wind. Potential cost advantages for airborne wind are the decreased material requirements and the possibility of using smaller and cheaper ships for maintenance due to the smaller system size. However, airborne wind is still very much an innovative concept with no large-scale operational systems thus it still has large uncertainties in many of its aspects. This report aimed to give some insight into multiple aspects of the design and operation of an airborne wind energy system on a large scale.

Single System Design

Since the goal was to design a large-scale wind farm, the first step was to design a single system with a capacity such that a farm design becomes feasible. This minimum system size was assumed to be 1MW, but it could still grow if a larger system proved to be more promising. In the previous report, the most promising concept was chosen. A trade-off was performed between a soft-wing ground-generation concept, a rigid-wing ground-generation concept and a rigid-wing fly-gen concept. It was concluded that for a larger scale, a rigid-wing fly-gen system was the most promising. To design a single system, relations were defined for each subsystem. These were implemented in a code to iterate and come up with a final optimal sizing. After the iteration process, it showed that a 1MW sizing was able to fulfil all the user requirements for the system, and thus this design was elaborated upon.

The complete airborne wind energy system consists of three main parts, the airborne element, the floating seaborne foundation, and the tether to connect these two elements. The output of the code is the sizes of the airborne element and the tether since these are the most important in terms of power yield.

The final airborne element was designed to have a wing span of 30m with 8 motor/generators connected to 3.2m diameter rotors to generate 1MW of power. This airborne element is attached to a 3.7-cm diameter tether, which is both a load-carrying component and able to transfer the power to the floating foundations. To operate this system offshore, a semi-submersible foundation was designed, this concept uses 3 hollow cylindrical floaters with ballast water. The size of the cylindrical floaters was designed for buoyancy, where it was determined that each floater has a diameter of 5 metres and a height of 10 metres. This height will be filled with about 3.5 metres of ballast water, which will lead to about 6.5 metres of the floater being submerged. The spacing of the floaters was designed for stability, where the system was allowed to have a tilt angle of 15° when the tension in the tether is at its maximum. This led to a spacing of the floaters of 44.3 meters.

Farm Integration

To design a farm layout, a site was selected in the North Sea that is assigned to be used for offshore wind energy. The spacing between the different systems is mostly dependent on the length of the tether and the angle of elevation. The distance between systems in the wind direction was calculated to be 566 metres and perpendicular to the wind direction 376 metres. These values were used to design eight grids of 105 systems, and one grid of 160 systems. A layout of these grids was designed based on the selected site where pathways for logistics, offshore substations and the energy grid were taken into account. This leads to a total farm area of 290 km^2 and a power density of 3.5 MW/km^2 which is a higher power density than using conventional wind turbines.

Financial Analysis

The ultimate enabler of the concept of airborne wind energy is the levelised cost of energy (LCoE), which must be comparable to conventional turbines to compete in the same market. A cost breakdown was made comparing the AWES to conventional wind turbines, which showed that even in a pessimistic case, the CapEx is lower for AWES than for conventional floating wind turbines. The Opex is similar for conventional and AWES, where the decommissioning costs for AWES is much lower. An LCoE estimation is performed using this cost breakdown. A requirement on the LCoE is set by the client of 50 €$/MWh$ which is similar to current conventional bottom fixed wind turbines. Floating wind turbines are expected to have an LCoE of 100 €$/MWh$ by 2025, highlighting the difficulty in meeting the requirement. Multiple scenarios were calculated with the most optimistic case leading to an LCoE of 49.5 €$/MWh$ and the most pessimistic case leading to 69 €$/MWh$ for a farm with a 20-year lifetime. This is a promising result, highlighting the possibility of the airborne wind energy system competing with conventional turbines in terms of costs. This shows that the team has achieved the first part of the mission need statement, being able to ”provide a cost-competitive way to harvest wind energy in deep water”.

Sustainability Analysis

The second part of the mission need statement is the requirement for the system to be more sustainable than conventional wind turbines. This is part of the project where the team has made a real contribution to the airborne wind energy sector due to the lack of published information.

The mass and height of an airborne wind energy system is much less than a conventional wind turbine, which has positive implications in many sustainable aspects. The total mass of an airborne wind energy is estimated to be only 40% of a conventional wind turbine, which directly decreases the use of materials. The airborne element is designed to be constructed using aluminium, which is much better recyclable than composite turbine blades. If the foundation is included, the total AWES is 99.8% recyclable mass-wise. Additionally, because of the limited system size, smaller and less polluting vessels can be used to transport and maintain the systems. Due to the semi-submersible foundation type, the AWES can be towed to their operational location fully assembled which enables construction and testing of the systems in sheltered conditions. From these results, the team concludes that the airborne wind energy system is more sustainable than conventional wind turbines and thus the second aspect of the mission need statement is also achieved.

Discussion

It seems that the team has achieved the goals stated in the mission need statement and has therefore shown that a gigawatt wind farm is possible using an airborne wind concept. However, it is not certain that airborne wind energy is actually a better way to harvest wind

energy than conventional turbines. Airborne wind energy shows its advantage in terms of material use and limited wake losses. Furthermore, airborne wind can have an increased capacity factor compared to conventional wind. The largest downside is the limited scale of a single system, a problem that this team has not been able to solve completely. A fly-gen system is a very complex system, where a single component failure can easily escalate in a complete system loss. Additionally, there are large uncertainties in the launch and landing on a dynamic platform. Therefore, the team believes that much more testing and development is needed for a megawatt-scale single system before the focus is to shift toward an offshore wind farm.

References

[1] J. Bogaert, F. Bononi Bello, G. van den Heuvel, *et al.*, "Dse project plan floating airborne wind energy system farm, group 19: Deep wattair," TU Delft, Tech. Rep., May 2023.

[2] J. Bogaert, F. Bononi Bello, G. van den Heuvel, *et al.*, "Dse baseline report floating airborne wind energy system farm, group 19: Deep wattair," TU Delft, Tech. Rep., May 2023.

[3] J. Bogaert, F. Bononi Bello, G. van den Heuvel, *et al.*, "Dse midterm report floating airborne wind energy system farm, group 19: Deep wattair," TU Delft, Tech. Rep., Jun. 2023.

[4] International Energy Agency. "Net zero by 2050." (2021), [Online]. Available: https://www.iea.org/reports/net-zero-by-2050.

[5] NetbeheerNL, "Het energiesysteem van de toekomst, Integrale infrastructuurverkenning 2030 -2050," 2021.

[6] DNV, "Floating offshore wind: The next five years," 2022.

[7] A. Schmitt and H. Zhou, "Eu energy outlook 2060 – how will the european electricity market develop over the next 37 years?" *Energy Brainpool*, 2022.

[8] R. García Sánchez, A. Pehlken, and M. Lewandowski, "On the sustainability of wind energy regarding material usage," Jan. 2014.

[9] B. Björkman and C. Samuelsson, "Chapter 6 - recycling of steel," in *Handbook of Recycling*, E. Worrell and M. A. Reuter, Eds., Boston: Elsevier, 2014, pp. 65–83, ISBN: 978-0-12-396459-5. DOI: https://doi.org/10.1016/B978-0-12-396459-5.00006-4. [Online]. Available: https://www.sciencedirect.com/science/article/pii/B9780123964595000064.

[10] A. Bonou, A. Laurent, and S. I. Olsen, "Life cycle assessment of onshore and offshore wind energy-from theory to application," *Applied Energy*, vol. 180, pp. 327–337, 2016, ISSN: 0306-2619. DOI: https://doi.org/10.1016/j.apenergy.2016.07.058. [Online]. Available: https://www.sciencedirect.com/science/article/pii/S0306261916309990.

[11] Irena. "Future of wind: Deployment, investment, technology, grid integration and socio-economic aspects." (2019), [Online]. Available: https://www.irena.org/-/media/Files/IRENA/Agency/Publication/2019/Oct/IRENA_Future_of_wind_2019_summ_EN.PDF.

[12] B. D. Agarwal, L. J. Broutman, and K. Chandrashekhara, *Analysis and performance of fiber compsites*, third. Wiley, 2015.

[13] M. Barile, L. Lecce, M. Iannone, S. Pappadà, and P. Roberti, "Thermoplastic composites for aerospace applications," in *Revolutionizing Aircraft Materials and Processes*, S. Pantelakis and K. Tserpes, Eds. Cham: Springer International Publishing, 2020, pp. 87–114, ISBN: 978-3-030-35346-9. DOI: 10.1007/978-3-030-35346-9_4. [Online]. Available: https://doi.org/10.1007/978-3-030-35346-9_4.

[14] P. Echeverri, T. Fricke, G. Homsy, and N. Tucker, "The energy kite, selected results from the design, development and testing of makani's airborne wind turbines," *Energies*, vol. Part I, II, III, Sep. 2020.

[15] N. Sergiienko, L. da Silva, E. Bachynski-Polić, B. Cazzolato, M. Arjomandi, and B. Ding, "Review of scaling laws applied to floating offshore wind turbines," *Renewable and Sustainable Energy Reviews*, vol. 162, 2022, ISSN: 1364-0321. DOI: https://doi.org/10.1016/j.rser.2022.112477. [Online]. Available: https://www.sciencedirect.com/science/article/pii/S1364032122003811.

[16] R. L. Reuben, "Marine materials," in *Materials in Marine Technology*. London: Springer London, 1994, pp. 79–160, ISBN: 978-1-4471-2011-7. DOI: 10.1007/978-1-4471-2011-7_4. [Online]. Available: https://doi.org/10.1007/978-1-4471-2011-7_4.

[17] H. Hu, X. Nie, and Y. Ma, "Corrosion and surface treatment of magnesium alloys," in *Magnesium Alloys*, F. Czerwinski, Ed. Rijeka: IntechOpen, 2014, ch. 3. DOI: 10.5772/58929. [Online]. Available: https://doi.org/10.5772/58929.

[18] R. L. Reuben, "Marine corrosion and biodeterioration," in *Materials in Marine Technology*. London: Springer London, 1994, pp. 45–78, ISBN: 978-1-4471-2011-7. DOI: 10.1007/978-1-4471-2011-7_3. [Online]. Available: https://doi.org/10.1007/978-1-4471-2011-7_3.

[19] *Pitting Corrosion Study In An Ae 44 Magnesium Alloy*, vol. All Days, NACE CORROSION, NACE-08232, Mar. 2008. eprint: https://onepetro.org/NACECORR/proceedings-pdf/CORR08/All-CORR08/NACE-08232/1805930/nace-08232.pdf.

[20] J. Bhandari, F. Khan, R. Abbassi, V. Garaniya, and R. Ojeda, "Modelling of pitting corrosion in marine and offshore steel structures – a technical review," *Journal of Loss Prevention in the Process Industries*, vol. 37, pp. 39–62, 2015, ISSN: 0950-4230. DOI: https://doi.org/10.1016/j.jlp.2015.06.008. [Online]. Available: https://www.sciencedirect.com/science/article/pii/S0950423015300024.

[21] F. Trevisi, “Configuration optimisation of kite-based wing turbines,” *DTU Wind Energy-M-0313*, 2019.

[22] Koninklijk Nederlands Meteorologisch Instituut. “Wind - model statistics for 1979-2013 at 10-200 meters above the north sea - knw end user pack of maps and time series.” (Mar. 2022), [Online]. Available: https://dataplatform.knmi.nl/dataset/knw-enduser-pack-1-0.

[23] D. I. A. Viré. “Fundamentals of wind energy i: Lecture 2.” (Sep. 2022).

[24] M. De Lellis, R. Reginatto, R. Saraiva, and A. Trofino, “The betz limit applied to airborne wind energy,” *Renewable Energy*, vol. 127, pp. 32–40, 2018, ISSN: 0960-1481. DOI: https://doi.org/10.1016/j.renene.2018.04.034.

[25] A. P. Ko, “Optimization of a multielement airfoil for a rigid airborne wind energy kite,” 2022.

[26] A. Pereira and J. Sousa, “A review on crosswind airborne wind energy systems: Key factors for a design choice,” *Energies*, vol. 16, no. 351, Dec. 2022. DOI: https://doi.org/10.3390/en16010351.

[27] U. D. of Transportation FEDERAL AVIATION ADMINISTRATION Flight Standards Service, *Helicopter Flying Handbook*. Oklahoma City, OK 73125: United States Department of Transportation, Federal Aviation Administration, Airman Testing Branch, 2019.

[28] G. White, “Biplane and tri-plane wing lift and efficiency,”

[29] J.-M. Moschetta and C. Thipyopas, “Optimization of a biplane micro air vehicle,” 2005.

[30] F. Bauer, “Multidisciplinary optimization of drag power kites,” Dissertation, Technical University of Munich, 2021.

[31] F. Bauer and R. M. Kennel, “Fault-tolerant power electronic system for drag power kites,” *Journal of Renewable Energy*, vol. 2018, pp. 1–37, 2018, ISSN: 2314-4386. DOI: 10.1155/2018/1306750. [Online]. Available: https://dx.doi.org/10.1155/2018/1306750.

[32] P. Barua, T. Sousa, and D. Scholz, “Empennage statistics and sizing methods for dorsal fins,” Apr. 2015.

[33] U. Eziefula, “Analysis of inelastic buckling of rectangular plates with a free edge using polynomial deflection functions,” *International Review of Applied Sciences and Engineering*, vol. 11, Apr. 2020. DOI: 10.1556/1848.2020.00003.

[34] J. R. Centre, I. for Energy, Transport, M. Ardelean, and P. Minnebo, *HVDC submarine power cables in the world: state-of-the-art knowledge*. Publications Office, 2017. DOI: doi/10.2790/023689.

[35] L. Liu, H. Zhao, W. Xu, R. Yuan, and Y. Guo, “Structural strength analysis of a tri-floater floating foundation for offshore vawt,” Apr. 2018. [Online]. Available: https://link.springer.com/content/pdf/10.1007/s11802-018-3434-9.pdf.

[36] A. Robertson, J. Jonkman, M. Masciola, *et al.*, “Definition of the semisubmersible floating system for phase ii of oc4,” Sep. 2014. DOI: 10.2172/1155123. [Online]. Available: https://www.osti.gov/biblio/1155123.

[37] R. Antonutti, C. Peyrard, L. Johanning, A. Incecik, and D. Ingram, “The effects of wind-induced inclination on the dynamics of semi-submersible floating wind turbines in the time domain,” *Renewable Energy*, vol. 88, pp. 83–94, 2016, ISSN: 0960-1481. DOI: https://doi.org/10.1016/j.renene.2015.11.020. [Online]. Available: https://www.sciencedirect.com/science/article/pii/S0960148115304389.

[38] J. Journée and W. Massie, “Offshore hydromechanics,” p. 570, Jan. 2001.

[39] M., Ikhennicheu, et al., “D2.1 review of the state of the art of mooring and anchoring designs, technical challenges and identification of relevant dlcs,” Corewind, Tech. Rep., Feb. 2020.

[40] L. A. Roque, L. T. Paiva, M. C. Fernandes, D. B. Fontes, and F. A. Fontes, “Layout optimization of an airborne wind energy farm for maximum power generation,” *Energy Reports*, vol. 6, pp. 165–171, 2020, The 6th International Conference on Energy and Environment Research - Energy and environment: challenges towards circular economy, ISSN: 2352-4847. DOI: https://doi.org/10.1016/j.egyr.2019.08.037. [Online]. Available: https://www.sciencedirect.com/science/article/pii/S2352484719306845.

[41] D. I. A. Viré. “Fundamentals of wind energy i: Lecture 4.” (Sep. 2022).

[42] G. Katsouris and A. Marina, “Cost modelling of floating wind farms,” ECN, Tech. Rep. ECN-E–15- 078, Mar. 2016.

[43] R. Ramachandran, C. J. Desmond, F. M. Judge, J.-J. Serraris, J. Murphy, and E. A. of Wind Energy, “Floating offshore wind turbines: Installation, operation, maintenance and decommissioning challenges and opportunities,” *Wind Energy Science Discussions*, Oct. 2021. DOI: 10.5194/wes-2021-120. [Online]. Available: https://doi.org/10.5194/wes-2021-120.

[44] L. Fagiano, M. Quack, F. Bauer, L. Carnel, and E. Oland, “Autonomous airborne wind energy systems: Accomplishments and challenges,” *Annual Review of Control, Robotics, and Autonomous Systems*, vol. 5, no. 1, pp. 603–631, 2022. DOI: 10.1146/annurev-control-042820-124658. eprint: https://doi.org/10.1146/annurev-control-042820-124658. [Online]. Available: https://doi.org/10.1146/annurev-control-042820-124658.

[45] S. Gudmundsson, *General Aviation Aircraft Design*. butterworth-heinemann, 2014. DOI: https://doi.org/10.1016/C2011-0-06824-2.

[46] S. O. L. Zijp, *Development of a life cycle cost model for conventional and unconventional aircraft*, 2014.

[47] G. Bedon, A. Dewan, W. van Schooten, R. Lindeboom, and B. van Hemert, “The sea-air-farm project: Demonstrating the potential of far offshore floating airborne wind farms,” Oct. 2017.

[48] A. Myhr, C. Bjerkseter, A. Ågotnes, and T. A. Nygaard, “Levelised cost of energy for offshore floating wind turbines in a life cycle perspective,” *Renewable Energy*, vol. 66, pp. 714–728, 2014, ISSN: 0960-1481. DOI: https://doi.org/10.1016/j.renene.2014.01.017. [Online]. Available: https://www.sciencedirect.com/science/article/pii/S0960148114000469.

[49] K. Blok and E. Nieuwlaar, *Introduction to Energy Analysis*, 3rd. Earthscan Routledge, 2021.

[50] H. Vos, *A whole-energy system perspective to floating wind turbines and airborne wind energy in the north sea region*, 2023.

[51] U. Ahrens, M. Diehl, and R. Schmehl, *Airborne Wind Energy*, 1st ed. Springer Berlin, Heidelberg, 2016.

A

Full Cost Breakdown

Table A.1: Cost Breakdown per MW

Cost Break down	HAWT	HAWT ES	RW FG pessimistic	RW FG optimistic
CAPEX	€ 1.799.576	€ 1.546.900	€ 3.578.166	€ 2.461.179
Development and management	€ 166.440	€ 141.500	€ 156.500	€ 156.500
Development services	€ 77.520	€ 65.000	€ 80.000	€ 80.000
Environmental surveys	€ 10.032	€ 8.500	€ 8.500	€ 8.500
Resource assessment	€ 7.524	€ 6.000	€ 6.000	€ 6.000
Geological surveys	€ 10.032	€ 8.500	€ 8.500	€ 8.500
Engineering and consultancy	€ 10.032	€ 8.500	€ 8.500	€ 8.500
Project management	€ 51.300	€ 45.000	€ 51.300	€ 45.000
Power Generation	1.509.560	€ 1.300.000	€ 990.718	€ 232.778
Wind Turbine	€ 1.509.560	€ 1.300.000	€ 0	€ 0
Airborne Element	€ 0	€ 0	€ 990.718	€ 232.778
Balance of plant	€ 1.923.180	€ 1.640.000	€ 1.778.680	€ 1.511.878
Array cable	€ 80.940	€ 70.000	€ 90.821	€ 77.198
Export cable	€ 228.000	€ 195.000	€ 255.834	€ 217.459
Cable accessories	€ 50.160	€ 45.000	€ 56.283	€ 47.841
Floating substructure	€ 1.094.400	€ 930.000	€ 935.800	€ 795.430
Mooring systems	€ 205.200	€ 175.000	€ 175.462	€ 149.143
Offshore substation	€ 171.000	€ 145.000	€ 171.000	€ 145.350
Onshore substation	€ 93.480	€ 80.000	€ 93.480	€ 79.458
Installation and commissioning	€ 313.614	€ 265.000	€ 273.368	€ 232.362
Inbound transport	€ 9.918	€ 8.000	€ 9.918	€ 8.430
Offshore cable installation	€ 159.600	€ 135.000	€ 179.084	€ 152.221
Mooring and anchoring	€ 77.520	€ 65.000	€ 35.000	€ 29.750
Floating substructure	€ 30.210	€ 25.000	€ 13.000	€ 11.050
Offshore substation installation	€ 27.360	€ 25.000	€ 27.360	€ 23.256
Onshore export cable installation	€ 6.498	€ 5.000	€ 6.498	€ 5.523
Offshore logistics	€ 2.508	€ 2.000	€ 2.508	€ 2.132
Contingency and insurance	€ 307.800	€ 260.000	€ 307.800	€ 260.000
Decommissioning	€ 162.450	€ 138.000	€ 83.782	€ 0
Floating substructure	€ 3.990	€ 3.000	€ 9.100	€ 0
Mooring and anchoring	€ 45.600	€ 40.000	€ 31.500	€ 0
Cable decommissioning	€ 83.220	€ 70.000	€ 18.558	€ 0
Substation decommissioning	€ 29.640	€ 25.000	€ 24.624	€ 0
Transport	€ 9.918	€ 8.000	€ 9.918	€ 0
Operations and maintenance	€ 80.484	€ 70.600	€ 71.100	€ 67.660
Operations	€ 27.360	€ 24.000	€ 24.000	€ 23.000
Maintenance	€ 50.160	€ 44.000	€ 44.000	€ 42.000
Offshore logistics and vessels	€ 2.508	€ 2.200	€ 2.200	€ 2.000
O&M port	€ 456	€ 400	€ 500	€ 500
Tether Replacements	€ 0	€ 0	€ 400	€ 160